
MULTI-AGENT NATURAL ACTOR-CRITIC REINFORCEMENT LEARNING ALGORITHMS

Prashant Trivedi

Industrial Engineering and Operations Research
Indian Institute of Technology Bombay India
trivedi.prashant15@iitb.ac.in

Nandyala Hemachandra

Industrial Engineering and Operations Research
Indian Institute of Technology Bombay India
nh@iitb.ac.in

ABSTRACT

Both single-agent and multi-agent actor-critic algorithms are an important class of Reinforcement Learning algorithms. In this work, we propose three fully decentralized multi-agent natural actor-critic (MAN) algorithms. The agents' objective is to collectively learn a joint policy that maximizes the sum of averaged long-term returns of these agents. In the absence of a central controller, agents communicate the information to their neighbors via a time-varying communication network while preserving privacy. We prove the convergence of all the 3 MAN algorithms to a globally asymptotically stable point of the ODE corresponding to the actor update; these use linear function approximations. We use the Fisher information matrix to obtain the natural gradients. The Fisher information matrix captures the curvature of the Kullback-Leibler (KL) divergence between policies at successive iterates. We also show that the gradient of this KL divergence between policies of successive iterates is proportional to the objective function's gradient. Our MAN algorithms indeed use this *representation* of the objective function's gradient. Under certain conditions on the Fisher information matrix, we prove that at each iterate, the optimal value via MAN algorithms can be better than that of the multi-agent actor-critic (MAAC) algorithm using the standard gradients. To validate the usefulness of our proposed algorithms, we implement all the 3 MAN algorithms on a bi-lane traffic network to reduce the average network congestion. We observe an almost 25% reduction in the average congestion in 2 MAN algorithms; the average congestion in another MAN algorithm is on par with the MAAC algorithm. We also consider a generic 15 agent MARL; the performance of the MAN algorithms is again as good as the MAAC algorithm. We attribute the better performance of the MAN algorithms to their use of the above representation.

Keywords Natural Gradients · Actor-Critic Methods · Networked Agents · Traffic Network Control · Stochastic Approximations · Function Approximations · Representation Learning

1 Introduction

Reinforcement Learning (RL) has been explored in recent years and is of great interest to researchers because of its broad applicability in many real-life scenarios. In RL, agent/agents interact with the environment and take decisions sequentially. It is applied successfully to various problems including elevator scheduling, robot control, etc. There are many instances where RL agents surpass human performance, such as openAI beating the world champion DOTA player, DeepMind beating the world champion of Alpha Star.

The sequential decision-making problems are generally modeled via a model-based approach called the Markov decision process (MDP). However, it requires the knowledge of system transitions and the rewards. In contrast, RL is a data-driven MDP framework for sequential decision-making tasks. The transition probability matrices and the reward functions are not assumed, but their realizations are available as observed data.

In RL, the purpose of an agent is to learn an optimal or nearly-optimal policy that maximizes the “reward function” or any user-provided reinforcement signals. However, in many realistic scenarios, there is more than one agent. To

A version of this paper is under review.

this end, many researchers explore the multi-agent reinforcement learning (MARL) methods, but most of them are centralized and hence relatively slow. Furthermore, these algorithms use the standard gradient, which comes with its limitations. For example, the standard gradients cannot capture the angles in the state space and may not be effective in many scenarios. The natural gradients are more suitable in such cases because they capture the intrinsic curvature in the state space. In this work, we are incorporating the natural gradients in a multi-agent RL framework.

In a multi-agent setup that we consider, the agents have some private information and a common goal. The goal can be achieved by deploying a central controller and converting the MARL problem into a single-agent RL problem. However, deploying a central controller often leads to scalability issues. On the other hand, if there is no central controller and the agents do not share any information, there is almost no hope of achieving the goal. An intermediate method is to share some parameters using (possibly) a time-varying and sparse communication matrix [Zhang et al., 2018]. The algorithms based on such intermediate methods are often attributed as consensus-based algorithms.

The consensus-based algorithm models can also be viewed as being intermediate between dynamic non-cooperative and cooperative game models. Non-cooperative games, as multi-agent systems, model situations where the agents do not have a common goal and do not communicate. On the contrary, cooperative games model situations where the central controller takes actions to achieve a common goal.

Algorithm 2 of [Zhang et al., 2018] is a consensus-based actor-critic algorithm and uses the standard gradient. We call it MAAC (multi-agent actor-critic) algorithm. However, MAAC lacks in capturing the intrinsic curvature present in the state space. To incorporate the natural gradients, we propose three multi-agent natural actor-critic (MAN) algorithms. These algorithms use the linear function approximations for the state value and the reward functions. The function approximations are often helpful if the state space or the action space is large or infinite. We prove the convergence of all the 3 MAN algorithms to a globally asymptotically stable equilibrium of an ordinary differential equation (ODE) obtained from the actor update. The equilibrium point gives the local optima of the objective function.

Being a first order method, the standard gradients methods overlooks the curvatures in the objective function. However, incorporating the Fisher information matrix to the standard gradients scales the parameter updates via a log-likelihood function. We show that this log-likelihood function is indeed the KL divergence between the consecutive policies and provides the gradient of the objective function up to a constant scaling (Section 2.1). Unlike the standard gradient method, where the updates are restricted to the parameter space only, the natural gradient based methods allow the updates to factor in the curvature of the objective function in policy distribution prediction space via the KL divergence between them. Thus, 2 of our MAN algorithms use a certain *representation* of the gradient of the objective function in terms gradient of this KL divergence. It turns out these 2 algorithms have much better empirical performance (see Section 5.1).

We also identify some sufficient conditions on the eigenvalues of the Fisher information matrix at any iterate that ensures the objective function of MAN algorithms to be better (see Theorem 3). We feel that this is a significant result about the effectiveness of the natural gradients in average reward actor-critic methods; to the best of our knowledge, this is the first such result on the role of natural gradients in RL. Also, the empirical performance of 2 of the MAN algorithms is significantly better than the MAAC algorithm, as outlined now.

To validate the usefulness of our proposed algorithms, we perform a comprehensive set of computational experiments in two settings: a bi-lane traffic network and an abstract MARL model. For the bi-lane network, we consider various arrival patterns at each traffic light (agent). The objective is to reduce network congestion by exploring massive traffic plans space involving signaling patterns across all traffic lights. To incorporate the ample state space (50^{16}) and action space (3^4), we use suitable linear function approximations for the state value function and the reward function. The abstract MARL setup consists of 15 agents with large state and action spaces and generic reward functions. Each agent's reward is private information and hence not known to other agents.

On a bi-lane traffic network model with two arrival patterns between various origin-destination (OD) pairs of the network [Bhatnagar, 2020] we often observe a significant reduction ($\approx 25\%$) in the average network congestion in 2 of our MAN algorithms. In these algorithms (that perform well), we have explicitly used the Fisher information matrix inverse estimate via the Sherman-Morrison update. One of our MAN algorithm that is only based on the advantage parameters and never estimates the Fisher information matrix inverse is on-par with MAAC. The abstract MARL setup has 15 states and 2 actions in each state [Dann et al., 2014, Zhang et al., 2018]. In that case, our MAN algorithms either outperform or are on-par with the MAAC algorithm with high confidence.

Organization of the paper: In Section 2 we introduce the multi-agent reinforcement learning (MARL) and a novel natural gradients framework. We then propose three MAN algorithms namely FI-MAN, AP-MAN, and FIAP-MAN, and provide some theoretical insights on their relative performance in Section 3. Convergence proofs of all the algorithms are available in Section 4. Finally, we provide the computational experiments for modeling traffic network control and another abstract multi-agent RL problem in Section 5.

The detailed proof of theorems and lemmas are available in Appendix A. More details of the computations and empirical observations are available in Appendix B. We provide some backgrounds on MDP, single-agent actor-critic algorithm, and the MAAC algorithm in Appendix C.

2 MARL framework and natural gradients

This section will describe the multi-agent reinforcement learning (MARL) framework and the notion of natural gradients. We begin by describing some basic notations and the multi-agent Markov decision process (MDP).

Let $N = \{1, 2, \dots, n\}$ denote the set of agents. Each agent is independently interacting with a stochastic environment and takes a local action. We consider a fully decentralized setup in which a communication network connects the agents. This network is used for exchanging information among agents in the absence of a central controller. The communication network is possibly time-varying and sparse. The network can help the agents to communicate some information such that the privacy of agents remains intact. Formally, the communication network is characterized by an undirected graph $\mathcal{G}_t = (N, \mathcal{E}_t)$, where N is the set of all nodes (or agents) and \mathcal{E}_t is the set of communication links available at time $t \in \mathbb{N}$. We say, agents $i, j \in N$ communicate at time t if $(i, j) \in \mathcal{E}_t$.

Let \mathcal{S} denote the common state space available to all the agents. At any time t , each agent observes a common state $s_t \in \mathcal{S}$, and takes a local action a_t^i from the set of available actions \mathcal{A}^i . The action a_t^i is taken as per a local policy $\pi^i : \mathcal{S} \times \mathcal{A}^i \rightarrow [0, 1]$, where $\pi^i(s_t, a_t^i)$ is the probability of taking action a_t^i in state s_t by agent $i \in N$. Let $\mathcal{A} = \prod_{i=1}^n \mathcal{A}^i$ is the joint action space of all the agents. To each state and action pair, every agent receives a finite reward from the local reward function $R^i : \mathcal{S} \times \mathcal{A} \rightarrow \mathbb{R}$. The state transition probability of MDP is given by $P : \mathcal{S} \times \mathcal{A} \times \mathcal{S} \rightarrow [0, 1]$. We assume that states are globally observed in the entire setup, whereas the rewards and actions are observed locally. However, using only local rewards and actions it is hard for any classical reinforcement learning algorithm to maximize the averaged reward determined by the joint actions of all the agents. To this end, we consider the multi-agent networked MDP given in [Zhang et al., 2018]. The multi-agent networked MDP is defined as $(\mathcal{S}, \{\mathcal{A}^i\}_{i \in N}, P, \{R^i\}_{i \in N}, \{\mathcal{G}_t\}_{t \geq 0})$, with each component described as above. Let the joint policy of all agents be denoted by $\pi : \mathcal{S} \times \mathcal{A} \rightarrow [0, 1]$ satisfying $\pi(s, a) = \prod_{i \in N} \pi^i(s, a^i)$. Let $a_t = (a_t^1, \dots, a_t^n)$ is the action taken by all the agents at time t . Depending on the action a_t^i taken by agent i at time t , the agent receives a random reward r_{t+1}^i with the expected value $R^i(s_t, a_t)$. Moreover, with probability $P(s_{t+1}|s_t, a_t)$ the multi-agent MDP shifts to next state $s_{t+1} \in \mathcal{S}$.

Due to large state and action space it is often useful to consider the parameterized policies [Grondman et al., 2012, Sutton and Barto, 2018]. We parameterize the local policy, $\pi^i(\cdot, \cdot)$ by $\theta^i \in \Theta^i \subseteq \mathbb{R}^{m_i}$, where Θ^i is the compact set. To find the global policy parameters we can pack all the local policy parameters as $\theta = [(\theta^1)^\top, \dots, (\theta^n)^\top]^\top \in \Theta \subseteq \mathbb{R}^{\sum_{i=1}^n m_i}$, where $\Theta = \prod_{i \in N} \Theta^i$. The parameterized joint policy is then given by $\pi_\theta(s, a) = \prod_{i \in N} \pi_{\theta^i}(s, a^i)$. The objective of the agents is to collectively find a joint policy π_θ that maximizes the averaged long-term return, provided each agent has local information only. For a given policy parameter θ , let the globally averaged long-term return be denoted by $J(\theta)$ and defined as

$$J(\theta) = \lim_{T \rightarrow \infty} \frac{1}{T} \mathbb{E} \left(\sum_{t=0}^{T-1} \frac{1}{n} \sum_{i \in N} r_{t+1}^i \right) = \sum_{s \in \mathcal{S}} d_\theta(s) \sum_{a \in \mathcal{A}} \pi_\theta(s, a) \bar{R}(s, a),$$

where $\bar{R}(s, a) = \frac{1}{n} \sum_{i \in N} R^i(s, a)$ is the globally averaged reward function. Let $\bar{r}_t = \frac{1}{n} \sum_{i \in N} r_t^i$. Thus $\bar{R}(s, a) = \mathbb{E}[\bar{r}_{t+1}|s_t = s, a_t = a]$. Therefore, the joint objective of the agents is to solve the following optimization problem

$$\max_{\theta} J(\theta) = \max_{\theta} \sum_{s \in \mathcal{S}} d_\theta(s) \sum_{a \in \mathcal{A}} \pi_\theta(s, a) \bar{R}(s, a). \quad (1)$$

Like the single-agent RL [Bhatnagar et al., 2009], we require the following regularity assumption on networked multi-agent MDP and parameterized policies.

A. 1. For any agent $i \in N$, the local policy function $\pi_{\theta^i}(s, a^i) > 0$ for any $s \in \mathcal{S}, a^i \in \mathcal{A}^i$ and $\theta^i \in \Theta^i$. Also $\pi_{\theta^i}(s, a^i)$ is continuously differentiable with respect to parameters θ^i over Θ^i . Moreover, for any $\theta \in \Theta$, P^θ is the transition matrix for the Markov chain $\{s_t\}_{t \geq 0}$ induced by policy π_θ , that is, for any $s, s' \in \mathcal{S}$,

$$P^\theta(s'|s) = \sum_{a \in \mathcal{A}} \pi_\theta(s, a) P(s'|s, a).$$

Furthermore, the Markov chain $\{s_t\}_{t \geq 0}$ is assumed to be ergodic under π_θ with stationary distribution $d_\theta(s)$ over \mathcal{S} .

The regularity assumption A. 1 on a multi-agent networked MDP is standard in the work of single agent actor-critic algorithms with function approximations [Konda and Tsitsiklis, 2000, Bhatnagar et al., 2009]. The continuous differentiability of policy $\pi_\theta(\cdot, \cdot)$ with respect to θ is required in policy gradient theorem [Sutton and Barto, 2018], and it is commonly satisfied by well-known class of functions such as neural networks or deep neural networks. Moreover, assumption A. 1 also implies that the Markov chain $\{(s_t, a_t)\}_{t \geq 0}$ has stationary distribution $\tilde{d}_\theta(s, a) = d_\theta(s) \cdot \pi_\theta(s, a)$ for any $s \in \mathcal{S}, a \in \mathcal{A}$.

Based on the objective function given in Equation (1) the global state-action value function associated with state-action pair (s, a) given a policy π_θ is defined as

$$Q_\theta(s, a) = \sum_{t \geq 0} \mathbb{E}[\bar{r}_{t+1} - J(\theta) | s_0 = s, a_0 = a, \pi_\theta]. \quad (2)$$

Note that the global state-action value function, $Q_\theta(s, a)$ given in Equation (2) is motivated from the gain and bias relation for the average reward criteria of the single agent MDP as given in say, Section 8.2.1 in [Puterman, 2014]. It captures the expected sum of fluctuations of the global rewards about the globally averaged objective function ('average adjusted sum of rewards' [Mahadevan, 1996]) when action $a = (a^1, a^2, \dots, a^n)$ is taken in state $s \in \mathcal{S}$ at time $t = 0$, and thereafter the policy π_θ is followed. Similarly, the global state value function is defined as

$$V_\theta(s) = \sum_{a \in \mathcal{A}} \pi_\theta(s, a) Q_\theta(s, a). \quad (3)$$

We will now provide the policy gradient theorem for the MARL setup [Zhang et al., 2018]. To this end, define the global advantage function $A_\theta(s, a) = Q_\theta(s, a) - V_\theta(s)$. For the multi-agent setup, the local advantage function $A_\theta^i : \mathcal{S} \times \mathcal{A} \rightarrow \mathbb{R}$ for each agent $i \in N$ is defined as $A_\theta^i(s, a) = Q_\theta(s, a) - \tilde{V}_\theta^i(s, a^{-i})$, where $\tilde{V}_\theta^i(s, a^{-i}) = \sum_{a^i \in \mathcal{A}^i} \pi_{\theta^i}^i(s, a^i) Q_\theta(s, a^i, a^{-i})$. Note that $\tilde{V}_\theta^i(s, a^{-i})$ represents the value of a state s to an agent $i \in N$ when the policy is parameterized by $\theta = [(\theta^1)^\top, (\theta^2)^\top, \dots, (\theta^n)^\top]$, and all other agents are taking action $a^{-i} = (a^1, \dots, a^{i-1}, a^{i+1}, \dots, a^n)$ in state s .

Theorem 1 (Policy gradient theorem for MARL [Zhang et al., 2018]). *Under the assumption A. 1, for any $\theta \in \Theta$, and each agent $i \in N$, the gradient of $J(\theta)$ with respect to θ^i is given by*

$$\begin{aligned} \nabla_{\theta^i} J(\theta) &= \mathbb{E}_{s \sim d_\theta, a \sim \pi_\theta} [\nabla_{\theta^i} \log \pi_{\theta^i}^i(s, a^i) \cdot A_\theta(s, a)] \\ &= \mathbb{E}_{s \sim d_\theta, a \sim \pi_\theta} [\nabla_{\theta^i} \log \pi_{\theta^i}^i(s, a^i) \cdot A_\theta^i(s, a)], \end{aligned}$$

where $J(\theta)$ is defined as in Equation (1).

The proof of this theorem is available in [Zhang et al., 2018]. We refer to $\psi^i(s, a^i) := \nabla_{\theta^i} \log \pi_{\theta^i}^i(s, a^i)$ as score function. It is often used to estimate the gradient of the global objective function. We will see in Section 3.2 that the same score function is called the compatible features. This is because the above policy gradient theorem with function approximations requires the compatibility condition (see Theorem 2 [Sutton et al., 1999]). The policy gradient theorem for MARL relates the gradient of the global objective function to each θ^i and the local advantage function $A_\theta^i(\cdot, \cdot)$. It also suggests that the gradient of the global objective function can be obtained solely using the local score function if agent $i \in N$ has an unbiased estimate of the advantage functions A_θ^i or A_θ . However, estimating the advantage function requires the rewards r_t^i of all the agents $i \in N$; therefore, these functions cannot be well estimated by any agent $i \in N$. To this end, [Zhang et al., 2018] have proposed two fully decentralized actor-critic algorithms based on the consensus network. These algorithms work in a fully decentralized fashion and empirically achieve the same performance as a centralized algorithm in the long run. However, we are using algorithm 2 of [Zhang et al., 2018] which we are calling as multi-agent actor-critic (MAAC) algorithm.

In the fully decentralized setup, we consider the weight matrix $C_t = [c_t(i, j)]$, depending on the network topology of communication network \mathcal{G}_t . Here $c_t(i, j)$ represents the weight of the message transmitted from agent i to agent j at time t . At any time t , the local parameters are updated by each agent using this weight matrix. For generality, we take the weight matrix C_t as random. This is either because \mathcal{G}_t is a time-varying graph or the randomness in the consensus algorithm [Boyd et al., 2006]. The weight matrix satisfy the following assumptions [Zhang et al., 2018].

A. 2. *The sequence of non-negative random matrices $\{C_t\}_{t \geq 0} \subseteq \mathbb{R}^{n \times n}$ satisfy the following:*

1. C_t is row stochastic, i.e., $C_t \mathbf{1} = \mathbf{1}$. Moreover, $\mathbb{E}(C_t)$ is column stochastic, i.e., $\mathbf{1}^\top \mathbb{E}(C_t) = \mathbf{1}^\top$. Furthermore, there exists a constant $\gamma \in (0, 1)$ such that, for any $c_t(i, j) > 0$, we have $c_t(i, j) \geq \gamma$.
2. Weight matrix C_t respects \mathcal{G}_t , i.e., $c_t(i, j) = 0$ if $(i, j) \notin \mathcal{E}_t$.

3. The spectral norm of $\mathbb{E}[C_t^\top (I - \mathbb{1}\mathbb{1}^\top/n)C_t]$ is smaller than one.
4. Given the σ -algebra generated by the random variables before time t , C_t is conditionally independent of r_{t+1}^i for any $i \in N$.

Assumption 1 of considering a doubly stochastic matrix is standard in the work of consensus-based algorithms. It is often helpful in the convergence of the update to a common vector [Bianchi et al., 2013]. To prove the stability of the consensus update (see Appendix A of [Zhang et al., 2018] for detailed proof), we require the lower bound on the weights of the matrix [Nedic and Ozdaglar, 2009]. Assumption 2 is required for the connectivity of \mathcal{G}_t . To provide the geometric convergence in distributed optimization, authors in [Nedic et al., 2017] provide the connection between the time-varying network and the spectral norm property. The same connection is needed for convergence in our work also. To this end, we have assumption 3 above. Assumption 4 on the conditional independence of C_t and r_{t+1} is common in many practical multi-agent systems. The Metropolis matrix [Xiao et al., 2005] given below satisfy all the above assumptions. It is defined only based on the local information of the agents. Let $N_t(i) := \{j \in N : (i, j) \in \mathcal{E}_t\}$ is set of neighbors of agent $i \in N$ at time t in the weight matrix C_t , and $d_t(i) = |N_t(i)|$ is the degree of agent $i \in N$. The weights $c_t(i, j)$ in the Metropolis matrix are given by

$$\begin{aligned} c_t(i, j) &= \frac{1}{1 + \max\{d_t(i), d_t(j)\}}, \quad \forall (i, j) \in \mathcal{E}_t \\ c_t(i, i) &= 1 - \sum_{j \in N_t(i)} c_t(i, j) \quad \forall i \in N. \end{aligned}$$

Now, we will outline the actor-critic algorithms along with the function approximations in a fully decentralized setting.

The actor-critic algorithm consists of two steps – critic step and actor step. At each time t , the actor suggests a policy parameters θ_t . The critic evaluates its value using the policy parameters and criticizes or gives the feedback to the actor. Using the feedback from critic, the actor then updates the policy parameters, and this continues until convergence. Let the global state value temporal difference (TD) error is defined as $\delta_t = \bar{r}_{t+1} - J(\theta) + V_\theta(s_{t+1}) - V_\theta(s_t)$. It is easy to see that the state value temporal difference error is an unbiased estimate of the advantage function A_θ [Sutton and Barto, 2018], i.e.,

$$\mathbb{E}[\delta_t \mid s_t = s, a_t = a, \pi_\theta] = A_\theta(s, a) \quad \forall s \in \mathcal{S}, a \in \mathcal{A}. \quad (4)$$

Often in many applications [Corke et al., 2005, Dall’Anese et al., 2013], the state space is either large or infinite. Therefore, the exact state value is not available. To this end, in this entire work we use the linear function approximations for state value function. Later on, we also use the linear function approximation for the advantage function in Section 3.2. Let the state value function $V_\theta(s)$ is approximated using the linear function as $V_\theta(v) := V_\theta(s; v) = v^\top \varphi(s)$, where $\varphi(s) = [\varphi_1(s), \dots, \varphi_L(s)]^\top \in \mathbb{R}^L$ is the feature associated with state s , and $v \in \mathbb{R}^L$. Note that $L \ll |\mathcal{S}|$, hence the value function is approximated using very small number of features. Moreover, let μ_t^i be the estimate of the objective function $J(\theta)$ by agent i at time t . It tracks the long-term return to each agent $i \in N$. The MAAC algorithm is based on the consensus network (details in Appendix C.3) and consists of the following updates for critic and objective function estimate

$$\tilde{\mu}_t^i = (1 - \beta_{v,t}) \cdot \mu_t^i + \beta_{v,t} \cdot r_{t+1}^i; \quad \mu_{t+1}^i = \sum_{j \in N} c_t(i, j) \tilde{\mu}_t^j \quad (5)$$

$$\tilde{v}_t^i = v_t^i + \beta_{v,t} \cdot \delta_t^i \cdot \nabla_v V_t(v_t^i); \quad v_{t+1}^i = \sum_{j \in N} c_t(i, j) \tilde{v}_t^j, \quad (6)$$

where $\beta_{v,t} > 0$ is the critic step-size and $\delta_t^i = r_{t+1}^i - \mu_t^i + V_{t+1}(v_t^i) - V_t(v_t^i)$ is the local TD error. Note that the estimate of advantage function as given in Equation (4) requires \bar{r}_{t+1} , which is not available to any agent $i \in N$. Therefore, we will parameterize the reward function $\bar{R}(\cdot, \cdot)$ used in the critic update as well. Let $\bar{R}(s, a)$ be approximated using a linear function as $\bar{R}(s, a; \lambda) = \lambda^\top f(s, a)$, where $f(s, a) = [f_1(s, a), \dots, f_M(s, a)]^\top \in \mathbb{R}^M$, $M \ll |\mathcal{S}||\mathcal{A}|$ are the features associated with state action pair (s, a) . To obtain the estimate of $\bar{R}(s, a)$ we use the following least square minimization

$$\min_{\lambda} \sum_{s \in \mathcal{S}, a \in \mathcal{A}} \tilde{d}_\theta(s, a) [\bar{R}(s, a) - \bar{R}(s, a; \lambda)]^2,$$

where $\bar{R}(s, a) := \frac{1}{n} \sum_{i \in N} R^i(s, a)$, and $\tilde{d}_\theta(s, a) = d_\theta(s) \cdot \pi_\theta(s, a)$. The above optimization can be written as

$$\min_{\lambda} \sum_{i \in N} \sum_{s \in \mathcal{S}, a \in \mathcal{A}} \tilde{d}_\theta(s, a) [R^i(s, a) - \bar{R}(s, a; \lambda)]^2,$$

Taking first order derivative with respect to λ implies that we should also do the following as a part of critic update:

$$\tilde{\lambda}_t^i = \lambda_t^i + \beta_{v,t} \cdot [r_{t+1}^i - \bar{R}_t(\lambda_t^i)] \cdot \nabla_{\lambda} \bar{R}_t(\lambda_t^i); \quad \lambda_{t+1}^i = \sum_{j \in N} c_t(i, j) \tilde{\lambda}_t^j, \quad (7)$$

where $\bar{R}_t(\lambda) := \bar{R}(s_t, a_t; \lambda)$ for any $\lambda \in \mathbb{R}^M$. The TD error with parametrized reward, $\bar{R}(\cdot)$ is given by $\tilde{\delta}_t^i = \bar{R}_t(\lambda_t^i) - \mu_t^i + V_{t+1}(v_t^i) - V_t(v_t^i)$. The actor will update the policy parameters as

$$\theta_{t+1}^i = \theta_t^i + \beta_{\theta,t} \cdot \tilde{\delta}_t^i \cdot \psi_t^i, \quad (8)$$

where $\beta_{\theta,t} > 0$ is the actor step size. Note that we have used $\tilde{\delta}_t^i \cdot \psi_t^i$ instead of $\nabla_{\theta^i} J(\theta)$ in the actor update. However, $\tilde{\delta}_t^i \cdot \psi_t^i$ may not be an unbiased estimate of the gradient of objective function $\nabla_{\theta^i} J(\theta)$, i.e.,

$$\mathbb{E}_{s_t \sim d_{\theta}, a_t \sim \pi_{\theta}} [\tilde{\delta}_t^i \cdot \psi_t^i] = \nabla_{\theta^i} J(\theta) + b, \quad (9)$$

where $b = \mathbb{E}_{s_t \sim d_{\theta}, a_t \sim \pi_{\theta}} [(f_t^\top \lambda_{\theta} - \bar{R}(s_t, a_t)) \psi_{t,\theta}^i] + \mathbb{E}_{s_t \sim d_{\theta}} [(\varphi_t^\top v_{\theta} - V_{\theta}(s_t)) \psi_{t,\theta}^i]$ is the bias term. If the above bias (approximation error) is very small then the convergence point of the ODE corresponding to the actor (will see in Section 4) is close to the local optima of $J(\theta)$. Therefore, while doing the asymptotic analysis we ignore the above bias term, and hence $\mathbb{E}_{s_t \sim d_{\theta}, a_t \sim \pi_{\theta}} [\tilde{\delta}_t^i \cdot \psi_t^i] \approx \nabla_{\theta^i} J(\theta)$. To prove the convergence of actor-critic algorithm we require the following conditions on the step sizes $\beta_{v,t}, \beta_{\theta,t}$

$$(a) \sum_t \beta_{v,t} = \sum_t \beta_{\theta,t} = \infty; \quad (b) \sum_t \beta_{v,t}^2 + \beta_{\theta,t}^2 < \infty, \quad (10)$$

moreover, $\beta_{\theta,t} = o(\beta_{v,t})$, and $\lim_t \frac{\beta_{v,t+1}}{\beta_{v,t}} = 1$, i.e., critic update is made at the faster time scale than the actor update. Condition in (a) ensure that the discrete time steps $\beta_{v,t}, \beta_{\theta,t}$ used in the critic and actor steps do cover the entire time axis while retaining $\beta_{v,t}, \beta_{\theta,t} \rightarrow 0$. We also require the error in the estimates used in the critic and the actor updates to be asymptotically negligible almost surely. Furthermore, condition in (b) asymptotically suppresses the variance in the estimates [Borkar, 2009].

The multi-agent actor-critic scheme given in the MAAC algorithm uses standard (or vanilla) gradients. However, they are most useful for reward functions that have single optima and whose gradients are isotropic in magnitude for any direction away from its optimum [Amari and Douglas, 1998]. None of these properties are valid in most of the reinforcement learning problems. Apart from this, the performance of standard gradient based reinforcement learning algorithms depends on the coordinate system used to define the objective function. This is one of the most significant drawbacks of standard gradient [Kakade, 2001, Bagnell and Schneider, 2003].

In many applications such as robotics, the state space contains angles, so the state space has manifolds (curvatures). The objective function will then be defined in that curved space, making the policy gradients methods inefficient. We thus require a method that incorporates knowledge about the curvature of the space into the gradient. The natural gradients are more ‘‘natural’’ choices in such cases. In the following section, we will describe the natural gradients and use them along with the policy gradient theorem in the multi-agent setup.

2.1 Natural gradients and the Fisher information matrix

Recall that our objective function J is parameterized by θ . For the single agent actor-critic methods involving natural gradients, $\tilde{\nabla} J(\theta)$, authors in [Bagnell and Schneider, 2003, Peters et al., 2003, Bhatnagar et al., 2009] have defined it via Fisher information matrix, $G(\theta)$ and standard gradients, $\nabla J(\theta)$ as

$$\tilde{\nabla}_{\theta} J(\theta) = G(\theta)^{-1} \nabla_{\theta} J(\theta), \quad (11)$$

where $G(\theta)$ is a positive definite matrix defined as

$$G(\theta) := \mathbb{E}_{s \sim d_{\theta}, a \sim \pi_{\theta}} [\nabla_{\theta} \log \pi_{\theta}(s, a) \nabla_{\theta} \log \pi_{\theta}(s, a)^\top]. \quad (12)$$

The above Fisher information matrix is the covariance of the score function. It can also be interpreted via KL-divergence¹ between the policy $\pi(\cdot, \cdot)$ parameterize at θ and $\theta + \Delta\theta$ as below [Martens, 2020, Ratliff, 2013]

$$KL(\pi_{\theta}(\cdot, \cdot) || \pi_{\theta+\Delta\theta}(\cdot, \cdot)) \approx \frac{1}{2} \Delta\theta^\top \cdot G(\theta) \cdot \Delta\theta. \quad (13)$$

¹<https://towardsdatascience.com/natural-gradient-ce454b3dcdafa>

The above expression is obtained from the second-order Taylor expansion of $\log \pi_{\theta+\Delta\theta}(s, a)$, and using the fact that the sum of the probabilities is one. In above, the right-hand term is a quadratic involving positive definite matrix $G(\theta)$, and hence $G(\theta)$ approximately captures the curvature of KL divergence between policy distributions at θ and $\theta + \Delta\theta$.

We now relate the Fisher information matrix, $G(\theta)$ to the objective function, $J(\theta)$. From Equation (13), KL is function of the Fisher information matrix and delta change in the policy parameters. We find the optimal step-size $\Delta\theta^*$ at iterate t via the following optimization problem

$$\begin{aligned} \Delta\theta^* &= \operatorname{argmax}_{\Delta\theta} J(\theta_t + \Delta\theta) \\ \text{s.t. } &KL(\pi_{\theta_t}(\cdot, \cdot) || \pi_{\theta_t + \Delta\theta}(\cdot, \cdot)) = c. \end{aligned} \quad (14)$$

Writing the Lagrangian $\mathcal{L}(\theta_t + \Delta\theta; \mu_t)$ (where μ_t is the Lagrangian multiplier) of above optimization problem and using the first order Taylor approximation, we have

$$\begin{aligned} \Delta\theta^* &= \operatorname{argmax}_{\Delta\theta} J(\theta_t + \Delta\theta) + \mu_t(KL(\pi_{\theta_t}(\cdot, \cdot) || \pi_{\theta_t + \Delta\theta}(\cdot, \cdot)) - c), \\ &\approx \operatorname{argmax}_{\Delta\theta} J(\theta_t) + \Delta\theta^\top \nabla J(\theta_t) + \frac{1}{2} \cdot \mu_t \cdot \Delta\theta^\top \cdot G(\theta_t) \cdot \Delta\theta - \mu_t c. \end{aligned}$$

Setting the derivative of above Lagrangian to zero, we have

$$\nabla J(\theta_t) + \mu_t \cdot \Delta\theta^{*\top} \cdot G(\theta_t) = 0 \implies \Delta\theta^* = -\frac{1}{\mu_t} G(\theta_t)^{-1} \nabla J(\theta_t), \quad (15)$$

i.e., upto the factor of μ_t , we get an optimal direction while taking the curvature of log-likelihood at point θ_t . Moreover, from Equations (13) and (15) we have

$$\nabla KL \approx G(\theta_t) \Delta\theta = -\frac{1}{\mu_t} \nabla J(\theta_t). \quad (16)$$

The above equation relates the gradient of the objective function to the gradient of KL divergence between the policies separated by $\Delta\theta$. It is a valuable observation because we can adjust the updates (of actor parameter) just by moving in the prediction space of the parameterized policy distributions. Thus, those MAN algorithms discussed later that rely on Fisher information matrix $G(\cdot)$ use the above *representation* for $\nabla J(\cdot)$. This again justifies the natural gradients as given in Equation (11). We recall these aspects in Section 3.5 for the Boltzmann policies.

2.2 Multi-agent natural policy gradient theorem and rank-one update of G_{t+1}^{i-1}

Similar to Equation (11), in the multi-agent setup the natural gradient of the objective function can be written for any agent $i \in N$ as

$$\tilde{\nabla}_{\theta^i} J(\theta) = G(\theta^i)^{-1} \nabla_{\theta^i} J(\theta), \quad (17)$$

where $G(\theta^i) = \mathbb{E}_{s \sim d_\theta, a \sim \pi_\theta} [\nabla_{\theta^i} \log \pi_{\theta^i}(s, a^i) \nabla_{\theta^i} \log \pi_{\theta^i}(s, a^i)^\top]$ is again a positive definite matrix for each agent $i \in N$. We will now present the policy gradient theorem for the multi-agent setup involving the natural gradients.

Theorem 2 (Policy gradient theorem for MARL with natural gradients). *Under assumption A.1, the natural gradient of $J(\theta)$ with respect to θ^i for each $i \in N$ is given by*

$$\begin{aligned} \tilde{\nabla}_{\theta^i} J(\theta) &= G(\theta^i)^{-1} \mathbb{E}_{s \sim d_\theta, a \sim \pi_\theta} [\nabla_{\theta^i} \log \pi_{\theta^i}(s, a^i) \cdot A_\theta(s, a)] \\ &= G(\theta^i)^{-1} \mathbb{E}_{s \sim d_\theta, a \sim \pi_\theta} [\nabla_{\theta^i} \log \pi_{\theta^i}(s, a^i) \cdot A_\theta^i(s, a)] \end{aligned}$$

Proof. The proof follows from the multi-agent policy gradient Theorem 1 and observing that $\tilde{\nabla}_{\theta^i} J(\theta) = G(\theta^i)^{-1} \nabla_{\theta^i} J(\theta)$. \square

It is known that the Fisher information matrix and its inverse are computationally heavy [Kakade, 2001, Peters and Schaal, 2008]. Whereas, we require $G(\theta^i)^{-1}$, $\forall i \in N$ in our natural gradient based multi-agent actor-critic methods. To this end, we derive the procedure for recursively estimating the $G(\theta^i)^{-1}$ for each agent $i \in N$ at the faster time scale. Let G_{t+1}^{i-1} , $t \geq 0$, be the t -th estimate of $G(\theta^i)^{-1}$. Consider the sample averages at time $t \geq 0$,

$$G_{t+1}^i = \frac{1}{t+1} \sum_{l=0}^t \psi_l^i \psi_l^{i\top},$$

where $\psi_t^i = \psi_t^i(s_t, a_t^i)$ is the score function at time t . Thus, G_{t+1}^i will be recursively obtained as

$$G_{t+1}^i = \left(1 - \frac{1}{t+1}\right) G_t^i + \frac{1}{t+1} \psi_t^i \psi_t^{i\top}.$$

More generally, one can consider the following recursion

$$G_{t+1}^i = (1 - \beta_{v,t}) G_t^i + \beta_{v,t} \psi_t^i \psi_t^{i\top}, \quad (18)$$

where $\beta_{v,t} > 0$ is the step size as earlier. Using the idea of stochastic convergence it is easy to see that if θ^i is held constant, G_{t+1}^i will converge to $G(\theta^i)$ with probability one. For all $i \in N$, we will write the recursion for the Fisher information matrix inverse G_{t+1}^{i-1} using the Sherman-Morrison matrix inversion [Sherman and Morrison, 1950] as follows

$$G_{t+1}^{i-1} = \frac{1}{1 - \beta_{v,t}} \left[G_t^{i-1} - \beta_{v,t} \frac{(G_t^{i-1} \psi_t^i)(G_t^{i-1} \psi_t^i)^\top}{1 - \beta_{v,t} + \beta_{v,t} \psi_t^{i\top} G_t^{i-1} \psi_t^i} \right]. \quad (19)$$

To ensure that the Fisher information inverse estimates are available before the actor update, the Sherman-Morrison update is done at a faster time scale $\beta_{v,t} > 0$.

We now give three multi-agent natural actor-critic (MAN) RL algorithms involving consensus matrices. Moreover, we will also investigate the relations among these algorithms and their effect on the quality of the local optima they attained.

3 Multi-agent natural actor-critic algorithms

This section provides three multi-agent natural actor-critic (MAN) reinforcement learning algorithms. Two of the three MAN algorithms explicitly use the Fisher information matrix inverse, whereas one only uses the linear function approximation of the advantage parameters.

3.1 FI-MAN: Fisher information based multi-agent natural actor-critic

The first algorithm uses the fact that the natural gradients can be obtained via the Fisher information matrix and its inverse as given in Equations (17) and (19). The updates of estimate of the objective function, critic, and the rewards parameters in FI-MAN algorithm are the same as given in Equations (5), (6), and (7). The major difference between the MAAC and the FI-MAN algorithm is in the actor update. FI-MAN algorithm uses the following actor update

$$\theta_{t+1}^i \leftarrow \theta_t^i + \beta_{\theta,t} \cdot G_t^{i-1} \cdot \tilde{\delta}_t \cdot \psi_t^i, \quad (20)$$

where $\beta_{v,t}, \beta_{\theta,t}$ are the critic and the actor step-sizes respectively, and satisfy the conditions given in Equation (10).

Note that the FI-MAN algorithm explicitly uses G_t^{i-1} in the actor update. Though the Fisher information inverse matrix is updated according to the Sherman-Morrison inverse at a faster time scale, it may be better to avoid the explicit use of the Fisher inverse in the actor update. To this end, we will use the linear function approximation of the advantage function. This leads to the AP-MAN algorithm, i.e., advantage parameters based multi-agent natural actor-critic algorithm.

3.2 AP-MAN: Advantage parameters based multi-agent natural actor critic

Consider the local advantage function, $A^i(s, a^i) : \mathcal{S} \times \mathcal{A} \rightarrow \mathbb{R}$ for each agent $i \in N$. Let the local advantage function $A^i(s, a^i)$ be parameterized as $A^i(s, a^i; w^i) = w^{i\top} \psi^i(s, a^i)$, where $\psi^i(s, a^i) = \nabla_{\theta^i} \log \pi_{\theta^i}^i(s, a^i)$ is compatible feature, and $w^i \in \mathbb{R}^K$, such that $K \ll |\mathcal{S}||\mathcal{A}|$. Recall that same $\psi^i(s, a^i)$ was used to represent the score function in the policy gradient theorem. However, it also serves as the compatible feature while approximating the advantage function as it satisfy the compatibility condition in the policy gradient theorem with function approximations (see Theorem 2 [Sutton et al., 1999]). The compatibility condition as given in [Sutton et al., 1999] is for single agent here we are using it explicitly for each agent $i \in N$. We can tune w^i in such a way that the estimate of least squared error in linear function approximation of advantage function is minimized, i.e.,

$$\mathcal{E}^{\pi_\theta}(w^i) = \frac{1}{2} \sum_{s \in \mathcal{S}, a^i \in \mathcal{A}^i} \tilde{d}_\theta(s, a^i) [w^{i\top} \psi^i - A^i(s, a^i)]^2, \quad (21)$$

FI-MAN: Fisher information based multi-agent natural actor critic

Input: Initial values of $\mu_0^i, \tilde{\mu}_0^i, v_0^i, \tilde{v}_0^i, \lambda_0^i, \tilde{\lambda}_0^i, \theta_0^i, G_0^{i-1} \forall i \in N$, initial state s_0 , and stepsizes $\{\beta_{v,t}\}_{t \geq 0}, \{\beta_{\theta,t}\}_{t \geq 0}$.

Each agent i implements $a_0^i \sim \pi_{\theta_0^i}(s_0, \cdot)$.

Initialize the step counter $t \leftarrow 0$.

repeat

for all $i \in N$ **do**

 Observe state s_{t+1} , and reward r_{t+1}^i .

 Update: $\tilde{\mu}_t^i \leftarrow (1 - \beta_{v,t}) \cdot \mu_t^i + \beta_{v,t} \cdot r_{t+1}^i$.

$\tilde{\lambda}_t^i \leftarrow \lambda_t^i + \beta_{v,t} \cdot [r_{t+1}^i - \bar{R}_t(\lambda_t^i)] \cdot \nabla_{\lambda} \bar{R}_t(\lambda_t^i)$, where $\bar{R}_t(\lambda_t^i) = \lambda_t^{i\top} f(s_t, a_t)$.

 Update: $\delta_t^i \leftarrow r_{t+1}^i - \mu_t^i + V_{t+1}(v_t^i) - V_t(v_t^i)$, where $V_{t+1}(v_t^i) = v_t^{i\top} \varphi(s_{t+1})$.

Critic Step: $\tilde{v}_t^i \leftarrow v_t^i + \beta_{v,t} \cdot \delta_t^i \cdot \nabla_v V_t(v_t^i)$,

 Update: $\tilde{\delta}_t^i \leftarrow \bar{R}_t(\lambda_t^i) - \mu_t^i + V_{t+1}(v_t^i) - V_t(v_t^i)$; $\psi_t^i \leftarrow \nabla_{\theta^i} \log \pi_{\theta^i}(s_t, a_t^i)$.

Actor Step: $\theta_{t+1}^i \leftarrow \theta_t^i + \beta_{\theta,t} \cdot G_t^{i-1} \cdot \tilde{\delta}_t^i \cdot \psi_t^i$.

 Send $\tilde{\mu}_t^i, \tilde{\lambda}_t^i, \tilde{v}_t^i$ to the neighbors over \mathcal{G}_t .

for all $i \in N$ **do**

Consensus Update: $\mu_{t+1}^i \leftarrow \sum_{j \in N} c_t(i, j) \tilde{\mu}_t^j$;

$\lambda_{t+1}^i \leftarrow \sum_{j \in N} c_t(i, j) \tilde{\lambda}_t^j$; $v_{t+1}^i \leftarrow \sum_{j \in N} c_t(i, j) \tilde{v}_t^j$.

Fisher Update: $G_{t+1}^{i-1} \leftarrow \frac{1}{1 - \beta_{v,t}} \left[G_t^{i-1} - \beta_{v,t} \frac{(G_t^{i-1} \psi_t^i)(G_t^{i-1} \psi_t^i)^\top}{1 - \beta_{v,t} + \beta_{v,t} \psi_t^{i\top} G_t^{i-1} \psi_t^i} \right]$.

 Update: $t \leftarrow t + 1$.

until Convergence;

where $\tilde{d}_\theta(s, a^i) = d_\theta(s) \cdot \pi_\theta(s, a^i)$ as defined earlier. Taking the derivative of Equation (21) we have $\nabla_{w^i} \mathcal{E}^{\pi_\theta}(w^i) = \sum_{s \in \mathcal{S}, a^i \in \mathcal{A}^i} \tilde{d}_\theta(s, a^i) [w^{i\top} \psi^i - A^i(s, a^i)] \psi^i$. Noting that parameterized TD error $\tilde{\delta}_t^i$ is an unbiased estimate of the local advantage function $A^i(s, a^i)$, we will use the following estimate of $\nabla_{w^i} \mathcal{E}^{\pi_\theta}(w^i)$,

$$\widehat{\nabla_{w^i} \mathcal{E}^{\pi_\theta}(w_t^i)} = (\psi_t^i \psi_t^{i\top} w_t^i - \tilde{\delta}_t^i \psi_t^i).$$

Hence the update of advantage parameter w^i in the AP-MAN algorithm is

$$\begin{aligned} w_{t+1}^i &= w_t^i - \beta_{v,t} \widehat{\nabla_{w^i} \mathcal{E}^{\pi_\theta}(w_t^i)} \\ &= (I - \beta_{v,t} \psi_t^i \psi_t^{i\top}) w_t^i + \beta_{v,t} \tilde{\delta}_t^i \psi_t^i. \end{aligned} \quad (22)$$

The updates of the objective function estimate, critic, and reward parameters in the AP-MAN algorithm are the same as given in Equations (5), (6), and (7). Additionally, in the critic step we have updates of the advantage parameters as given in Equation (22). AP-MAN actor-critic algorithm uses the following actor update

$$\theta_{t+1}^i \leftarrow \theta_t^i + \beta_{\theta,t} \cdot w_{t+1}^i. \quad (23)$$

The pseudo-code of the algorithm involving advantage parameters is given in the AP-MAN algorithm.

Remark 1. We want to emphasize that the AP-MAN does not explicitly use the inverse of Fisher information matrix, $G(\theta^i)^{-1}$ in the actor update (as also in [Bhatnagar et al., 2009]); hence it requires fewer computations. However, it involves the linear function approximation of the advantage function, as given in Equation (22) that requires $\psi_t^i \psi_t^{i\top}$ which is an unbiased estimate of the Fisher information matrix (see Equation (12)). We will see later in Section 3.4 that the performance of AP-MAN is almost the same as MAAC. We empirically verify this in the computational experiments Section 5.

Remark 2. The advantage function is a linear combination of $Q(s, a)$ and $V(s)$; therefore, the linear function approximation of the advantage function alone enjoys the benefits of approximating the $Q(s, a)$ or $V(s)$. Moreover, MAAC uses the linear function approximation of $V(s)$; hence, we expect the behavior of AP-MAN to be similar to that of MAAC; this comes out in our computational experiments in 5.

Note that FI-MAN is based solely on the Fisher matrix and AP-MAN on the advantage function approximation. The FIAP-MAN algorithm, i.e., Fisher information and advantage parameter based multi-agent natural actor-critic algorithm combines them in a certain way. We see in Section 3.4 and 5.1.2 the benefits of this combination. In particular, in Section 5.1.2 we illustrate these benefits in 2 arrival distributions in the traffic network congestion model.

AP-MAN: Advantage parameters based multi-agent natural actor critic

Input: Initial values of $\mu_0^i, \tilde{\mu}_0^i, v_0^i, \tilde{v}_0^i, \lambda_0^i, \tilde{\lambda}_0^i, \theta_0^i, w_0^i \forall i \in N$, initial state s_0 , and stepsizes $\{\beta_{v,t}\}_{t \geq 0}, \{\beta_{\theta,t}\}_{t \geq 0}$. Each agent i implements $a_0^i \sim \pi_{\theta_0^i}(s_0, \cdot)$.

Initialize the step counter $t \leftarrow 0$.

repeat

for all $i \in N$ **do**

Observe state s_{t+1} , and reward r_{t+1}^i .

Update: $\tilde{\mu}_t^i \leftarrow (1 - \beta_{v,t}) \cdot \mu_t^i + \beta_{v,t} \cdot r_{t+1}^i$.

$\tilde{\lambda}_t^i \leftarrow \lambda_t^i + \beta_{v,t} \cdot [r_{t+1}^i - \bar{R}_t(\lambda_t^i)] \cdot \nabla_{\lambda} \bar{R}_t(\lambda_t^i)$, where $\bar{R}_t(\lambda_t^i) = \lambda_t^{i\top} f(s_t, a_t)$.

Update: $\delta_t^i \leftarrow r_{t+1}^i - \mu_t^i + V_{t+1}(v_t^i) - V_t(v_t^i)$, where $V_{t+1}(v_t^i) = v_t^{i\top} \varphi(s_{t+1})$.

Critic Step: $\tilde{v}_t^i \leftarrow v_t^i + \beta_{v,t} \cdot \delta_t^i \cdot \nabla_v V_t(v_t^i)$.

Update: $\tilde{\delta}_t^i \leftarrow \bar{R}_t(\lambda_t^i) - \mu_t^i + V_{t+1}(v_t^i) - V_t(v_t^i)$; $\psi_t^i \leftarrow \nabla_{\theta^i} \log \pi_{\theta_t^i}(s_t, a_t^i)$.

Update: $w_{t+1}^i \leftarrow (I - \beta_{v,t} \psi_t^i \psi_t^{i\top}) w_t^i + \beta_{v,t} \tilde{\delta}_t^i \psi_t^i$.

Actor Step: $\theta_{t+1}^i \leftarrow \theta_t^i + \beta_{\theta,t} \cdot w_{t+1}^i$.

Send $\tilde{\mu}_t^i, \tilde{\lambda}_t^i, \tilde{v}_t^i$ to the neighbors over \mathcal{G}_t .

for all $i \in N$ **do**

Consensus Update: $\mu_{t+1}^i \leftarrow \sum_{j \in N} c_t(i, j) \tilde{\mu}_t^j$;

$\lambda_{t+1}^i \leftarrow \sum_{j \in N} c_t(i, j) \tilde{\lambda}_t^j$; $v_{t+1}^i \leftarrow \sum_{j \in N} c_t(i, j) \tilde{v}_t^j$.

Update: $t \leftarrow t + 1$.

until Convergence;

3.3 FIAP-MAN: Fisher information and advantage parameter based multi-agent natural actor-critic

Recall from Section 3.2, for each agent $i \in N$, the local advantage function $A^i(s, a^i) : \mathcal{S} \times \mathcal{A} \rightarrow \mathbb{R}$ is parameterized as $A^i(s, a^i; w^i) = w^{i\top} \psi^i(s, a^i)$, where $\psi^i(s, a^i)$ are the compatible features as before, and $w^i \in \mathbb{R}^K$ such that $K \ll |\mathcal{S}| |\mathcal{A}|$. In AP-MAN the Fisher inverse $G(\theta^i)^{-1}$ is not estimated explicitly, however in FIAP-MAN we explicitly estimate $G(\theta^i)^{-1}$ along with the advantage parameters and hence use the following estimate of $\nabla_{w^i} \mathcal{E}^{\pi_{\theta^i}}(w^i)$

$$\widehat{\nabla_{w^i} \mathcal{E}^{\pi_{\theta^i}}(w_t^i)} = G_t^{i-1} (\psi_t^i \psi_t^{i\top} w_t^i - \tilde{\delta}_t^i \psi_t^i).$$

The update of advantage parameters, w^i along with the critic update of algorithm is given by

$$\begin{aligned} w_{t+1}^i &= w_t^i - \beta_{v,t} \widehat{\nabla_{w^i} \mathcal{E}^{\pi_{\theta^i}}(w_t^i)} \\ &= w_t^i - \beta_{v,t} G_t^{i-1} (\psi_t^i \psi_t^{i\top} w_t^i - \tilde{\delta}_t^i \psi_t^i) \\ &= (1 - \beta_{v,t}) w_t^i + \beta_{v,t} G_t^{i-1} \tilde{\delta}_t^i \psi_t^i. \end{aligned} \quad (24)$$

The updates of the objective function estimate, critic, and reward parameters in the FIAP-MAN algorithm are the same as given in Equations (5), (6), and (7). FIAP-MAN algorithm uses the following actor update

$$\theta_{t+1}^i \leftarrow \theta_t^i + \beta_{\theta,t} \cdot w_{t+1}^i. \quad (25)$$

The pseudo code of the algorithm involving advantage parameters and the Fisher information matrix inverse is given in FIAP-MAN algorithm.

3.4 Relationship between actor updates in algorithms

In this section, we investigate the relation between the actor updates of the MAAC and 3 MAN algorithms. In particular, we compare the actor parameters and the objective functions in all the algorithms.

Recall that the actor update for each agent $i \in N$ in FIAP-MAN algorithm is $\theta_{t+1}^i = \theta_t^i + \beta_{\theta,t} w_{t+1}^i$, where $w_{t+1}^i = (1 - \beta_{v,t}) w_t^i + \beta_{v,t} G_t^{i-1} \tilde{\delta}_t^i \psi_t^i$. Therefore, the actor update of FIAP-MAN is written as

$$\begin{aligned} \theta_{t+1}^i &= \theta_t^i + \beta_{\theta,t} \left[(1 - \beta_{v,t}) w_t^i + \beta_{v,t} G_t^{i-1} \tilde{\delta}_t^i \psi_t^i \right] \\ &= \theta_t^i + \beta_{\theta,t} (1 - \beta_{v,t}) w_t^i + \beta_{v,t} \left\{ \beta_{\theta,t} G_t^{i-1} \tilde{\delta}_t^i \psi_t^i \right\}. \end{aligned} \quad (26)$$

FIAP-MAN: Fisher information and advantage parameters based multi-agent natural actor-critic

Input: Initial values of $\mu_0^i, \tilde{\mu}_0^i, v_0^i, \tilde{v}_0^i, \lambda_0^i, \tilde{\lambda}_0^i, \theta_0^i, w_0^i, G_0^{i-1} \forall i \in N$, initial state s_0 , and stepsizes $\{\beta_{v,t}\}_{t \geq 0}, \{\beta_{\theta,t}\}_{t \geq 0}$.

Each agent i implements $a_0^i \sim \pi_{\theta_0^i}(s_0, \cdot)$.

Initialize the step counter $t \leftarrow 0$.

repeat

for all $i \in N$ **do**

 Observe state s_{t+1} , and reward r_{t+1}^i .

 Update: $\tilde{\mu}_t^i \leftarrow (1 - \beta_{v,t}) \cdot \mu_t^i + \beta_{v,t} \cdot r_{t+1}^i$.

$\tilde{\lambda}_t^i \leftarrow \lambda_t^i + \beta_{v,t} \cdot [r_{t+1}^i - \bar{R}_t(\lambda_t^i)] \cdot \nabla_{\lambda} \bar{R}_t(\lambda_t^i)$, where $\bar{R}_t(\lambda_t^i) = \lambda_t^{i\top} f(s_t, a_t)$.

 Update: $\delta_t^i \leftarrow r_{t+1}^i - \mu_t^i + V_{t+1}(v_t^i) - V_t(v_t^i)$, where $V_{t+1}(v_t^i) = v_t^{i\top} \varphi(s_{t+1})$.

Critic Step: $\tilde{v}_t^i \leftarrow v_t^i + \beta_{v,t} \cdot \delta_t^i \cdot \nabla_v V_t(v_t^i)$.

 Update: $\tilde{\delta}_t^i \leftarrow \bar{R}_t(\lambda_t^i) - \mu_t^i + V_{t+1}(v_t^i) - V_t(v_t^i)$; $\psi_t^i \leftarrow \nabla_{\theta^i} \log \pi_{\theta_t^i}(s_t, a_t^i)$.

 Update: $w_{t+1}^i \leftarrow (1 - \beta_{v,t}) w_t^i + \beta_{v,t} G_t^{i-1} \tilde{\delta}_t^i \psi_t^i$.

Actor Step: $\theta_{t+1}^i \leftarrow \theta_t^i + \beta_{\theta,t} \cdot w_{t+1}^i$.

 Send $\tilde{\mu}_t^i, \tilde{\lambda}_t^i, \tilde{v}_t^i$ to the neighbors over \mathcal{G}_t .

for all $i \in N$ **do**

Consensus Update: $\mu_{t+1}^i \leftarrow \sum_{j \in N} c_t(i, j) \tilde{\mu}_t^j$;

$\lambda_{t+1}^i \leftarrow \sum_{j \in N} c_t(i, j) \tilde{\lambda}_t^j$; $v_{t+1}^i \leftarrow \sum_{j \in N} c_t(i, j) \tilde{v}_t^j$.

Fisher Update: $G_{t+1}^{i-1} \leftarrow \frac{1}{1 - \beta_{v,t}} \left[G_t^{i-1} - \beta_{v,t} \frac{(G_t^{i-1} \psi_t^i)(G_t^{i-1} \psi_t^i)^\top}{1 - \beta_{v,t} + \beta_{v,t} \psi_t^{i\top} G_t^{i-1} \psi_t^i} \right]$.

 Update: $t \leftarrow t + 1$.

until Convergence;

This update is almost the same as the actor update of the FI-MAN algorithm with an additional term involving advantage parameters w_t^i . However, the contribution of the second term is negligible after some time t . Moreover, the third term in Equation (26) is a positive fraction of the second term in the actor update of FI-MAN algorithm (see Equation (20)). Therefore, the actor parameters in FIAP-MAN and FI-MAN are almost the same after some time t . Hence, both the algorithms converge almost to the same optimal point.

Similarly, consider the actor update of the AP-MAN algorithm, i.e., $\theta_{t+1}^i = \theta_t^i + \beta_{\theta,t} w_{t+1}^i$, where $w_{t+1}^i = (I - \beta_{v,t} \psi_t^i \psi_t^{i\top}) w_t^i + \beta_{v,t} \tilde{\delta}_t^i \psi_t^i$, thus we have

$$\begin{aligned} \theta_{t+1}^i &= \theta_t^i + \beta_{\theta,t} \left[(I - \beta_{v,t} \psi_t^i \psi_t^{i\top}) w_t^i + \beta_{v,t} \tilde{\delta}_t^i \psi_t^i \right] \\ &= \theta_t^i + \beta_{\theta,t} (I - \beta_{v,t} \psi_t^i \psi_t^{i\top}) w_t^i + \beta_{v,t} \left\{ \beta_{\theta,t} \tilde{\delta}_t^i \psi_t^i \right\}. \end{aligned} \quad (27)$$

Again, the second term in the above equation is negligible after some time t , and the third term is a positive fraction of the second term in the actor update of the MAAC algorithm (see Equation (8)). Hence the actor update in the AP-MAN algorithm is almost the same as the MAAC algorithm; therefore, both converge to the same optimal point.

The above arguments show that the FI-MAN and FIAP-MAN converge to the same optimal point, and AP-MAN and MAAC also converge to a same optimal point; possibly same as optimal point of the FI-MAN algorithm. We now show that, under some conditions, FI-MAN indeed finds an optimum at least as good as MAAC. The following theorem compares the objective functions with natural gradients and standard gradients.

Theorem 3. Let θ_t^M and θ_t^N are the actor parameters for the MAAC and FI-MAN algorithms at time $t \geq 0$, such that $\theta_t^M = \theta_t^N$, so $J(\theta_t^M) = J(\theta_t^N)$, and $\nabla J(\theta_t^M) = \nabla J(\theta_t^N)$. Then

$$\begin{aligned} J(\theta_{t+1}^N) &\geq J(\theta_{t+1}^M), \text{ if } \sigma_{\min}(G(\theta_t^N)) \leq 1, \text{ and} \\ J(\theta_{t+1}^N) &\leq J(\theta_{t+1}^M), \text{ if } \sigma_{\max}(G(\theta_t^N)) \geq 1, \end{aligned} \quad (28)$$

where $\sigma_{\max}(G(\theta_t^N))$, and $\sigma_{\min}(G(\theta_t^N))$ are the maximum and the minimum singular values of the Fisher information matrix $G(\theta_t^N)$ respectively.

Moreover, if the sequences $\{\sigma_{\min}(G(\theta_t^N))\}_{t \geq 0}$ and $\{\sigma_{\max}(G(\theta_t^N))\}_{t \geq 0}$ are monotonically decreasing, then

$$\begin{aligned} J(\theta^{N^*}) &\geq J(\theta^{M^*}), \text{ if } \sigma_{\min}(G(\theta^{N^*})) \leq 1, \\ J(\theta^{N^*}) &\leq J(\theta^{M^*}), \text{ if } \sigma_{\max}(G(\theta^{N^*})) \geq 1, \end{aligned} \quad (29)$$

where θ^{N^*} and θ^{M^*} are the limiting points of the actor parameters in the FI-MAN and MAAC algorithms respectively, and $\sigma_{\min}(G(\theta^{N^*}))$ and $\sigma_{\max}(G(\theta^{N^*}))$ are the smallest and the largest singular values of the limiting Fisher information matrix respectively.

Proof. Consider the difference $J(\theta_{t+1}^M) - J(\theta_{t+1}^N)$ and apply the Taylor expansion

$$\begin{aligned} &= (J(\theta_t^M) - J(\theta_t^N)) + \Delta\theta_t^{M^\top} \nabla J(\theta_t^M) - \Delta\theta_t^{N^\top} \tilde{\nabla} J(\theta_t^N) + o(\|\Delta\theta_t^M\|^2) - o(\|\Delta\theta_t^N\|^2) \\ &\stackrel{(i)}{=} \Delta\theta_t^{M^\top} \nabla J(\theta_t^M) - \Delta\theta_t^{N^\top} G(\theta_t^N)^{-1} \nabla J(\theta_t^N) + o(\|\Delta\theta_t^M\|^2) - o(\|\Delta\theta_t^N\|^2) \\ &\stackrel{(ii)}{=} ((\theta_{t+1}^M - \theta_t^M)^\top - (\theta_{t+1}^N - \theta_t^N)^\top G(\theta_t^N)^{-1}) \nabla J(\theta_t^N) + o(\|\Delta\theta_t^M\|^2) - o(\|\Delta\theta_t^N\|^2) \\ &\stackrel{(iii)}{=} \beta_{\theta_t^M} \nabla J(\theta_t^M)^\top \nabla J(\theta_t^M) - \beta_{\theta_t^N} (G(\theta_t^N)^{-1} \nabla J(\theta_t^N))^\top (G(\theta_t^N)^{-1} \nabla J(\theta_t^N)) + o(\|\Delta\theta_t^M\|^2) - o(\|\Delta\theta_t^N\|^2) \\ &\stackrel{(iv)}{=} \beta_{\theta_t^N} (\|\nabla J(\theta_t^N)\|^2 - \|G(\theta_t^N)^{-1} \nabla J(\theta_t^N)\|^2) + o(\|\Delta\theta_t^M\|^2) - o(\|\Delta\theta_t^N\|^2), \end{aligned} \quad (30)$$

where (i) follows because $J(\theta_t^M) = J(\theta_t^N)$, and $\tilde{\nabla} J(\theta_t^N) = G(\theta_t^N)^{-1} \nabla J(\theta_t^N)$. (ii) uses the fact that $\Delta\theta_t^M = \theta_{t+1}^M - \theta_t^M$; $\Delta\theta_t^N = \theta_{t+1}^N - \theta_t^N$, and $\nabla J(\theta_t^M) = \nabla J(\theta_t^N)$. (iii) is the consequence of actor updates in MAAC and FI-MAN algorithms. Finally, (iv) follows from the fact that for any $t \geq 0$, $\beta_{\theta_t^M} = \beta_{\theta_t^N}$.

From the above Equation (30), and using the fact that for any matrix \mathbf{A} , and a vector \mathbf{v} , we have $\|\mathbf{A}\mathbf{v}\| \leq \|\mathbf{A}\| \|\mathbf{v}\| = \sqrt{\sigma_{\max}(\mathbf{A})} \|\mathbf{v}\|$, therefore,

$$J(\theta_{t+1}^M) - J(\theta_{t+1}^N) \geq \beta_{\theta_t^N} \left(1 - \frac{1}{\sigma_{\max}(G(\theta_t^N))}\right) \|\nabla J(\theta_t^N)\|^2 + o(\|\Delta\theta_t^M\|^2) - o(\|\Delta\theta_t^N\|^2). \quad (31)$$

Ignoring the higher order terms in Equation (31) we have,

$$\begin{aligned} J(\theta_{t+1}^M) - J(\theta_{t+1}^N) &\geq \beta_{\theta_t^N} \left(1 - \frac{1}{\sigma_{\max}(G(\theta_t^N))}\right) \|\nabla J(\theta_t^N)\|^2 \\ &\geq 0 \text{ if } \sigma_{\max}(G(\theta_t^N)) \geq 1. \end{aligned}$$

Again from Equation (30) and using the fact that $\|\mathbf{A}\mathbf{v}\| \geq \sigma_{\min}(\mathbf{A}) \|\mathbf{v}\|$, we have

$$J(\theta_{t+1}^M) - J(\theta_{t+1}^N) \leq \beta_{\theta_t^N} \left(1 - \frac{1}{\sigma_{\min}^2(G(\theta_t^N))}\right) \|\nabla J(\theta_t^N)\|^2 + o(\|\Delta\theta_t^M\|^2) - o(\|\Delta\theta_t^N\|^2) \quad (32)$$

Ignoring the higher order terms in the Equation (32) we have,

$$\begin{aligned} J(\theta_{t+1}^M) - J(\theta_{t+1}^N) &\leq \beta_{\theta_t^N} \left(1 - \frac{1}{\sigma_{\min}^2(G(\theta_t^N))}\right) \|\nabla J(\theta_t^N)\|^2 \\ &\leq 0 \text{ if } \sigma_{\min}(G(\theta_t^N)) \leq 1. \end{aligned}$$

This ends the proof of the first part, i.e.,

$$\begin{aligned} J(\theta_{t+1}^N) &\geq J(\theta_{t+1}^M), \text{ if } \sigma_{\min}(G(\theta_t^N)) \leq 1, \text{ and} \\ J(\theta_{t+1}^N) &\leq J(\theta_{t+1}^M), \text{ if } \sigma_{\max}(G(\theta_t^N)) \geq 1. \end{aligned} \quad (33)$$

Next, take $t \rightarrow \infty$ in above equations we have

$$\begin{aligned} \lim_{t \rightarrow \infty} J(\theta_{t+1}^N) &\geq \lim_{t \rightarrow \infty} J(\theta_{t+1}^M), \text{ if } \lim_{t \rightarrow \infty} \sigma_{\min}(G(\theta_t^N)) \leq 1, \text{ and} \\ \lim_{t \rightarrow \infty} J(\theta_{t+1}^N) &\leq \lim_{t \rightarrow \infty} J(\theta_{t+1}^M), \text{ if } \lim_{t \rightarrow \infty} \sigma_{\max}(G(\theta_t^N)) \geq 1. \end{aligned}$$

We now argue that above limits indeed exist. To this end, recall that the singular values of any matrix (or the eigenvalues in case of symmetric matrices) are the continuous function of the entries of the matrix [Zedek, 1965]. Therefore, from the assumption that $\{\sigma_{\min}(G(\theta_t^N))\}_{t \geq 0}$ and $\{\sigma_{\max}(G(\theta_t^N))\}_{t \geq 0}$ are monotonically decreasing sequences, and noting that, $\sigma_{\min}(G(\theta_t^N)) > 0$, $\forall t \geq 0$ (as $G(\theta_t^N)$ is a positive definite matrix for all $t \geq 0$), and from Equation

(33), $\sigma_{\max}(G(\theta_t^N)) \geq 1$, $\forall t \geq 0$, we have $\lim_{t \rightarrow \infty} \sigma_{\min}(G(\theta_t^N)) \leq 1$ and $\lim_{t \rightarrow \infty} \sigma_{\max}(G(\theta_t^N)) \geq 1$. Moreover, $\lim_{t \rightarrow \infty} J(\theta_{t+1}^N)$ and $\lim_{t \rightarrow \infty} J(\theta_{t+1}^M)$ will exist from the convergence analysis of the algorithms available in Section 4. Therefore, we have

$$\begin{aligned} J(\theta^{N^*}) &\geq J(\theta^{M^*}), \text{ if } \sigma_{\min}(G(\theta^{N^*})) \leq 1, \\ J(\theta^{N^*}) &\leq J(\theta^{M^*}), \text{ if } \sigma_{\max}(G(\theta^{N^*})) \geq 1. \end{aligned}$$

□

□

Note that $\forall t \geq 0$, $G(\theta_t^N)$ is a symmetric matrix and hence $\sigma(G(\theta_t^N)) = \lambda^2(G(\theta_t^N))$, where $\lambda(G(\theta_t^N))$ is the eigenvalue of matrix $G(\theta_t^N)$. Thus, Equations (28) and (29) can equivalently be stated in terms of maximum and minimum eigenvalues of $G(\theta_t^N)$.

Remark 3. Note that the requirements for the Theorem to hold are not hard to satisfy. For instance at $t = 0$ we have $\theta_0^M = \theta_0^N = 0$, and hence $J(\theta_0^M) = J(\theta_0^N)$, and $\nabla J(\theta_0^M) = \nabla J(\theta_0^N)$. Moreover, we observe in the computational experiments in Sections 5.1 and 5.2 that $\{\sigma_{\min}(G(\theta_t^N))\}_{t \geq 0}$ and $\{\sigma_{\max}(G(\theta_t^N))\}_{t \geq 0}$ are indeed monotonically decreasing sequences.

Remark 4. The sufficient conditions that the sequences $\{\sigma_{\min}(G(\theta_t^N))\}_{t \geq 0}$ and $\{\sigma_{\max}(G(\theta_t^N))\}_{t \geq 0}$ are monotonically decreasing sequences can also be replaced by $\sigma_{\min}(G(\theta_t^N)) \leq 1$, $\forall t \geq 0$, and $\sigma_{\max}(G(\theta_t^N)) \geq 1$, $\forall t \geq 0$. However, we may need some extra conditions for existence of the limits.

Theorem 3 suffices that the FIAP-MAN algorithm also finds a better local optimum than MAAC and AP-MAN algorithms provided $\lambda_{\min}(G(\theta_t^N)) \leq 1$, $\forall t$. In fact, in our experiments in Section 5 we observe that $\lambda_{\max}(G(\theta_t^N)) < 1$ and hence second case in Theorem 3 does not arise. Thus, the FI-MAN or FIAP-MAN are at least as good as AP-MAN or MAAC algorithms. We illustrate these aspects in the RL tasks of reducing congestion in a traffic network in Section 5.1 and the abstract MARL model in Section 5.2.

Remark 5. Though the Fisher information matrix captures the curvature of the KL divergence between the policies parameterized at consecutive iterates, the MAN algorithms may not be regarded as second-order methods. It is because the Fisher information matrix is not the Hessian of the ‘objective function’ $J(\cdot)$. However, being the curvature of the KL divergence, we observe a period to period improvement in the objective function if the maximum eigenvalue of the Fisher matrix is less than 1, which holds in our experiments in Section 5.

In the next subsection, we will highlight some consequences of using the Boltzmann policy.

3.5 KL divergence based natural gradients for Boltzmann policy

One specific policy that is often used in RL literature is the Boltzmann policy [Doan et al., 2021]. Recall, the parameterized Boltzmann policy is given as

$$\pi_{\theta_t}(s, a) = \frac{\exp(q_{s,a}^\top \theta_t)}{\sum_{b \in \mathcal{A}} \exp(q_{s,b}^\top \theta_t)}, \quad (34)$$

where $q_{s,a}^\top$ is the feature for any (s, a) .

Lemma 1. For the Boltzmann policy as given in Equation (34) the KL divergence between policy parameterized by θ_t and $\theta_t + \Delta\theta$ is given by

$$KL(\pi_{\theta_t}(s, a) || \pi_{\theta_t + \Delta\theta}(s, a)) = \mathbb{E} \left[\log \left(\sum_{b \in \mathcal{A}} \pi_{\theta_t}(s, b) \exp(\Delta q_{s,ba}^\top \Delta\theta) \right) \right], \quad (35)$$

where $\Delta q_{s,ba}^\top = q_{s,b}^\top - q_{s,a}^\top$.

The proof of this lemma is deferred to Appendix A.2. The above KL divergence represents that we have a non-zero curvature if the action taken is better than the averaged action. From above equation we also observe that $\exp(\Delta q_{s,ba}^\top \Delta\theta) \neq 1$ if and only if $\Delta q_{s,ba}$ is orthogonal to $\Delta\theta$. So, except when they are orthogonal, $\log(\sum_{b \in \mathcal{A}} \pi_{\theta_t}(s, b) \cdot \exp(\Delta q_{s,ba}^\top \Delta\theta)) \neq 0$ as $\sum_{b \in \mathcal{A}} \pi_{\theta_t}(s, b) = 1$. Thus, the curvature is non-zero, large or smaller depends on the direction $\Delta\theta$ makes with that of feature difference $q_{s,b}^\top - q_{s,a}^\top$; if the angle is zero, it is better.

Next lemma provide the derivative of KL divergence between policy π_{θ_t} , and $\pi_{\theta_t + \Delta\theta}$.

Lemma 2. For the Boltzmann policy as given in Equation (34) we have

$$\nabla KL(\pi_{\theta_t}(\cdot, \cdot) || \pi_{\theta_t + \Delta\theta}(\cdot, \cdot)) = -\mathbb{E}[\nabla \log \pi_{\theta_t + \Delta\theta}(s, a)]. \quad (36)$$

Proof of this lemma is available in Appendix A.3. Recall, Equation (13) provides the approximate derivative of KL divergence based on second order Taylor approximation of the objective function as

$$\nabla KL(\pi_{\theta_t}(\cdot, \cdot) || \pi_{\theta_t + \Delta\theta}(\cdot, \cdot)) \approx G(\theta_t) \Delta\theta. \quad (37)$$

Thus, from Equations (15), (36), and (37), for Boltzmann policies we have

$$\nabla KL(\pi_{\theta_t}(\cdot, \cdot) || \pi_{\theta_t + \Delta\theta}(\cdot, \cdot)) \approx G(\theta_t) \Delta\theta = -\mathbb{E}[\nabla \log \pi_{\theta_t + \Delta\theta}(s, a)] = -\frac{1}{\mu_t} \nabla J(\theta_t), \quad (38)$$

i.e., $\nabla \log \pi_{\theta_t + \Delta\theta} = \psi_{\theta_{t+1}}$ is an unbiased estimate of $\nabla J(\theta_t)$ upto scaling of μ_t for the Boltzmann policies. Also, from Equation (9) we have $\delta_t \psi_t$ as a biased estimate of $\nabla J(\theta_t)$, implying that the Boltzmann policies can have better estimate of $\nabla J(\theta_t)$. Using $\psi_{\theta_{t+1}}$ in the actor update of MAAC we have,

$$\theta_{t+1} = \theta_t + \beta_{\theta,t} \psi_{\theta_t + \Delta\theta} = \theta_t + \beta_{\theta,t} \psi_{\theta_{t+1}},$$

which is a fixed point equation in θ_{t+1} ; might be theoretically helpful, but not implementable, because θ_{t+1} itself requires $\psi_{\theta_{t+1}}$. Thus, in our computations we stick to the biased estimate, i.e., $\delta_t \psi_t$. Similarly, for the FI-MAN algorithm, we have a fixed point equation as

$$\theta_{t+1} = \theta_t + \beta_{\theta,t} G_t^{-1} \psi_{\theta_{t+1}},$$

which is again theoretically sound, but for the same reason, it is not implementable. However, similar to Equation (16), we again have Equation (38) relating the gradient of the objective function to the gradient of KL divergence between the policies separated by $\Delta\theta$ which renders actor updates in the prediction space. In other words, these algorithms use the *representation* of the gradient of the objective function given by Equation (38) in the prediction space of the policy distributions.

We now prove the convergence of FI-MAN, AP-MAN, and FIAP-MAN algorithms. The proofs majorly use the idea of two-time scale stochastic approximations from [Borkar, 2009, Bhatnagar et al., 2009].

4 Convergence analysis

In this section, we will provide the convergence proofs of the 3 MAN algorithms. We need the following assumptions on the features $\varphi(s)$ of the value function, and $f(s, a)$ of the rewards for any $s \in \mathcal{S}, a \in \mathcal{A}$. This assumption is similar to [Zhang et al., 2018], and also used in the convergence proof for single-agent natural actor-critic [Bhatnagar et al., 2009].

A. 3. *The feature vectors $\varphi(s)$, and $f(s, a)$ associated with the value function and the reward function are uniformly bounded for any $s \in \mathcal{S}, a \in \mathcal{A}$. Moreover, let the feature matrix $\Phi \in \mathbb{R}^{|\mathcal{S}| \times L}$ have $[\varphi_l(s), s \in \mathcal{S}]^\top$ as its l -th column for any $l \in [L]$, and feature matrix $F \in \mathbb{R}^{|\mathcal{S}| \times M}$ have $[f_m(s, a), s \in \mathcal{S}, a \in \mathcal{A}]^\top$ as its m -th column for any $m \in [M]$, then Φ and F have full column rank, and for any $\omega \in \mathbb{R}^L, \Phi\omega \neq \mathbb{1}$.*

Apart from the above assumption A. 3, let $D_\theta^s = [d_\theta(s), s \in \mathcal{S}]$, and $\bar{R}_\theta = [\bar{R}_\theta(s), s \in \mathcal{S}]^\top \in \mathbb{R}^{|\mathcal{S}|}$ with $\bar{R}_\theta(s) = \sum_a \pi_\theta(s, a) \cdot \bar{R}(s, a)$. Define the operator $T_\theta^V : \mathbb{R}^{|\mathcal{S}|} \rightarrow \mathbb{R}^{|\mathcal{S}|}$ for any state value vector $V \in \mathbb{R}^{|\mathcal{S}|}$ as,

$$T_\theta^V(V) = \bar{R}_\theta - J(\theta) \mathbb{1} + P^\theta V.$$

The proofs of all 3 MAN algorithms are done in two steps: (a) convergence of the estimate of the objective function and the critic update keeping the actor parameters θ^i fixed for all the agents $i \in N$, and (b) convergence of actor parameters to an asymptotically stable equilibrium of the ODE corresponding to the actor update. To this end, we require the following assumption on Fisher information matrix G_t^i and its inverse G_t^{i-1} . This assumption is used by [Bhatnagar et al., 2009] in the case of single-agent natural actor-critic algorithms, here we have suitably modified it for multi-agent setup.

A. 4. *For each agent $i \in N$, the recursions of the Fisher information matrix G_t^i , and its inverse G_t^{i-1} as given in Equations (18) and (19) respectively satisfy the following*

$$\sup_{t, \theta^i, s, a^i} \|G_t^i\| < \infty; \quad \sup_{t, \theta^i, s, a^i} \|G_t^{i-1}\| < \infty.$$

Assumption A. 4 ensures that the FI-MAN algorithm and FIAP-MAN actor-critic algorithm does not stuck in the non-stationary point. A sufficient condition for both requirements of assumption A. 4 is following: for each agent $i \in N$, for some scalars $c_1^i, c_2^i > 0$,

$$c_1^i \|x^i\|^2 \leq x^{i\top} \psi_{s, a^i}^i \psi_{s, a^i}^{i\top} x^i \leq c_2^i \|x^i\|^2, \quad \forall s \in \mathcal{S}, a^i \in \mathcal{A}^i, x^i \in \mathbb{R}^K, \text{ and } \theta^i \in \mathbb{R}^{m_i}.$$

Therefore, for each agent $i \in N$ we have

$$\bar{c}_1^i \|x^i\|^2 \leq x^{i\top} G_t^i x^i \leq \bar{c}_2^i \|x^i\|^2, \quad \forall t \geq 0,$$

and the eigenvalues of G_t^i lie between some positive scalars \bar{c}_1^i , and \bar{c}_2^i . Since, $\bar{c}_1^i, \bar{c}_2^i > 0 \quad \forall i \in N$, thus from the Propositions A.9 and A.15 of [Bertsekas, 1997] the algorithms will not stuck at non-stationary points. Moreover, recall Equation (18), and using stochastic approximation technique we know that G_t^i will converge asymptotically to $G(\theta^i)$ almost surely if θ^i is held fixed (this is easy to verify by comparing it with the stochastic approximation scheme given in [Borkar, 2009]).

To ensure the existence of local optima of $J(\theta)$ we make the following assumptions on policy parameters θ_t^i for each agent $i \in N$.

A. 5. *The policy parameters θ_t^i update includes a projection operator $\Gamma^i : \mathbb{R}^{m_i} \rightarrow \Theta^i \subset \mathbb{R}^{m_i}$, that projects any θ_t^i onto a compact set Θ^i . Moreover, $\Theta = \prod_{i=1}^n \Theta^i$ is large enough to include at least one local minimum of $J(\theta)$.*

For each agent $i \in N$, let $\hat{\Gamma}^i$ is the transformed projection operator defined for any $\theta \in \Theta$ with $h : \Theta \rightarrow \mathbb{R}^{\sum_{i \in N} m_i}$ being a continuous function as follows:

$$\hat{\Gamma}^i(h(\theta)) = \lim_{0 < \eta \rightarrow 0} \frac{\Gamma^i(\theta^i + \eta h(\theta)) - \theta^i}{\eta}. \quad (39)$$

If the above limit is not unique, $\hat{\Gamma}^i(h(\theta))$ denotes the set of all possible limit points of Equation (39). The above projection operator is used to prove the convergence of the policy parameters. It is an often-used technique to ensure boundedness of iterates in stochastic approximation algorithms. However, in computations, we do not require a projection operator because the iterates remain bounded.

We begin by proving the convergence of the critic updates given in Equations (5), (6), and (7). The following theorem will be common in the proof of all the 3 MAN algorithms.

Theorem 4. *Under assumptions A. 1, A. 2, and A. 3, for any policy π_θ , with sequences $\{\lambda_t^i\}, \{\mu_t^i\}, \{v_t^i\}$ generated from critic updates, we have $\lim_t \mu_t^i = J(\theta)$, $\lim_t \lambda_t^i = \lambda_\theta$, and $\lim_t v_t^i = v_\theta$ a.s. for any agent $i \in N$, where $J(\theta)$, λ_θ , and v_θ are unique solutions to*

$$\begin{aligned} F^\top D_{\theta^s}^{s,a} (\bar{R} - F\lambda_\theta) &= 0, \\ \Phi^\top D_{\theta^s}^s [T_{\theta^V}^V (\Phi v_\theta) - \Phi v_\theta] &= 0. \end{aligned}$$

Proof of this theorem follows from [Zhang et al., 2018]. For the sake of completeness, we briefly present the proof in Appendix A.1.

4.1 Convergence of FI-MAN actor-critic algorithm

To prove the convergence of FI-MAN algorithm we will first show the convergence of recursion for the Fisher information matrix inverse as given in Equation (19).

Theorem 5. *For each agent $i \in N$, and any given parameter θ^i , G_t^{i-1} , $t \geq 1$, as given in Equation (19), we have $G_t^{i-1} \rightarrow G(\theta^i)^{-1}$ as $t \rightarrow \infty$ with probability one.*

Proof. Consider the following $\forall i \in N$,

$$\begin{aligned} \|G_t^{i-1} - G(\theta^i)^{-1}\| &= \|G(\theta^i)^{-1} G(\theta^i) G_t^{i-1} - G(\theta^i)^{-1} G_t^i G_t^{i-1}\| \\ &= \|G(\theta^i)^{-1} (G(\theta^i) - G_t^i) G_t^{i-1}\| \\ &\leq \sup_{\theta^i} \|G(\theta^i)^{-1}\| \sup_{t,s,a^i} \|G_t^{i-1}\| \|G(\theta^i) - G_t^i\| \\ &\rightarrow 0 \text{ as } t \rightarrow \infty. \end{aligned}$$

The inequality above follows from the induced matrix norm property and assumption A. 4. \square \square

To prove the convergence of the actor update we can view $-r_{t+1}^i$ as the cost incurred at time t . Hence we can transform the problem by considering the cost functions instead of reward functions. Because of the above, the actor recursion is

$$\theta_{t+1}^i \leftarrow \theta_t^i - \beta_{\theta,t} \cdot G_t^{i-1} \cdot \tilde{\delta}_t^i \cdot \psi_t^i.$$

The convergence of the FI-MAN actor-critic algorithm with linear function approximation is given in the following theorem.

Theorem 6. Under the assumptions A. 1 - A. 5, the sequence $\{\theta_t^i\}_{t \geq 0}$ obtained from the actor step of the FI-MAN algorithm converges almost surely to a point in a set of asymptotically stable equilibrium of the ODE

$$\dot{\theta}^i = \hat{\Gamma}^i[-G(\theta^i)^{-1}\mathbb{E}_{s_t \sim d_{\theta}, a_t \sim \pi_{\theta}}(\tilde{\delta}_{t,\theta}^i \psi_t^i)], \quad \forall i \in N. \quad (40)$$

Proof. Let $\mathcal{F}_{t,1} = \sigma(\theta_\tau, \tau \leq t)$ be the σ -field generated by $\{\theta_\tau\}_{\tau \leq t}$. Let

$$\begin{aligned} \xi_{t+1,1}^i &= -G(\theta_t^i)^{-1} \left\{ \tilde{\delta}_t^i \psi_t^i - \mathbb{E}_{s_t \sim d_{\theta_t}, a_t \sim \pi_{\theta_t}}(\tilde{\delta}_t^i \psi_t^i | \mathcal{F}_{t,1}) \right\} \\ \xi_{t+1,2}^i &= -G(\theta_t^i)^{-1} \mathbb{E}_{s_t \sim d_{\theta_t}, a_t \sim \pi_{\theta_t}}((\tilde{\delta}_t^i - \tilde{\delta}_{t,\theta_t}^i) \psi_t^i | \mathcal{F}_{t,1}) \end{aligned}$$

where $\tilde{\delta}_{t,\theta_t}^i$ is defined as

$$\tilde{\delta}_{t,\theta_t}^i = f_t^\top \lambda_{\theta_t} - J(\theta_t) + \varphi_{t+1}^\top v_{\theta_t} - \varphi_t^\top v_{\theta_t}.$$

The actor update in the FI-MAN algorithm with local projection then becomes,

$$\theta_{t+1}^i = \Gamma^i[\theta_t^i - \beta_{\theta,t} G(\theta_t^i)^{-1} \mathbb{E}_{s_t \sim d_{\theta_t}, a_t \sim \pi_{\theta_t}}(\tilde{\delta}_t^i \psi_t^i | \mathcal{F}_{t,1}) + \beta_{\theta,t} \xi_{t+1,1}^i + \beta_{\theta,t} \xi_{t+1,2}^i]. \quad (41)$$

Note that $\xi_{t+1,2}^i = o(1)$ since critic converges at the faster time scale, i.e., $\tilde{\delta}_t^i \rightarrow \tilde{\delta}_{t,\theta_t}^i$. Moreover, let $M_t^{1,i} = \sum_{\tau=0}^t \beta_{\theta,\tau} \xi_{\tau+1,1}^i$, then $\{M_t^{1,i}\}$ is a martingale sequence. The sequences $\{z_t^i\}$, $\{\psi_t^i\}$, $\{G_t^{i-1}\}$, and $\{\varphi_t^i\}$ are all bounded (by assumptions), and so is the sequence $\{\xi_{t,1}^i\}$ (Here $z_t^i = [\mu_t^i, (\lambda_t^i)^\top, (v_t^i)^\top]^\top$ is similar to the vector used in the proof of Theorem 4). Hence, we have $\sum_t \mathbb{E}[|M_{t+1}^{1,i} - M_t^{1,i}|^2 | \mathcal{F}_{t,1}] < \infty$ a.s., and the martingale sequence $\{M_t^{1,i}\}$ converges a.s. [Neveu, 1975]. Thus assumption 4 in A. 6 (given in Appendix C.2) is satisfied. Hence for any $\epsilon > 0$, we have $\lim_{t \rightarrow \infty} \mathbb{P}[\sup_{p \geq t} |\sum_{\tau=t}^p \beta_{\theta,\tau} \xi_{\tau+1,1}^i| \geq \epsilon] = 0$.

We now argue that $g^{1,i}(\theta_t) = -G(\theta_t^i)^{-1} \mathbb{E}_{s_t \sim d_{\theta_t}, a_t \sim \pi_{\theta_t}}(\tilde{\delta}_t^i \psi_t^i | \mathcal{F}_{t,1})$ is continuous in θ_t^i . To see this, note that

$$\begin{aligned} g^{1,i}(\theta_t) &= -G(\theta_t^i)^{-1} \mathbb{E}_{s_t \sim d_{\theta_t}, a_t \sim \pi_{\theta_t}}(\tilde{\delta}_t^i \psi_t^i | \mathcal{F}_{t,1}) \\ &= -G(\theta_t^i)^{-1} \sum_{s_t \in \mathcal{S}, a_t \in \mathcal{A}} d_{\theta_t}(s_t) \cdot \pi_{\theta_t}(s_t, a_t) \cdot \tilde{\delta}_{t,\theta_t}^i \cdot \psi_{t,\theta_t}^i. \end{aligned}$$

Firstly, ψ_{t,θ_t}^i is continuous by assumption A. 1. The term $d_{\theta_t}(s_t) \cdot \pi_{\theta_t}(s_t, a_t)$ is continuous in θ_t^i since it is the stationary distribution and solution to $d_{\theta_t}(s) \cdot \pi_{\theta_t}(s, a) = \sum_{s' \in \mathcal{S}, a' \in \mathcal{A}} P^{\theta_t}(s', a' | s, a) \cdot d_{\theta_t}(s') \cdot \pi_{\theta_t}(s', a')$ and $\sum_{s \in \mathcal{S}, a \in \mathcal{A}} d_{\theta_t}(s) \cdot \pi_{\theta_t}(s, a) = 1$, where $P^{\theta_t}(s', a' | s, a) = P(s' | s, a) \cdot \pi_{\theta_t}(s', a')$. The unique solution to this set of linear equations can be verified to be continuous in θ_t , noting that $\pi_{\theta_t}(s, a) > 0$ by assumption A. 1. Moreover, $\tilde{\delta}_{t,\theta_t}^i$ is continuous in θ_t^i since v_{θ_t} is the unique solution to the linear equation $\Phi^\top D_\theta^s [T_\theta^V(\Phi v_\theta) - \Phi v_\theta] = 0$ and can be verified to be continuous in θ_t . Thus it concludes that $g^{1,i}(\theta_t)$ is continuous in θ_t^i .

Now using Kushner-Clark lemma (see appendix C.2) the update in Equation (41) converges a.s to the set of asymptotically stable equilibria of ODE Equation (40) for each $i \in N$. This concludes the proof. \square \square

Next, we provide the convergence of the AP-MAN algorithm. Recall, AP-MAN does not use the estimate of the Fisher information inverse; instead, it uses the linear function approximation of the advantage parameters.

4.2 Convergence of AP-MAN actor-critic algorithm

The convergence of critic step, the reward parameters and the estimate of the objective function are the same as in Theorem 4. Thus, we will focus on the convergence of the advantage parameters and the actor updates as given in the AP-MAN algorithm. Similar to the FI-MAN algorithm we again consider the transformed problem; rewards replaced with costs. This transformation, however, only affects the recursion given in Equation (22). Thus the transformed recursion can be written as

$$w_{t+1}^i \leftarrow (I - \beta_{v,t} \psi_t^i \psi_t^{i\top}) w_t^i - \beta_{v,t} \tilde{\delta}_{t,\theta}^i \psi_t^i. \quad (42)$$

Theorem 7. For each agent $i \in N$, under a given parameter θ^i , the w_t^i , $t \geq 0$ satisfy $w_t^i \rightarrow -G(\theta^i)^{-1} \mathbb{E}[\tilde{\delta}_{t,\theta}^i \psi_t^i]$ as $t \rightarrow \infty$ with probability one.

Proof. For each $i \in N$, the ODE associated with the recursion in Equation (42) for given θ is

$$\dot{w}^i = \mathbb{E}_{s_t \sim d_\theta, a_t \sim \pi_\theta} [-\psi_t^i \psi_t^{i\top} w^i - \tilde{\delta}_{t,\theta}^i \psi_t^i] := g^{2,i}(w^i) \quad (43)$$

It is easy to see that $g^{2,i}(w^i)$ is Lipschitz continuous in w^i . Let $g_{\infty}^{2,i}(w^i) = \lim_{r \rightarrow \infty} \frac{g^{2,i}(rw^i)}{r}$. Note that $g_{\infty}^{2,i}(w^i)$ exists and satisfy $g_{\infty}^{2,i}(w^i) = -G(\theta^i)w^i$. For the ODE $\dot{w}^i = -G(\theta^i)w^i$ the origin is an asymptotically stable equilibrium with $V_1(w^i) = w^{i\top} w^i / 2$ as the associated Lyapunov function (since $G(\theta^i)$ is positive definite). Now define a sequence $\{M_t^{2,i}\}$ as $M_t^{2,i} = \hat{g}^{2,i}(w_t^i) - \mathbb{E}[\hat{g}^{2,i}(w_t^i) | \mathcal{F}_{t,2}]$, where $\hat{g}^{2,i}(w_t^i) = -\psi_t^i \psi_t^{i\top} w^i - \tilde{\delta}_t^i \psi_t^i$ and $\mathcal{F}_{t,2} = \sigma(w_r^i, M_r^{2,i}, r \leq t)$. Note that $\{M_t^{2,i}\}$ is the martingale difference sequence. Thus there exists a constant $C_0 < \infty$ such that

$$\mathbb{E}[\|M_{t+1}^{2,i}\|^2 | \mathcal{F}_{2,t}] \leq C_0(1 + \|w_t^i\|^2) \quad \forall t \geq 0.$$

For the ODE given in Equation (43) consider the function $V_2(w^i)$ defined by

$$V_2(w^i) = \frac{1}{2}(w^i + G(\theta^i)^{-1}\mathbb{E}[\tilde{\delta}_{t,\theta}^i \psi_t^i])^\top (w^i + G(\theta^i)^{-1}\mathbb{E}[\tilde{\delta}_{t,\theta}^i \psi_t^i]).$$

Since $G(\theta^i)^{-1}$ is a positive definite, we have

$$\begin{aligned} \frac{dV_2(w^i)}{dt} &= \nabla V_2(w^i)^\top \dot{w}^i \\ &= -(w^i + G(\theta^i)^{-1}\mathbb{E}[\tilde{\delta}_{t,\theta}^i \psi_t^i])^\top (G(\theta^i)w^i + \mathbb{E}[\tilde{\delta}_{t,\theta}^i \psi_t^i]) \\ &= -(w^i + G(\theta^i)^{-1}\mathbb{E}[\tilde{\delta}_{t,\theta}^i \psi_t^i])^\top G(\theta^i) (w^i + G(\theta^i)^{-1}\mathbb{E}[\tilde{\delta}_{t,\theta}^i \psi_t^i]) \\ &< 0 \quad \forall w^i \neq -G(\theta^i)^{-1}\mathbb{E}[\tilde{\delta}_{t,\theta}^i \psi_t^i]. \end{aligned}$$

Thus $w(\theta^i) = -G(\theta^i)^{-1}\mathbb{E}[\tilde{\delta}_{t,\theta}^i \psi_t^i]$ is an asymptotically stable equilibrium solution for the ODE given in Equation (43). Now, from the Theorem 2.2 of [Borkar and Meyn, 2000] recursion (42) converges to $w(\theta^i)$ with probability one. \square

We now consider the convergence of the AP-MAN algorithm.

Theorem 8. *Under the assumptions A. 1 - A. 5, the sequence $\{\theta_t^i\}$ obtained from the actor step of the AP-MAN algorithm converges a.s. to a point in a set of asymptotically stable equilibrium of*

$$\dot{\theta}^i = \hat{\Gamma}^i[-G(\theta^i)^{-1}\mathbb{E}_{s_t \sim d_{\theta^i}, a_t \sim \pi_{\theta^i}}(\tilde{\delta}_{t,\theta}^i \psi_t^i)], \quad \forall i \in N. \quad (44)$$

Proof. Let $\mathcal{F}_{t,3} = \sigma(\theta_\tau, \tau \leq t)$ be the sigma field generated by $\{\theta_\tau\}_{\tau \leq t}$. The actor update in the AP-MAN algorithm with local projection becomes

$$\theta_{t+1}^i = \Gamma^i[\theta_t^i - \beta_{\theta,t}\mathbb{E}_{s_t \sim d_{\theta_t}, a_t \sim \pi_{\theta_t}}(G(\theta_t^i)^{-1}\tilde{\delta}_t^i \psi_t^i | \theta_t^i) + \beta_{\theta,t}\xi_{t+1,3}^i].$$

Note that $\xi_{t+1,3}^i = o(1)$ since critic converges at the faster time scale. The rest of the proof follows as that of Theorem 6. \square

4.3 Convergence of FIAP-MAN actor-critic algorithm

The critic convergence, the convergence of reward parameters, and the estimate of the objective function are the same as in Theorem 4 thus, we will give proof for actor convergence only. Similar to FI-MAN and AP-MAN algorithms, we again consider the transformed problem; rewards replaced with costs. This transformation, however, only affects the recursion given in Equation (24). Therefore, we consider the following recursion

$$w_{t+1}^i = (1 - \beta_{v,t})w_t^i - \beta_{v,t}G_t^{i-1}\tilde{\delta}_t^i \psi_t^i. \quad (45)$$

Theorem 9. *For each agent $i \in N$, under a given parameter θ^i , the w_t^i , $t \geq 0$ given in Equation (45) satisfy $w_t^i \rightarrow -G(\theta^i)^{-1}\mathbb{E}[\tilde{\delta}_{t,\theta}^i \psi_t^i]$ as $t \rightarrow \infty$ with probability one.*

Proof. To prove this, we first note that for each $i \in N$, $\sup_{t,\theta^i,s_t,a_t} \|G_t^{i-1}\tilde{\delta}_t^i \psi_t^i\| < \infty$ with probability one. For the conditions given in Equation (10) there exists N_0 such that for all $t \geq N_0$, w_{t+1}^i is a convex combination of w_t^i and a uniformly bounded quantity, $G_t^{i-1}\tilde{\delta}_t^i \psi_t^i$. The overall sequence w_t^i of iterates, for any $w_0^i \in \mathbb{R}^{m_i}$ remains bounded with probability one. One can re-write the Equation (45) as

$$w_{t+1}^i \leftarrow (1 - \beta_{v,t})w_t^i - \beta_{v,t}G(\theta^i)^{-1}\mathbb{E}[\tilde{\delta}_{t,\theta}^i \psi_t^i | \theta^i] - M_t^{3,i} + \beta_{v,t}\xi_{t+1,4}^i + \beta_{v,t}\xi_{t+1,5}^i,$$

where $M_t^{3,i} = \beta_{v,t} G(\theta^i)^{-1} (\tilde{\delta}_t^i \psi_t^i - \mathbb{E}[\tilde{\delta}_t^i \psi_t^i | \theta^i])$, $\xi_{t+1,4}^i = (G(\theta^i)^{-1} - G_t^{i-1}) \tilde{\delta}_t^i \psi_t^i$, and $\xi_{t+1,5}^i = G(\theta^i)^{-1} \mathbb{E}[(\tilde{\delta}_t^i - \tilde{\delta}_t^i) \psi_t^i | \theta^i]$ respectively. From Theorem 4 and 5 both $\xi_{t+1,4}^i$ and $\xi_{t+1,5}^i$ are $o(1)$. It is easy to see that the sequence $\{\sum_{r=0}^{t-1} M^5(r)\}$ is a convergent martingale sequence. Let $m_T = \min\{m \geq p | \sum_{r=p}^m \beta_{v,r} \geq T\}$, then $\sum_{r=p}^{m_T} \beta_{v,r} G(\theta^i)^{-1} (\tilde{\delta}_r^i \psi_r^i - \mathbb{E}[\tilde{\delta}_r^i \psi_r^i | \theta_r^i]) \rightarrow 0$ almost surely as $p \rightarrow \infty$. Next, consider the ODE associated with Equation (45),

$$\dot{w}^i = -w^i - G(\theta^i)^{-1} \mathbb{E}[\tilde{\delta}_{t,\theta}^i \psi_t^i] := g^{3,i}(w^i) \quad (46)$$

Note that $g^{3,i}(w^i)$ is Lipschitz continuous in w^i , and hence the ODE (46) is well-posed. Let $g_\infty^3(w^i) = \lim_{r \rightarrow \infty} \frac{g^3(rw^i)}{r} = -w^i$. For the ODE $\dot{w}^i = -w^i$ the origin is unique globally asymptotically stable equilibrium with $V_3(w^i) = w^{i\top} w^i / 2$ as the associated Lyapunov function. Similar to Theorem 7 one can show that $w(\theta^i) = -G(\theta^i)^{-1} \mathbb{E}[\tilde{\delta}_{t,\theta}^i \psi_t^i]$ is an asymptotically stable attractor for the ODE given in Equation (46). The proof follows from Theorem 2.2 of [Borkar and Meyn, 2000]. \square

Theorem 10. *Under the assumptions A. 1 - A. 5 the sequence $\{\theta_t^i\}$ obtained from the actor step of the FIAP-MAN algorithm converges a.s. to a point in a set of asymptotically stable equilibrium of*

$$\dot{\theta}^i = \hat{\Gamma}^i [-G(\theta^i)^{-1} \mathbb{E}_{s_t \sim d_\theta, a_t \sim \pi_\theta} (\tilde{\delta}_{t,\theta}^i \psi_{t,\theta}^i)], \quad \forall i \in N. \quad (47)$$

The proof of the above theorem is similar to the Theorem 8. We avoid writing it because of repetition.

Remark 6. *Though the ODE corresponding to the actor update in all the 3 MAN algorithms seems similar, we want to emphasize that they come from three different algorithms, each with a different critic update. Thus all the three algorithms will attain different optimums as justified in our experiment in Section 5.1. Moreover, we also note that the optimal value obtained from FI-MAN and FIAP-MAN are close to each other, and AP-MAN and MAAC are also close. This observation is theoretically justified in Section 3.4.*

To validate the usefulness of our proposed MAN algorithms, we implement them on a bi-lane traffic network and an abstract multi-agent RL model. The detailed experiments are provided in the next section.

5 Performance of algorithms in traffic network and abstract MARL models

In this section, we provide comparative and comprehensive experiments in two different setups. Firstly, we model traffic network control as a multi-agent reinforcement learning problem. A similar model is available in [Bhatnagar, 2020] in a related but different context. Here, each traffic light is an agent, and the collective objective of these traffic lights is to minimize the average *network congestion*. Another setup that we consider is an abstract multi-agent RL model with 15 agents, 15 states, and 2 actions in each state. The model, algorithm parameters, rewards, and the features used in the linear function approximations are the same as given in [Dann et al., 2014, Zhang et al., 2018].

All the computations are done in python 3.8 on a machine equipped with 8 GB RAM and an Intel i5 processor. For the traffic network control, we use TraCI, i.e., ‘‘Traffic Control Interface’’. TraCI uses a TCP-based client/server architecture to provide access to sumo-gui² in python, thereby sumo act as a server [Krajewicz et al., 2012]. For detailed documentation on TraCI, we refer to <https://sumo.dlr.de/docs/TraCI.html>. We now describe the traffic network and the arrival processes that we consider.

5.1 Performance of algorithms for traffic network controls

Consider the bi-lane traffic network shown in Figure 1. The network consists of $N_1, N_2, S_1, S_2, E_1, E_2, W_1$, and W_2 that act as the source and the destination nodes. T_1, T_2, T_3 , and T_4 represents the traffic lights and act as agents. All the edges in the network are assumed to be of equal length. The agent’s objective is to find a traffic signaling plan such that the overall network congestion is minimized, provided the congestion to each traffic light is private information and hence not available to other traffic lights.

The sumo-gui requires the user to provide T , the total number of time steps the simulation needs to be performed, and N_v , the number of vehicles used in each simulation. As per the architecture of sumo-gui, vehicles arrive uniformly from the interval $\{1, 2, \dots, T\}$. Once a vehicle arrives, it has to be assigned a source and a destination node. We assign the source node to each incoming vehicle according to various distributions. Different arrival patterns can be incorporated by considering different source node assignment distributions. We use two different arrival patterns to

²The sumo-gui can be installed using: <https://www.eclipse.org/sumo/>

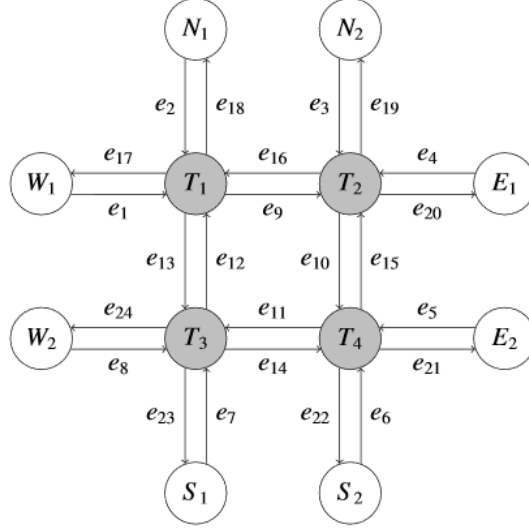


Figure 1: A bi-lane traffic network with four traffic lights T_1, T_2, T_3, T_4 . All the other nodes $N_1, N_2, S_1, S_2, E_1, E_2, W_1$, and W_2 act as the source and destination nodes.

capture high or low number of vehicles assigned to the source nodes in the network. Let $p_{s,m}$ be the probability that a vehicle is assigned a source node s if arrival pattern is m . Table 1 gives probabilities, $p_{s,m}$ for 2 arrival patterns ($m \in \{1, 2\}$) that we consider. The destination node is sampled uniformly from the nodes except the source node. We assume that vehicles follow the shortest path from the source node to the destination node. However, if there are multiple paths with the same path length, then any one of them can be chosen with uniform probability.

Source node (s)	Arrival pattern (m)	
	$m = 1$	$m = 2$
W_1	$\frac{3}{16}$	$\frac{1}{28}$
W_2	$\frac{1}{16}$	$\frac{1}{28}$
N_1	$\frac{1}{16}$	$\frac{3}{14}$
N_2	$\frac{3}{16}$	$\frac{3}{14}$
E_1	$\frac{3}{16}$	$\frac{1}{28}$
E_2	$\frac{1}{16}$	$\frac{1}{28}$
S_1	$\frac{1}{16}$	$\frac{3}{14}$
S_2	$\frac{3}{16}$	$\frac{3}{14}$

Table 1: Probability $p_{s,m}$ for all the nodes and arrival patterns. $m = 1$ assigns high probabilities to the nodes, N_2, S_2 and E_1, W_1 . $m = 2$ assigns high probabilities to all north and south nodes, N_1, S_1, N_2, S_2 and low probability to all east-west nodes, E_1, E_2, W_1, W_2 .

In arrival pattern 1, i.e., $m = 1$, we have $p_{s,m}$ higher for North-South nodes N_2, S_2 , and East-West nodes E_1, W_1 . Thus, we expect to see heavy congestion for traffic light T_2 ; almost same congestion for traffic lights T_1 and T_4 ; and the least congestion for traffic light T_3 . For the arrival pattern 2, i.e., $m = 2$ more vehicles are assigned to all the North-South nodes. So we expect that all the traffic lights will be equally congested. For completeness, we now provide the distribution of the number of vehicles assigned to a source node s at time t for a given arrival pattern m .

Let N_t is the number of vehicles arrived at time t , and N_t^s be the number of vehicles assigned to source node s at time t . Thus, $N_t = \sum_s N_t^s$. Since arrivals are uniform in $\{0, 1, \dots, T\}$, it is easy to see that N_t is a binomial random variable with parameters $(N_v, \frac{1}{T})$. Therefore, we have

$$\mathbb{P}(N_t = r) = \binom{N_v}{r} \left(\frac{1}{T}\right)^r \left(1 - \frac{1}{T}\right)^{N_v - r}, \quad \forall r = 0, 1, \dots, N_v.$$

Moreover, using the law of total probability, for all $m \in \{1, 2\}$, we obtain

$$\mathbb{P}(N_t^s = k \mid m) = \binom{N_v}{k} \left(\frac{p_{s,m}}{T}\right)^k \left(1 - \frac{p_{s,m}}{T}\right)^{N_v-k}, \quad \forall k = 0, 1, \dots, N_v, \quad (48)$$

i.e., the distribution of N_t^s for a given arrival pattern m is also binomial with parameters $(N_v, \frac{p_{s,m}}{T})$. For more details see Appendix B.2.3.

In our experiments we take simulation time $T = 180000$ seconds. The total simulation time $T = 180000$ seconds is divided into simulation cycles (called decision epoch) of $T_c = 120$ seconds each. Thus, there are 1500 decision epochs. The number of vehicles are taken as $N_v = 50000$. We now describe the decentralized MARL framework for the traffic network shown in Figure 1.

5.1.1 Decentralized framework for traffic network control

In this section, we model the above traffic network control as a fully decentralized MARL problem with traffic lights as agents, $N = \{T_1, T_2, T_3, T_4\}$. Let E_{in} denote the set of edges directed towards the traffic lights,

$$E_{in} = \{e_1, e_2, e_{12}, e_{16}, e_3, e_4, e_9, e_{15}, e_8, e_7, e_{11}, e_{13}, e_5, e_6, e_{10}, e_{14}\}.$$

We assume that the maximum capacity of each lane in the network is $C = 50$. The state space of the system consists of the number of vehicles in the lanes belonging to E_{in} . Hence, the size of the state space is 50^{16} . At every decision epoch each traffic light follows one of the following traffic signal plans for the next $T_c = 120$ simulation steps.

1. Equal green time of $\frac{T_c}{2}$ for both North-South and East-West lanes
2. $\frac{3T_c}{4}$ green time for North-South and $\frac{T_c}{4}$ green time for East-West lanes
3. $\frac{T_c}{4}$ green time for North-South and $\frac{3T_c}{4}$ green time for East-West lanes.

Thus the total number of actions available at each traffic light is $3^4 = 81$. The rewards given to each agent is equal to the negative of the average number of vehicles stopped at its corresponding traffic light. Note that the rewards are privately available to each traffic light only. We aim to maximize the expected time average of the globally averaged rewards, which is equivalent to minimize the (time average of) number of stopped vehicles in the system. Since the state space is huge (50^{16}), we will use the linear function approximation for the state value function and the reward function. The approximate state value for state s is $V(s; v) = v^\top \varphi(s)$, where $\varphi(s) \in \mathbb{R}^L$, $L \ll |\mathcal{S}|$, is the feature vector for the state s . Moreover, the reward function is approximated as $R(s, a; \lambda) = \lambda^\top f(s, a)$ where $f(s, a) \in \mathbb{R}^M$, $M \ll |\mathcal{S}||\mathcal{A}|$ are the features associated with each state-action pair (s, a) . Next, we describe the features we are using in the experiments [Bhatnagar, 2020].

Let x_t^i denote the number of vehicles in lane $e_i \in E_{in}$ at time t . We normalize x_t^i via maximum capacity of a lane, C to obtain $z_t^i = x_t^i / C$. We define $\xi(s)$ as a vector having components containing z_t^i , as well as components with products of two or three z_t^i 's. The product terms are of the form $z_t^i z_t^j$ and $z_t^i z_t^j z_t^l$ where all terms in the product correspond to the same traffic light.

$$\xi(s) = (z_t^1, z_t^2, \dots, z_t^{16}, z_t^1 z_t^2, \dots, z_t^6 z_t^5, z_t^1 z_t^2 z_t^{12}, \dots, z_t^5 z_t^6 z_t^{10})$$

The feature vector $\varphi(s)$ is defined as having all the components of $\xi(s)$ along with an additional bias component, 1. Thus, $\varphi(s) = (1, \xi(s))^\top$. The length of $\xi(s)$ is $16 + 4 \times (4^2 + 4^3) = 336$. Hence, the length of the feature vector, $\varphi(s)$ is $L = 1 + 336 = 337$. For each agent $i \in N$, we parameterize the local policy $\pi^i(s, a^i)$ using the Boltzmann distribution as follows:

$$\pi_{\theta^i}^i(s, a^i) = \frac{\exp(q_{s,a^i}^\top \cdot \theta^i)}{\sum_{b^i \in \mathcal{A}^i} \exp(q_{s,b^i}^\top \cdot \theta^i)}, \quad (49)$$

where $q_{s,b^i} \in \mathbb{R}^{m_i}$ is the feature vector of dimension same as θ^i , for any $s \in \mathcal{S}$ and $b^i \in \mathcal{A}^i$, for all $i \in N$. The feature vector q_{s,a^i} for each $i \in N$ is given by:

$$q_{s,a^i} = (1, a^{i,1}\xi(s), a^{i,2}\xi(s), a^{i,3}\xi(s))^\top,$$

where the $\xi(s)$ is defined as earlier, and $a^{i,j}$ are the binary numbers defined as:

$$a^{i,j} = \begin{cases} 1 & \text{if signal plan } j \text{ is selected in action } a^i \\ 0 & \text{otherwise,} \end{cases} \quad \forall i \in N.$$

The length of q_{s,a^i} , i.e., $m_i = 3 \times 336 + 1 = 1009$. For the Boltzmann policy function $\pi_{\theta^i}^i(s, a^i)$ we have [Bhatnagar et al., 2009],

$$\nabla_{\theta^i} \log \pi_{\theta^i}^i(s, a^i) = q_{s,a^i} - \sum_{b^i \in A^i} \pi_{\theta^i}^i(s, b^i) q_{s,b^i}.$$

The features $f(s, a)$ for the rewards function are taken in a similar way as q_{s,a^i} for each $i \in N$, thus $M = 4 \times 3 \times 336 + 1 = 4033$.

We implement all the 3 MAN algorithms and compared the average network congestion with the MAAC algorithm. For all $i \in N$, the initial value of parameters $\mu_0^i, \tilde{\mu}_0^i, v_0^i, \tilde{v}_0^i, \lambda_0^i, \tilde{\lambda}_0^i, \theta_0^i, w_0^i$ are taken as zero vectors of appropriate dimensions. The Fisher information matrix inverse, G_0^{i-1} is initialized to I , $\forall i \in N$. The critic and actor step sizes are taken as $\beta_{v,t} = \frac{1}{(t+1)^{0.65}}$, and $\beta_{\theta,t} = \frac{1}{(t+1)^{0.85}}$ respectively. Note that these step sizes satisfy the conditions given in Equation (10). We assume that the communication graph \mathcal{G}_t is a complete graph at all time instances t and the consensus matrix is constant with $c_t(i, j) = \frac{1}{4}$ for all pairs i, j of agents. Although we do not use the eligibility traces in the convergence analysis, we use them ($\lambda = 0.25$ for TD(λ) [Sutton and Barto, 2018]) to provide better performance in case of function approximations. We believe that the convergence of MAN algorithms while incorporating eligibility traces are easy to follow, so we avoid them here. We now provide the details of the performance of all the algorithms for both arrival patterns.

5.1.2 Performance on traffic network for arrival pattern 1

Recall, for arrival pattern 1 we assign high probability $p_{s,m}$ to the source nodes N_2, S_2 and E_1, E_2 and low probability to other source nodes. Table 2 gives average network congestion (averaged over 10 runs, and round off to 5 decimal places), standard deviation and 95% confidence interval.

Algorithms	Avg network congestion	Standard Deviation	Confidence Interval (95%)
MAAC	14.01687	0.08405	(13.96478, 14.06896)
FI-MAN	12.02819	1.48071	(11.11045, 12.94593)
AP-MAN	14.07899	0.08266	(14.02776, 14.13022)
FIAP-MAN	11.28657	1.04137	(10.64113, 11.93201)

Table 2: For the arrival pattern 1 this table gives the average network congestion, standard deviation and 95% confidence interval at the last decision epoch. FIAP-MAN has $\approx 18\%$, and FI-MAN has $\approx 14\%$ less congestion than MAAC. The congestion for the AP-MAN algorithm is almost the same as the MAAC algorithm with high confidence.

We observe an $\approx 18\%$ reduction in average congestion for FIAP-MAN and $\approx 14\%$ reduction for FI-MAN algorithms compared to the MAAC algorithm. These observations are theoretically justified in Theorem 3 in Section 3.4, as for the Boltzmann policy, we observe that the spectrum of the Fisher information matrix is bounded by 1.

To show that these algorithms have attained the steady state, we provide average congestion, and the correction factor (CF), i.e., the 95% confidence value which is defined as $CF = 1.96 \times \frac{std \, dv n}{\sqrt{10}}$ for last 200 decision epochs in Table 8 of Appendix B.2.1. We observe that average network congestion for FI-MAN and FIAP-MAN are almost (upto 1st decimal) on decreasing trend w.r.t. network congestion however this decay is very slow (0.1 in 200 epochs) suggesting that algorithms are converging to a local minima.

Thus, we see that algorithms involving the natural gradients have better or as good performance as those involving standard gradients. Figure 2 shows the (time) average network congestion for single run (thus lower the better).

For almost 180 decision epochs, all the algorithms have the same (time) average network congestion. However, after 180 decision epochs, FI-MAN and FIAP-MAN follow different paths and hence find different local minima as shown in Theorem 3. We want to emphasize that the Theorem 3 is for maximization framework. As mentioned above in Section 5.1.1, we are also maximizing the globally average rewards, which is equivalent to minimizing the (time average of) number of stopped vehicles.

Actor parameter comparison for arrival pattern 1

Recall, Theorem 3 provides the sufficient conditions for $J(\theta_{t+1}^N) \geq J(\theta_{t+1}^M)$ if $\theta_t^N = \theta_t^M$. However, we observe that $\lambda_{\max}(G(\theta_t^N)) < 1$ for all $t \geq 2$. Therefore, we have $J(\theta_{t+1}^N) \geq J(\theta_{t+1}^M)$ for all $t \geq 2$, and hence at each iterate the average network congestion in FI-MAN, and FIAP-MAN algorithms are better than MAAC algorithm. To investigate this further, we plot the norm of difference of the actor parameter of all the 3 MAN algorithms with MAAC algorithms

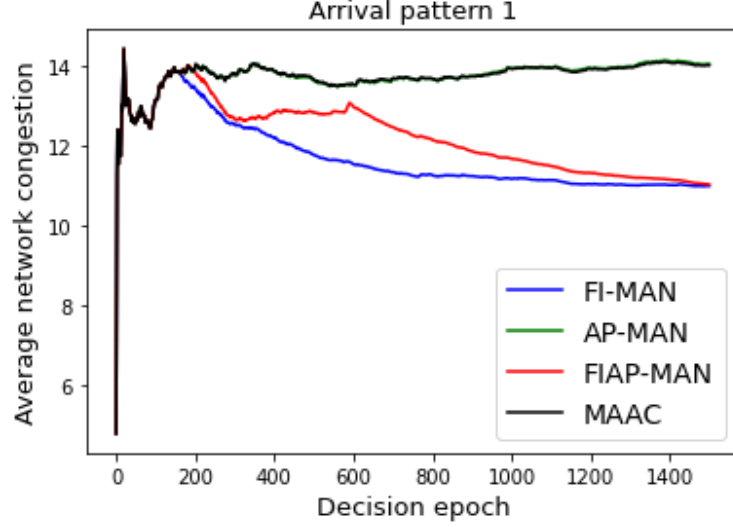


Figure 2: (Time) average network congestion for all the algorithms with arrival pattern 1. The congestion is least for FIAP-MAN and FI-MAN. However, MAAC and AP-MAN have almost the same congestion. Thus 2 (FI-MAN and FIAP-MAN) of the 3 natural gradients based algorithms finds better optima, and the third one (AP-MAN) is on par with MAAC. Moreover, for few initial decision epochs ≈ 180 , all the algorithms have almost the same performance, but afterward, they find different directions and end in different optima.

for each agent. For traffic light T_1 (or agent 1) these differences are shown in Figure 3 (for other agents see Figure 8 in Appendix B.2.1).

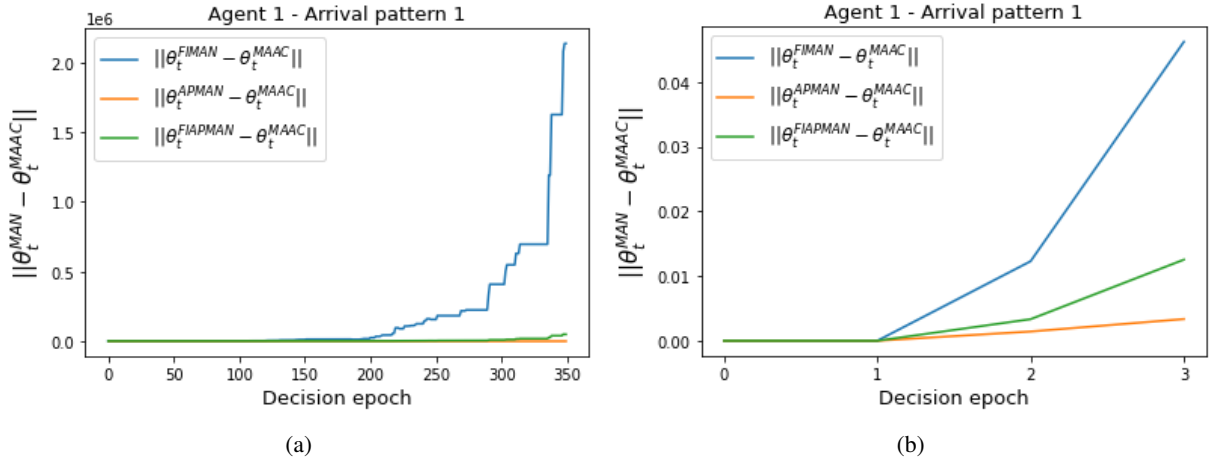


Figure 3: Norm of difference in the actor parameter of agent 1 for all the 3 MAN algorithms with MAAC algorithm for arrival pattern 1. Figure (a) is shown for 350 decision epochs; to show that the differences in the actor parameter are from decision epoch 2 itself, we zoom it in figure (b) in the left panel. However, the significant differences are observed only after ≈ 180 epochs. This illustrates Theorem 3 and related discussions in Section 3.4.

We observe that all the 3 MAN algorithms pick up θ_2 (i.e., the actor parameter at decision epoch 2) that is different from that of the MAAC scheme at varying degrees, with FI-MAN being a bit more ‘farther.’ However, a significant difference is observed around decision epoch ≈ 180 . For better understanding, the same graphs are also shown in the logarithmic scale for agent 1 and agent 2 in Figure 4.

We see that the norm difference is linearly increasing in FI-MAN and FIAP-MAN algorithms, whereas it is almost flat for the AP-MAN algorithm. So, the iterates of these 2 algorithms are exponentially separating from those of the MAAC. This again substantiates our analysis in Section 3.4.

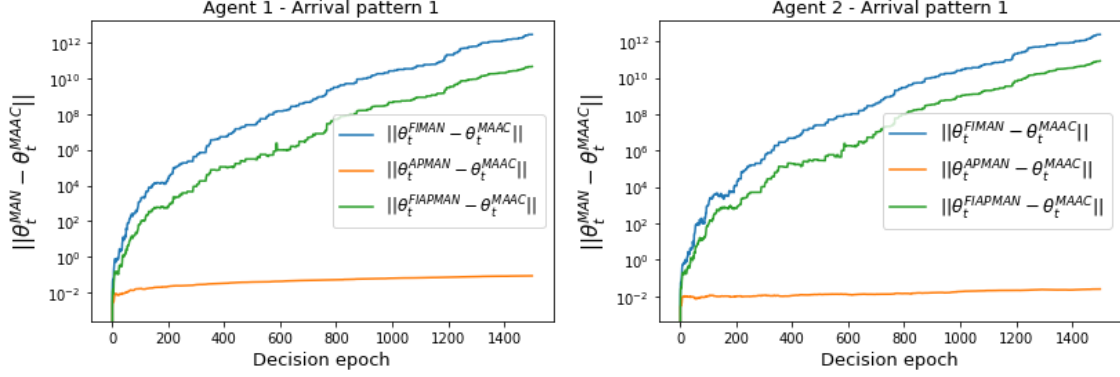


Figure 4: Norm of differences of the actor parameter for agents 1 and 2 with traffic arrival pattern 1 in logarithmic scale illustrating Theorem 3 and related discussions in Section 3.4.

Though we aim to minimize the network congestion, in Table 3 we also provide the average congestion and the correction factor (CF) to each traffic light for last decision epoch (Table 8 in Appendix B.2.1 shows these values for last 200 decision epochs). Expectedly, in all the algorithms, the average congestion for traffic light T_2 is highest; almost same for traffic lights T_1, T_4 ; and least for traffic light T_3 .

Algorithms	Congestion (Avg \pm CF)			
	T_1	T_2	T_3	T_4
MAAC	3.733 ± 0.067	4.336 ± 0.050	2.249 ± 0.013	3.699 ± 0.040
FI-MAN	2.613 ± 0.110	4.492 ± 0.868	2.359 ± 0.161	2.564 ± 0.038
AP-MAN	3.748 ± 0.073	4.338 ± 0.046	2.247 ± 0.013	3.746 ± 0.039
FIAP-MAN	2.711 ± 0.214	3.785 ± 0.371	1.907 ± 0.148	2.883 ± 0.147

Table 3: The average congestion and correction factor (CF) for each traffic light for arrival pattern 1 (described in Section 5.1.2). CF is defined as $1.96 \times \frac{\text{std } \frac{dvn}{\sqrt{10}}}$. For more details see Table 8 in Appendix B.2.1

5.1.3 Performance on traffic network for arrival pattern 2

Recall, in arrival pattern 1 nodes N_2, S_2 and E_1, W_1 are assigned more $p_{s,m}$. We now change the $p_{s,m}$'s and consider arrival pattern 2. Here the traffic origins N_1, N_2, S_1 and S_2 have higher probabilities of being assigned a vehicle. Since $p_{s,m}$ for all these nodes is $\frac{3}{14}$, and for all other nodes it is $\frac{1}{28}$, we expect that all the traffic lights will have almost same average congestion. This observation is reported in Appendix B.2.2. Table 4 present the average network congestion (averaged over 10 runs, and round off to 5 decimal places), standard deviation and 95% confidence interval for arrival pattern 2.

Algorithms	Avg network congestion	Standard deviation	Confidence Interval (95%)
MAAC	13.64571	0.19755	(13.52327, 13.76815)
FI-MAN	10.16988	0.11877	(10.09627, 10.24349)
AP-MAN	13.77573	0.18925	(13.65843, 13.89303)
FIAP-MAN	10.19858	0.21248	(10.06689, 10.33027)

Table 4: For the arrival pattern 2 (described in Section 5.1.3), table gives the average network congestion, standard deviation and 95% confidence interval at last decision epoch. FI-MAN and FIAP-MAN has $\approx 25\%$ less average network congestion than MAAC. The performance of AP-MAN is almost similar to the MAAC algorithm as shown in Theorem 3 and in Section 3.4.

We observe an $\approx 25\%$ reduction in the average congestion for FI-MAN and FIAP-MAN algorithms compared to the MAAC algorithm. AP-MAN is on par with the MAAC algorithm. This again shows the usefulness of the natural gradient based algorithms. As opposed to arrival pattern 1 where FIAP-MAN has slightly better performance than FI-MAN algorithm, in arrival pattern 2, both algorithms have almost similar average network congestion. Moreover,

the standard deviation in arrival pattern 1 is much higher than in arrival pattern 2. Figure 5 shows the (time) average congestion for single simulation run of all the algorithms.

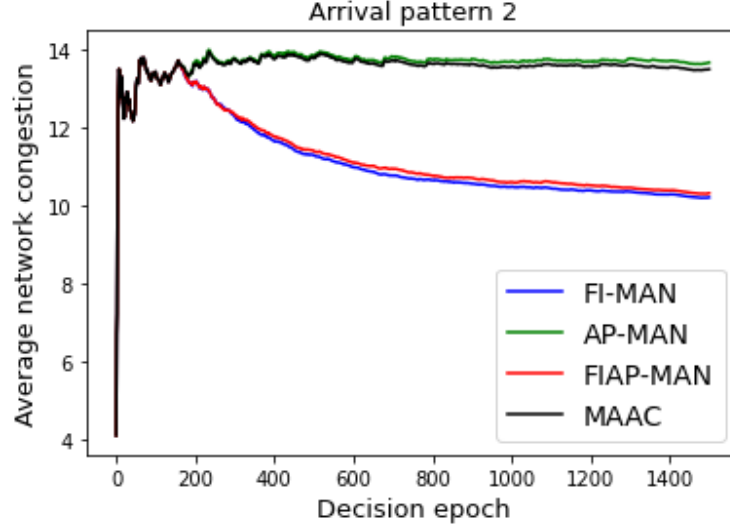


Figure 5: (Time) average network congestion for arrival pattern 2. Again, for few initial decision epochs ≈ 180 all the algorithms have almost same performance, but afterwards they find different directions, and hence ends in different optima.

Actor parameter comparison for arrival pattern 2

Similar to arrival pattern 1, in Figure 6 we plot the norm of the difference for traffic light T_1 (for other traffic lights (agents) see Figure 9 of Appendix B.2.2). For better understanding, the same graphs are also shown in the logarithmic scale for agent 1 and agent 2 in Figure 7. Again, we see that the norm difference is linearly increasing in FI-MAN and FIAP-MAN algorithms, whereas it is almost flat for the AP-MAN algorithm. So, the iterates of these 2 algorithms are exponentially separating from MAAC. This again substantiates our analysis in Section 3.4. Moreover, we also compute the average congestion and (simulation) correction factor for each traffic light. Table 5 shows these values for last decision epoch (See Table 9 for last 200 decision epochs). As expected, the average congestion to each traffic light is almost the same.

Algorithms	Congestion (Avg \pm CF)			
	T_1	T_2	T_3	T_4
MAAC	3.481 ± 0.070	3.379 ± 0.034	3.348 ± 0.032	3.438 ± 0.033
FI-MAN	2.532 ± 0.047	2.530 ± 0.040	2.519 ± 0.045	2.589 ± 0.045
AP-MAN	3.511 ± 0.064	3.404 ± 0.032	3.376 ± 0.034	3.485 ± 0.033
FIAP-MAN	2.566 ± 0.041	2.534 ± 0.034	2.543 ± 0.041	2.556 ± 0.036

Table 5: The average congestion and correction factor (CF) for each traffic light for arrival pattern 2 (described in Section 5.1.3). CF is defined as $1.96 \times \frac{\text{std } d\mathbf{v}_n}{\sqrt{10}}$. For more details see Table 9.

We now present another computational experiment where we consider an abstract MARL with $n = 15$ agents. The model, algorithm parameters, including transition probabilities, rewards, and features for state value function, and rewards are the same as given in [Dann et al., 2014, Zhang et al., 2018]

5.2 Performance of algorithms in abstract MARL model

The abstract MARL model that we consider consists of $n = 15$ agents and $|\mathcal{S}| = 15$ states. Each agent $i \in N$ is endowed with the binary valued actions $\mathcal{A}^i \in \{0, 1\}$. Therefore, the total number of actions are 2^{15} . Each element of the transition probability is a random number uniformly generated from the interval $[0, 1]$. These values are normalized to incorporate the stochasticity. To ensure the ergodicity we add a small constant 10^{-5} to each entry of the transition matrix. The mean reward $R^i(s, a)$ are sampled uniformly from the interval $[0, 4]$ for each agent

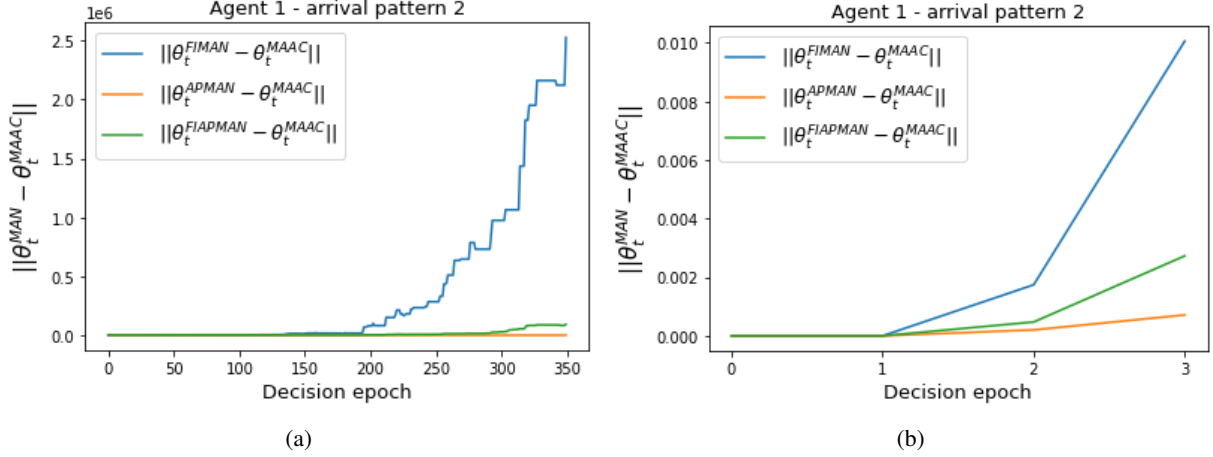


Figure 6: Norm of difference in the actor parameter of agent 1 for all the 3 MAN algorithms with MAAC algorithm. Figure (a) is shown for 350 decision epochs; to show that the differences in the actor parameter are from decision epoch 2 itself, we zoom it in Figure (b). However, the significant differences are observed only after ≈ 180 epochs. This illustrates Theorem 3 and related discussions in Section 3.4.

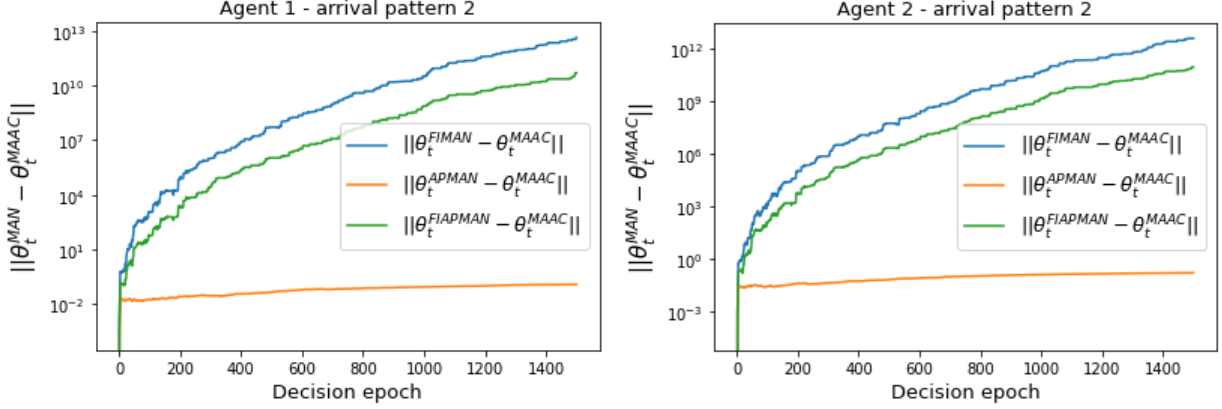


Figure 7: Norm of differences of the actor parameter for agents 1 and 2 with traffic arrival pattern 2 in logarithmic scale illustrating Theorem 3 and related discussions in Section 3.4.

$i \in N$, and for each state-action pair (s, a) . The instantaneous rewards r_t^i are sampled uniformly from the interval $[R^i(s, a) - 0.5, R^i(s, a) + 0.5]$. We parameterize the policy using the Boltzmann distribution as given in Equation (49) with $m_i = 5 \forall i \in N$. All the feature vectors (for the state value and the reward functions) are sampled uniformly from the set $[0, 1]$ of suitable dimensions. More details of the multi-agent model are available in Appendix B.1.

We compared all 3 MAN actor-critic algorithms with MAAC. We observe that the globally averaged return from all the algorithms is almost close to each other (for details, see Table 6 of Appendix B.1). To provide more details, we compute the relative V values for each agent $i \in N$ that is defined as $V(s, v^i) = v^{i\top} \varphi(s)$. Thus, the higher the value, the better is the algorithm. The relative values corresponding to the FI-MAN and FIAP-MAN algorithm are more than the MAAC almost for all agents, suggesting that the natural gradient based algorithms are better than the standard gradient as far as the relative values are concerned. The detailed observations are available in Appendix B.1.

6 Related work

Reinforcement learning has been extensively studied and explored by researchers because of its varied applications, and usefulness in many real world applications [Fax and Murray, 2004, Corke et al., 2005, Dall’Anese et al., 2013]. Single-agent reinforcement learning models are well explained in many works including [Bertsekas, 1995,

[Sutton and Barto, 2018, Bertsekas, 2019]. The average reward reinforcement learning algorithms are available in [Mahadevan, 1996, Dewanto et al., 2020].

Various algorithms to compute the optimal policy for single-agent RL are available; these are mainly categorized as off-policy and on-policy algorithms in literature [Sutton and Barto, 2018]. Moreover, because of the large state and action space, it is often helpful to consider the function approximations of the state value functions [Sutton et al., 1999]. To this end, actor-critic algorithms with function approximations are introduced in [Konda and Tsitsiklis, 2000]. In actor-critic algorithms, the actor updates the policy parameters, and the critic evaluates the policy’s value for the actor parameters until convergence. The convergence of linear architecture in actor-critic methods is known. The algorithm in [Konda and Tsitsiklis, 2000] uses the standard gradient while estimating the objective function. However, as mentioned in Section 2, we outlined some drawbacks of using standard gradients [Ratliff, 2013, Martens, 2020].

To the best of our knowledge, the idea of natural gradients begins from the work of [Amari and Douglas, 1998]. Afterward, it has been extended to learning in [Amari, 1998]. The policy gradient theorem involving the natural gradients is explored in [Kakade, 2001]. For recent developments and work on natural gradients we refer to [Martens, 2020]; see also lecture slides by Roger Grosse³. For the discounted reward, [Agarwal et al., 2021, Mei et al., 2020] recently showed that despite the non-concavity in the objective function, the policy gradient methods under tabular setting with softmax policy characterization find the global optima. However, to the best of our knowledge, such a result is not available for average reward criteria with actor-critic methods and the general class of policy we are using in this work. Moreover, we also see in our computations in Section 5.1 that MAN algorithms are stabilizing at different local optima. Actor-critic methods involving the natural gradients for single-agent are available in [Peters and Schaal, 2008, Bhatnagar et al., 2009]. On the contrary, we deal with the multi-agent setup where all agents have private rewards but have a common objective. For a comparative survey of the MARL algorithms, we refer to [Busoniu et al., 2008, Tuyls and Weiss, 2012, Zhang et al., 2021b].

The MARL algorithms given in [Zhang et al., 2021b] are majorly centralized, and hence relatively slow. However, in many situations [Corke et al., 2005, Dall’Anese et al., 2013] deploying a centralized agent is inefficient and costly. Recently, [Zhang et al., 2018] gave two different actor-critic algorithms in a fully decentralized setup; one based on approximating the state-action value function and the other approximating the state value function. Another work in the same direction is available in [Heredia and Mou, 2019, Suttle et al., 2020, Zhang et al., 2021a]. We build on algorithm 2 of the [Zhang et al., 2018] and incorporate the natural gradients into it. The algorithms that we propose uses the natural gradients similar to [Bhatnagar et al., 2009]. We propose three algorithms incorporating natural gradients into multi-agent RL based on Fisher’s information matrix inverse, approximation of advantage parameters, or both. Using the ideas of stochastic approximation [Borkar and Meyn, 2000, Borkar, 2009, Kushner and Clark, 2012], we prove the convergence of all the proposed algorithms.

7 Discussion

In this paper, we propose three multi-agent natural actor-critic (MAN) reinforcement learning algorithms. Instead of using a central controller for taking action each time, our algorithms use the consensus matrix and are fully decentralized. These MAN algorithms majorly use the Fisher information matrix and the advantage function approximations. All the three algorithms are shown to converge, possibly to different local optima.

We have formally proved that under certain conditions on the eigenvalues of the Fisher information matrix, FI-MAN and FIAP-MAN can find the better optima than MAAC. However, our third algorithm, AP-MAN, is empirically on par with the MAAC. We observe that the Fisher information matrix in these natural gradient based algorithms captures the curvature of the Kullback-Leibler divergence between the policies at consecutive iterates. Indeed, we show that the KL divergence is proportional to the gradient of the objective function; the use of natural gradients offered a *new representation* of the gradient of the objective function in the prediction space of policy distributions which improved the search for better policies.

To validate the usefulness of our algorithm, we empirically evaluate them on a bi-lane traffic network model to minimize the overall congestion in the network in a fully decentralized fashion. Our observation is that sometimes our MAN algorithms can reduce the network congestion by almost $\approx 25\%$ compared to the MAAC algorithm. Moreover, we also consider an abstract MARL with $n = 15$ agents; in that case, also the MAN algorithms are at least as good as the MAAC algorithm with high confidence.

Based on these observations, we like to pursue further some of the open challenges in the multi-agent actor-critic domain. In particular, we like to pursue the finite-time analysis of MAAC and all the 3 MAN algorithms. Our

³<https://csc2541-f17.github.io/slides/lec05a.pdf>

MAN algorithms use different representations via the natural gradients involving the Fisher information matrix and the advantage parameters; this aspect of *representation learning in RL* can also be investigated further.

References

- [Agarwal et al., 2021] Agarwal, A., Kakade, S. M., Lee, J. D., and Mahajan, G. (2021). On the theory of policy gradient methods: Optimality, approximation, and distribution shift. *Journal of Machine Learning Research*, 22(98):1–76.
- [Amari, 1998] Amari, S. I. (1998). Natural gradient works efficiently in learning. *Neural computation*, 10(2):251–276.
- [Amari and Douglas, 1998] Amari, S. I. and Douglas, S. C. (1998). Why natural gradient? In *Proceedings of the 1998 IEEE International Conference on Acoustics, Speech and Signal Processing, ICASSP’98 (Cat. No. 98CH36181)*, volume 2, pages 1213–1216. IEEE.
- [Bagnell and Schneider, 2003] Bagnell, J. A. and Schneider, J. (2003). Covariant policy search. In *Proceedings of the 18th International Joint Conference on Artificial intelligence*, pages 1019–1024.
- [Bertsekas, 1995] Bertsekas, D. P. (1995). *Dynamic programming and optimal control*, volume 1. Athena scientific Belmont, MA.
- [Bertsekas, 1997] Bertsekas, D. P. (1997). *Nonlinear Programming*. Athena scientific, 3rd edition.
- [Bertsekas, 2019] Bertsekas, D. P. (2019). *Reinforcement learning and optimal control*. Athena scientific.
- [Bhatnagar, 2020] Bhatnagar, S. (2020). Single and multi-agent reinforcement learning in changing environments. Master’s thesis, Industrial Engineering and Operations Research, IIT Bombay.
- [Bhatnagar et al., 2009] Bhatnagar, S., Sutton, R. S., Ghavamzadeh, M., and Lee, M. (2009). Natural actor–critic algorithms. *Automatica*, 45(11):2471–2482.
- [Bianchi et al., 2013] Bianchi, P., Fort, G., and Hachem, W. (2013). Performance of a distributed stochastic approximation algorithm. *IEEE Transactions on Information Theory*, 59(11):7405–7418.
- [Borkar, 2009] Borkar, V. S. (2009). *Stochastic approximation: a dynamical systems viewpoint*, volume 48. Springer.
- [Borkar and Meyn, 2000] Borkar, V. S. and Meyn, S. P. (2000). The ode method for convergence of stochastic approximation and reinforcement learning. *SIAM Journal on Control and Optimization*, 38(2):447–469.
- [Boyd et al., 2006] Boyd, S., Ghosh, A., Prabhakar, B., and Shah, D. (2006). Randomized gossip algorithms. *IEEE Transactions on Information Theory*, 52(6):2508–2530.
- [Busoniu et al., 2008] Busoniu, L., Babuska, R., and De Schutter, B. (2008). A comprehensive survey of multiagent reinforcement learning. *IEEE Transactions on Systems, Man, and Cybernetics, Part C (Applications and Reviews)*, 38(2):156–172.
- [Corke et al., 2005] Corke, P., Peterson, R., and Rus, D. (2005). Networked robots: Flying robot navigation using a sensor net. In *Robotics Research. The Eleventh International Symposium*, pages 234–243. Springer.
- [Dall’Anese et al., 2013] Dall’Anese, E., Zhu, H., and Giannakis, G. B. (2013). Distributed optimal power flow for smart microgrids. *IEEE Transactions on Smart Grid*, 4(3):1464–1475.
- [Dann et al., 2014] Dann, C., Neumann, G., Peters, J., et al. (2014). Policy evaluation with temporal differences: A survey and comparison. *Journal of Machine Learning Research*, 15:809–883.
- [Dewanto et al., 2020] Dewanto, V., Dunn, G., Eshragh, A., Gallagher, M., and Roosta, F. (2020). Average-reward model-free reinforcement learning: a systematic review and literature mapping. *arXiv preprint arXiv:2010.08920*.
- [Doan et al., 2021] Doan, T. T., Maguluri, S. T., and Romberg, J. (2021). Finite-time performance of distributed temporal-difference learning with linear function approximation. *SIAM Journal on Mathematics of Data Science*, 3(1):298–320.
- [Fax and Murray, 2004] Fax, J. A. and Murray, R. M. (2004). Information flow and cooperative control of vehicle formations. *IEEE Transactions on Automatic Control*, 49(9):1465–1476.
- [Grondman et al., 2012] Grondman, I., Busoniu, L., Lopes, G. A., and Babuska, R. (2012). A survey of actor-critic reinforcement learning: Standard and natural policy gradients. *IEEE Transactions on Systems, Man, and Cybernetics, Part C (Applications and Reviews)*, 42(6):1291–1307.
- [Heredia and Mou, 2019] Heredia, P. C. and Mou, S. (2019). Distributed multi-agent reinforcement learning by actor-critic method. *IFAC-PapersOnLine*, 52(20):363–368.

- [Kakade, 2001] Kakade, S. M. (2001). A natural policy gradient. *Advances in Neural Information Processing Systems*, 14.
- [Konda and Tsitsiklis, 2000] Konda, V. R. and Tsitsiklis, J. N. (2000). Actor-critic algorithms. In *Advances in Neural Information Processing Systems*, pages 1008–1014. Citeseer.
- [Krajzewicz et al., 2012] Krajzewicz, D., Erdmann, J., Behrisch, M., and Bieker, L. (2012). Recent development and applications of sumo-simulation of urban mobility. *International Journal on Advances in Systems and Measurements*, 5(3&4).
- [Kushner and Yin, 2003] Kushner, H. and Yin, G. G. (2003). *Stochastic approximation and recursive algorithms and applications*, volume 35. Springer Science & Business Media.
- [Kushner and Clark, 2012] Kushner, H. J. and Clark, D. S. (2012). *Stochastic approximation methods for constrained and unconstrained systems*, volume 26. Springer Science & Business Media.
- [Mahadevan, 1996] Mahadevan, S. (1996). Average reward reinforcement learning: Foundations, algorithms, and empirical results. *Machine Learning*, 22(1):159–195.
- [Martens, 2020] Martens, J. (2020). New insights and perspectives on the natural gradient method. *Journal of Machine Learning Research*, 21(146):1–76.
- [Mei et al., 2020] Mei, J., Xiao, C., Szepesvari, C., and Schuurmans, D. (2020). On the global convergence rates of softmax policy gradient methods. In *International Conference on Machine Learning*, pages 6820–6829. PMLR.
- [Metivier and Priouret, 1984] Metivier, M. and Priouret, P. (1984). Applications of a Kushner and Clark lemma to general classes of stochastic algorithms. *IEEE Transactions on Information Theory*, 30(2):140–151.
- [Nedic et al., 2017] Nedic, A., Olshevsky, A., and Shi, W. (2017). Achieving geometric convergence for distributed optimization over time-varying graphs. *SIAM Journal on Optimization*, 27(4):2597–2633.
- [Nedic and Ozdaglar, 2009] Nedic, A. and Ozdaglar, A. (2009). Distributed subgradient methods for multi-agent optimization. *IEEE Transactions on Automatic Control*, 54(1):48–61.
- [Neveu, 1975] Neveu, Jacques translated by Speed, T. (1975). *Discrete-parameter martingales*, volume 10. North-Holland Amsterdam.
- [Peters and Schaal, 2008] Peters, J. and Schaal, S. (2008). Natural actor-critic. *Neurocomputing*, 71(7-9):1180–1190.
- [Peters et al., 2003] Peters, J., Vijayakumar, S., and Schaal, S. (2003). Reinforcement learning for humanoid robotics. In *3rd IEEE-RAS International Conference on Humanoid Robots (ICHR 2003)*, pages 1–20.
- [Puterman, 2014] Puterman, M. L. (2014). *Markov decision processes: discrete stochastic dynamic programming*. John Wiley & Sons.
- [Ratliff, 2013] Ratliff, N. (2013). Information geometry and natural gradients. Available at https://ipvs.informatik.uni-stuttgart.de/mlr/wp-content/uploads/2015/01/mathematics_for_intelligent_systems_lecture12_notes_I.pdf. Last accessed August 20, 2021.
- [Sherman and Morrison, 1950] Sherman, J. and Morrison, W. J. (1950). Adjustment of an inverse matrix corresponding to a change in one element of a given matrix. *The Annals of Mathematical Statistics*, 21(1):124–127.
- [Suttle et al., 2020] Suttle, W., Yang, Z., Zhang, K., Wang, Z., Başar, T., and Liu, J. (2020). A multi-agent off-policy actor-critic algorithm for distributed reinforcement learning. *IFAC-PapersOnLine*, 53(2):1549–1554.
- [Sutton and Barto, 2018] Sutton, R. S. and Barto, A. G. (2018). *Reinforcement learning: An introduction*. MIT press.
- [Sutton et al., 1999] Sutton, R. S., McAllester, D. A., Singh, S. P., Mansour, Y., et al. (1999). Policy gradient methods for reinforcement learning with function approximation. In *NIPS*, volume 99, pages 1057–1063. Citeseer.
- [Tuyts and Weiss, 2012] Tuyts, K. and Weiss, G. (2012). Multiagent learning: Basics, challenges, and prospects. *AI Magazine*, 33(3).
- [Xiao et al., 2005] Xiao, L., Boyd, S., and Lall, S. (2005). A scheme for robust distributed sensor fusion based on average consensus. In *IPSN 2005. Fourth International Symposium on Information Processing in Sensor Networks, 2005.*, pages 63–70. IEEE.
- [Zedek, 1965] Zedek, M. (1965). Continuity and location of zeros of linear combinations of polynomials. *Proceedings of the American Mathematical Society*, 16(1):78–84.
- [Zhang et al., 2021a] Zhang, K., Yang, Z., and Başar, T. (2021a). Decentralized multi-agent reinforcement learning with networked agents: recent advances. *Frontiers of Information Technology & Electronic Engineering*, 22(6):802–814.

[Zhang et al., 2021b] Zhang, K., Yang, Z., and Başar, T. (2021b). Multi-agent reinforcement learning: A selective overview of theories and algorithms. *Handbook of Reinforcement Learning and Control*, pages 321–384.

[Zhang et al., 2018] Zhang, K., Yang, Z., Liu, H., Zhang, T., and Basar, T. (2018). Fully decentralized multi-agent reinforcement learning with networked agents. In *International Conference on Machine Learning*, pages 5872–5881. PMLR.

A Proof of theorems and lemmas

In this section, we provide the proofs of some important theorems and lemmas stated in the main text.

A.1 Proof of Theorem 4

Recall Theorem 4: Under assumptions A. 1, A. 2, and A. 3, for any policy π_θ , with sequences $\{\lambda_t^i\}, \{\mu_t^i\}, \{v_t^i\}$ generated from critic updates, we have $\lim_t \mu_t^i = J(\theta)$, $\lim_t \lambda_t^i = \lambda_\theta$, and $\lim_t v_t^i = v_\theta$ a.s. for any agent $i \in N$, where $J(\theta)$, λ_θ , and v_θ are unique solutions to

$$\begin{aligned} F^\top D_\theta^{s,a}(\bar{R} - F\lambda_\theta) &= 0, \\ \Phi^\top D_\theta^s[T_\theta^V(\Phi v_\theta) - \Phi v_\theta] &= 0. \end{aligned}$$

Proof. The proof is similar to the Theorem 4.9 of [Zhang et al., 2018]. Define the following $z_t^i = [\mu_t^i, (\lambda_t^i)^\top, (v_t^i)^\top]^\top \in \mathbb{R}^{1+M+L}$. Firstly, we will use the following lemma from [Zhang et al., 2018] to give the bounds on z_t^i (for proof see [Zhang et al., 2018]).

Lemma 3. Under assumptions A. 1, A. 2, A. 3 the sequence $\{z_t^i\}$ satisfy $\sup_t \|z_t^i\| < \infty$ a.s., for all $i \in N$.

Now consider the actor step given in Equation (20)

$$\begin{aligned} \theta_{t+1}^i &= \theta_t^i + \beta_{\theta,t} \cdot G_t^{i-1} \cdot \tilde{\delta}_t^i \cdot \psi_t^i \\ &= \theta_t^i + \beta_{v,t} \cdot \frac{\beta_{\theta,t}}{\beta_{v,t}} \cdot G_t^{i-1} \cdot \tilde{\delta}_t^i \cdot \psi_t^i. \end{aligned} \quad (50)$$

By assumption, $\frac{\beta_{\theta,t}}{\beta_{v,t}} \rightarrow 0$. Also note that $\tilde{\delta}_t^i \cdot \psi_t^i$ is bounded by assumptions and Lemma 3. Moreover, G_t^{i-1} is bounded by assumption A. 4. Thus, the actor update in Equation (50) can be traced via an ODE $\dot{\theta}^i = 0$. Hence we can fix the value of θ_t as constant θ while analyzing the critic-step at the faster time scale. Note that above argument of taking $\theta_t \equiv \theta$ while analyzing the critic step is common to all the 3 MAN algorithms. The only difference is in actor update Equation (50), nonetheless a similar argument concludes that $\theta_t \equiv \theta$.

Let $\mathcal{F}_{t,4} = \sigma(r_\tau, \mu_\tau, \lambda_\tau, v_\tau, s_\tau, a_\tau, C_{\tau-1}, \tau \leq t)$ be the filtration which is an increasing σ -algebra over time t . Define the following for notation convenience. Let $r_t = [r_t^1, \dots, r_t^n]^\top$, $v_t = [(v_t^1)^\top, \dots, (v_t^n)^\top]^\top$, $\delta_t = [(\delta_t^1)^\top, \dots, (\delta_t^n)^\top]^\top$, and $z_t = [(z_t^1)^\top, \dots, (z_t^n)^\top]^\top \in \mathbb{R}^{n(1+M+L)}$. Moreover, let $A \otimes B$ represents the Kronecker product of matrices A and B . Let $y_t = [(y_t^1)^\top, \dots, (y_t^n)^\top]^\top$, where $y_{t+1}^i = [r_{t+1}^i - \mu_t^i, (r_{t+1}^i - f_t^\top \lambda_t^i) f_t^\top, \delta_t^i \varphi_t^\top]^\top$. Recall, $f_t = f(s_t, a_t)$, and $\varphi_t = \varphi(s_t)$. Let I be the identity matrix of the dimension $(1 + M + L) \times (1 + M + L)$. Then update of z_t can be written as

$$z_{t+1} = (C_t \otimes I)(z_t + \beta_{v,t} \cdot y_{t+1}).$$

Let $\mathbb{1} = (1, \dots, 1)$ represents the vector of all 1's. We define the operator $\langle z \rangle = \frac{1}{n}(\mathbb{1}^\top \otimes I)z = \frac{1}{n} \sum_{i \in N} z^i$. This $\langle z \rangle \in \mathbb{R}^{1+M+L}$ represents the average of the vectors in $\{z^1, z^2, \dots, z^n\}$. For notational simplicity let $k = 1 + M + L$. Moreover, let $\mathcal{J} = (\frac{1}{n} \mathbb{1} \mathbb{1}^\top) \otimes I \in \mathbb{R}^{nk \times nk}$ is the projection operator that projects a vector into the consensus subspace $\{\mathbb{1} \otimes u : u \in \mathbb{R}^k\}$. Thus $\mathcal{J}z = \mathbb{1} \otimes \langle z \rangle$. Now define the disagreement vector $z_\perp = \mathcal{J}_\perp z = z - \mathbb{1} \otimes \langle z \rangle$, where $\mathcal{J}_\perp = I - \mathcal{J}$. Here I is $nk \times nk$ dimensional identity matrix. The iteration z_t can be separated as the sum of a vector in disagreement space and a vector in consensus space, i.e., $z_t = z_{\perp,t} + \mathbb{1} \otimes \langle z_t \rangle$. The proof of critic step convergence consists of two steps.

Step 01: To show $\lim_t z_{\perp,t} = 0$ a.s. From Lemma 3 we have $\mathbb{P}[\sup_t \|z_t\| < \infty] = 1$, i.e., $\mathbb{P}[\cup_{K \in \mathbb{Z}^+} \{\sup_t \|z_t\| < K\}] = 1$. It suffices to show that $\lim_t z_{\perp,t} \mathbb{1}_{\{\sup_t \|z_t\| < K\}} = 0$ for any $K \in \mathbb{Z}^+$. Lemma B.5 in [Zhang et al., 2018] proves the boundedness of $\mathbb{E}[\|\beta_{v,t}^{-1} z_{\perp,t}\|^2]$ over the set $\{\sup_t \|z_t\| \leq K\}$, for any $K > 0$. We state the lemma here.

Lemma 4. Under assumptions A. 2, and A. 3 for any $K > 0$, we have

$$\sup_t \mathbb{E}[\|\beta_{v,t}^{-1} z_{\perp,t}\|^2 \mathbb{1}_{\{\sup_t \|z_t\| \leq K\}}] < \infty.$$

From Lemma 4 we obtain that for any $K > 0$, $\exists K_1 < \infty$ such that for any $t \geq 0$, $\mathbb{E}[\|z_{\perp,t}\|^2] < K_1 \beta_{v,t}^2$ over the set $\{sup_t \|z_t\| < K\}$. Since $\sum_t \beta_{v,t}^2 < \infty$, by Fubini's theorem we have $\sum_t \mathbb{E}(\|z_{\perp,t}\|^2 \mathbb{1}_{\{sup_t \|z_t\| < K\}}) < \infty$. Thus, $\sum_t \|z_{\perp,t}\|^2 \mathbb{1}_{\{sup_t \|z_t\| < K\}} < \infty$ a.s. Therefore, $\lim_t z_{\perp,t} \mathbb{1}_{\{sup_t \|z_t\| < K\}} = 0$ a.s. Since $\{sup_t \|z_t\| < \infty\}$ wp 1, thus $\lim_t z_{\perp,t} = 0$ a.s. This ends the proof of step 01.

Step 02: To show the convergence of the consensus vector $\mathbb{1} \otimes \langle z_t \rangle$. First, note that the iteration of $\langle z_t \rangle$ can be written as

$$\begin{aligned} \langle z_{t+1} \rangle &= \frac{1}{N} (\mathbb{1}^\top \otimes I) (C_t \otimes I) (\mathbb{1} \otimes \langle z_t \rangle + z_{\perp,t} + \beta_{v,t} y_{t+1}) \\ &= \langle z_t \rangle + \beta_{v,t} \langle (C_t \otimes I) (y_{t+1} + \beta_{v,t}^{-1} z_{\perp,t}) \rangle. \end{aligned}$$

Hence the update of $\langle z_t \rangle$ becomes

$$\langle z_{t+1} \rangle = \langle z_t \rangle + \beta_{v,t} \mathbb{E}(\langle y_{t+1} \rangle | \mathcal{F}_{t,4}) + \beta_{v,t} \xi_{t+1}, \quad (51)$$

where

$$\begin{aligned} \xi_{t+1} &= \langle (C_t \otimes I) (y_{t+1} + \beta_{v,t}^{-1} z_{\perp,t}) \rangle - \mathbb{E}(\langle y_{t+1} \rangle | \mathcal{F}_{t,4}), \\ \langle y_{t+1} \rangle &= [\bar{r}_{t+1} - \langle \mu_t \rangle, (\bar{r}_{t+1} - f_t^\top \langle \lambda_t \rangle) f_t^\top, \langle \delta_t \rangle \varphi_t^\top]^\top, \end{aligned}$$

where $\langle \delta_t \rangle = \bar{r}_{t+1} - \langle \mu_t \rangle + \varphi_{t+1}^\top \langle v_t \rangle - \varphi_t^\top \langle v_t \rangle$. Note that $\mathbb{E}(\langle y_{t+1} \rangle | \mathcal{F}_{t,4})$ is Lipschitz continuous in $\langle z_t \rangle = (\langle \mu_t \rangle, \langle \lambda_t \rangle^\top, \langle v_t \rangle^\top)^\top$. Moreover, ξ_{t+1} is martingale difference sequence and satisfy

$$\mathbb{E}[\|\xi_{t+1}\|^2 | \mathcal{F}_{t,4}] \leq \mathbb{E}[\|y_{t+1} + \beta_{v,t}^{-1} z_{\perp,t}\|_{S_t}^2 | \mathcal{F}_{t,4}] + \|\mathbb{E}(\langle y_{t+1} \rangle) | \mathcal{F}_{t,4}\|^2, \quad (52)$$

where $S_t = \frac{C_t^\top \mathbb{1} \mathbb{1}^\top C_t \otimes I}{n^2}$ has bounded spectral norm. Bounding first and second terms in rhs of Equation (52) we have, for any $K > 0$

$$\mathbb{E}[\|\xi_{t+1}\|^2 | \mathcal{F}_{t,4}] \leq K_2(1 + \|\langle z_t \rangle\|^2), \quad (53)$$

over the set $\{sup_t \|z_t\| \leq K\}$ for some $K_2 < \infty$. The ODE associated with the Equation (51) has the form

$$\langle \dot{z} \rangle = \begin{pmatrix} \langle \dot{\mu} \rangle \\ \langle \dot{\lambda} \rangle \\ \langle \dot{v} \rangle \end{pmatrix} = \begin{pmatrix} -1 & 0 & 0 \\ 0 & -F^\top D_\theta^{s,a} F & 0 \\ -\Phi^\top D_\theta^s \mathbb{1} & 0 & \Phi^\top D_\theta^s (P^\theta - I) \Phi \end{pmatrix} \begin{pmatrix} \langle \mu \rangle \\ \langle \lambda \rangle \\ \langle v \rangle \end{pmatrix} + \begin{pmatrix} J(\theta) \\ F^\top D_\theta^{s,a} \bar{R} \\ \Phi^\top D_\theta^s \bar{R} \theta \end{pmatrix}. \quad (54)$$

Let the rhs of equation (54) be $h(\langle z \rangle)$. It is easy to verify that $h(\langle z \rangle)$ is Lipschitz continuous in $\langle z \rangle$. Also, recall that $D_\theta^{s,a} = \text{diag}[d_\theta(s) \cdot \pi_\theta(s, a), s \in \mathcal{S}, a \in \mathcal{A}]$. Using assumption A. 1, and Perron-Frobenius theorem the stochastic matrix P^θ has a eigenvalue of 1, and remaining eigenvalues have real part less than 1. Hence $(P^\theta - I)$ has one eigenvalue zero, and all other eigenvalues with negative real parts. Same follows for the matrix $\Phi^\top D_\theta^s (P^\theta - I) \Phi$, since Φ is full rank column matrix. The simple eigen-vector ν of the matrix satisfy $\Phi \nu = \alpha \mathbb{1}$ for some $\alpha \neq 0$. However, this will not happen because of the assumption A. 3. Hence the ODE given in Equation (54) has unique globally asymptotically stable equilibrium $[J(\theta), \lambda_\theta^\top, v_\theta^\top]^\top$ satisfying

$$-\langle \mu \rangle + J(\theta) = 0; \quad F^\top D_\theta^{s,a} (\bar{R} - F \lambda_\theta) = 0; \quad \Phi^\top D_\theta^s [T_\theta^V (\Phi v_\theta) - \Phi v_\theta] = 0,$$

where $[J(\theta), \lambda_\theta^\top, v_\theta^\top]^\top$ are the unique equilibrium solutions to the above equations. Moreover, from Lemma 3, and Lemma 4, the sequence $\{z_t\}$ is bounded almost surely, so is the sequence $\{\langle z_t \rangle\}$. Specializing Corollary 8 and Theorem 9 on page 74-75 in [Borkar, 2009] we have $\lim_t \langle \mu_t \rangle = J(\theta)$, $\lim_t \langle \lambda_t \rangle = \lambda_\theta$, and $\lim_t \langle v_t \rangle = v_\theta$ a.s. over the set $\{sup_t \|z_t\| \leq K\}$ for any $K > 0$. This concludes the proof of step 02. The proof of Theorem thus follows from Lemma 3 and results from step 01. Thus, we have $\lim_t \mu_t^i = J(\theta)$, $\lim_t \lambda_t^i = \lambda_\theta$, and $\lim_t v_t^i = v_\theta$ a.s. for any $i \in N$. \square

A.2 Proof of Lemma 1

Recall the Lemma: For the Boltzmann policy as given in Equation (34) the KL divergence between policy parameterized by θ_t and $\theta_t + \Delta\theta$ is given by

$$KL(\pi_{\theta_t}(s, a) || \pi_{\theta_t + \Delta\theta}(s, a)) = \mathbb{E} \left[\log \left(\sum_{b \in \mathcal{A}} \pi_{\theta_t}(s, b) \cdot \exp(\Delta q_{s,ba}^\top \Delta\theta) \right) \right], \quad (55)$$

where $\Delta q_{s,ba}^\top = q_{s,b}^\top - q_{s,a}^\top$.

Proof. Recall, KL divergence is defined as

$$\begin{aligned}
 KL(\pi_{\theta_t}(\cdot, \cdot) || \pi_{\theta_t + \Delta\theta}(\cdot, \cdot)) &= \mathbb{E} \left[\log \left(\frac{\pi_{\theta_t}(s, a)}{\pi_{\theta_t + \Delta\theta}(s, a)} \right) \right] = \mathbb{E} \left[\log \left(\frac{\frac{\exp(q_{s,a}^\top \theta_t)}{\sum_{c \in \mathcal{A}} \exp(q_{s,c}^\top \theta_t)}}{\frac{\exp(q_{s,a}^\top (\theta_t + \Delta\theta))}{\sum_{b \in \mathcal{A}} \exp(q_{s,b}^\top (\theta_t + \Delta\theta))}} \right) \right] \\
 &= \mathbb{E} \left[\log \left(\exp(q_{s,a}^\top (\theta_t - (\theta_t + \Delta\theta))) \cdot \frac{\sum_{b \in \mathcal{A}} \exp(q_{s,b}^\top (\theta_t + \Delta\theta))}{\sum_{c \in \mathcal{A}} \exp(q_{s,c}^\top \theta_t)} \right) \right] \\
 &= \mathbb{E} \left[-q_{s,a}^\top \Delta\theta + \log \left(\sum_{b \in \mathcal{A}} \left(\frac{\exp(q_{s,b}^\top \theta_t) \cdot \exp(q_{s,b}^\top \Delta\theta)}{\sum_{c \in \mathcal{A}} \exp(q_{s,c}^\top \theta_t)} \right) \right) \right] \\
 &= \mathbb{E} \left[-q_{s,a}^\top \Delta\theta + \log \left(\sum_{b \in \mathcal{A}} \pi_{\theta_t}(s, b) \cdot \exp(q_{s,b}^\top \Delta\theta) \right) \right] \\
 &= \mathbb{E} \left[\log \left(\sum_{b \in \mathcal{A}} \pi_{\theta_t}(s, b) \cdot \frac{\exp(q_{s,b}^\top \Delta\theta)}{\exp(q_{s,a}^\top \Delta\theta)} \right) \right] \\
 &= \mathbb{E} \left[\log \left(\sum_{b \in \mathcal{A}} \pi_{\theta_t}(s, b) \cdot \exp((q_{s,b}^\top - q_{s,a}^\top) \Delta\theta) \right) \right] \\
 &= \mathbb{E} \left[\log \left(\sum_{b \in \mathcal{A}} \pi_{\theta_t}(s, b) \cdot \exp(\Delta q_{s,ba}^\top \Delta\theta) \right) \right].
 \end{aligned}$$

□

A.3 Proof of Lemma 2

Recall the Lemma: For the Boltzmann policy as given in Equation (34), we have

$$\nabla KL(\pi_{\theta_t}(\cdot, \cdot) || \pi_{\theta_t + \Delta\theta}(\cdot, \cdot)) = -\mathbb{E}[\nabla \log \pi_{\theta_t + \Delta\theta}(s, a)]. \quad (56)$$

Proof. Recall, $KL(\pi_{\theta_t}(\cdot, \cdot) || \pi_{\theta_t + \Delta\theta}(\cdot, \cdot))$ for the Boltzmann policy is given in Lemma 1. Thus, $\nabla KL(\pi_{\theta_t}(\cdot, \cdot) || \pi_{\theta_t + \Delta\theta}(\cdot, \cdot))$ is

$$\begin{aligned}
 &= \nabla \mathbb{E} \left[\log \left(\sum_{b \in \mathcal{A}} \pi_{\theta_t}(s, b) \cdot \exp(\Delta q_{s,ba}^\top \Delta\theta) \right) \right] \\
 &= \mathbb{E} \left[\nabla \log \left(\sum_{b \in \mathcal{A}} \pi_{\theta_t}(s, b) \cdot \exp(\Delta q_{s,ba}^\top \Delta\theta) \right) \right] \quad (\because \mathcal{A} \text{ is finite}) \\
 &= \mathbb{E} \left[\frac{1}{\sum_{b \in \mathcal{A}} \pi_{\theta_t}(s, b) \cdot \exp(\Delta q_{s,ba}^\top \Delta\theta)} \cdot \sum_{b \in \mathcal{A}} \pi_{\theta_t}(s, b) \cdot \Delta q_{s,ba} \cdot \exp(\Delta q_{s,ba}^\top \Delta\theta) \right] \\
 &= \mathbb{E} \left[\sum_{b \in \mathcal{A}} \pi_{\theta_t}(s, b) \cdot \Delta q_{s,ba} \cdot \left(\frac{\exp(\Delta q_{s,ba}^\top \Delta\theta)}{\sum_{c \in \mathcal{A}} \pi_{\theta_t}(s, c) \cdot \exp(\Delta q_{s,ca}^\top \Delta\theta)} \right) \right] \\
 &= \mathbb{E} \left[\sum_{b \in \mathcal{A}} \Delta q_{s,ba} \cdot \left(\frac{\pi_{\theta_t}(s, b) \cdot \exp(\Delta q_{s,ba}^\top \Delta\theta)}{\sum_{c \in \mathcal{A}} \pi_{\theta_t}(s, c) \cdot \exp(\Delta q_{s,ca}^\top \Delta\theta)} \right) \right] \\
 &= \mathbb{E} \left[\sum_{b \in \mathcal{A}} \Delta q_{s,ba} \cdot \left(\frac{\frac{\exp(q_{s,b}^\top \theta_t)}{\sum_{e \in \mathcal{A}} \exp(q_{s,e}^\top \theta_t)} \cdot \frac{\exp(q_{s,b}^\top \Delta\theta)}{\exp(q_{s,a}^\top \Delta\theta)}}{\sum_{c \in \mathcal{A}} \frac{\exp(q_{s,c}^\top \theta_t)}{\sum_{d \in \mathcal{A}} \exp(q_{s,d}^\top \theta_t)} \cdot \frac{\exp(q_{s,c}^\top \Delta\theta)}{\exp(q_{s,a}^\top \Delta\theta)}} \right) \right] \\
 &= \mathbb{E} \left[\sum_{b \in \mathcal{A}} \Delta q_{s,ba} \cdot \left(\frac{\exp(q_{s,b}^\top (\theta_t + \Delta\theta))}{\sum_{c \in \mathcal{A}} \exp(q_{s,c}^\top (\theta_t + \Delta\theta))} \right) \right]
 \end{aligned}$$

$$\begin{aligned}
&= \mathbb{E} \left[\sum_{b \in \mathcal{A}} (q_{s,b}^\top - q_{s,a}^\top) \cdot \pi_{\theta_t + \Delta \theta}(s, b) \right] \\
&= -\mathbb{E} \left[q_{s,a}^\top - \sum_{b \in \mathcal{A}} q_{s,b}^\top \cdot \pi_{\theta_t + \Delta \theta}(s, b) \right] \\
&= -\mathbb{E}[\nabla \log \pi_{\theta_t + \Delta \theta}(s, a)].
\end{aligned}$$

□

□

B Further details on computational experiments

In this section, we will provide further details of the computational experiments for traffic network control and the abstract multi-agent reinforcement learning setup.

B.1 Experiments for abstract multi-agent reinforcement learning model

We will provide the details of the experiments for an abstract multi-agent RL model we have considered in Section 5.2.

The abstract MARL model that we consider consists of $n = 15$ agents and $|\mathcal{S}| = 15$ states. Each agent, $i \in N$ is endowed with the binary valued actions, $\mathcal{A}^i = \{0, 1\}$. Therefore, total number of actions are 2^{15} . Each element of the transition probability is a random number uniformly generated from the interval $[0, 1]$. These values are normalized to be stochastic. To ensure the ergodicity we add a small constant 10^{-5} to each entry of the transition matrix. The mean reward $R^i(s, a)$ is sampled uniformly from the interval $[0, 4]$ for each agent $i \in N$, and each state-action pair (s, a) . The instantaneous rewards r_t^i are sampled uniformly from the interval $[R^i(s, a) - 0.5, R^i(s, a) + 0.5]$. We parameterize the policy using the Boltzmann distribution as

$$\pi_{\theta^i}^i(s, a^i) = \frac{\exp(q_{s,a^i}^\top \cdot \theta^i)}{\sum_{b^i \in \mathcal{A}^i} \exp(q_{s,b^i}^\top \cdot \theta^i)} \quad (57)$$

where $q_{s,b^i} \in \mathbb{R}^{m_i}$ is the feature vector of dimension same as θ^i , for any $s \in \mathcal{S}$, and $b^i \in \mathcal{A}^i$, for all $i \in N$. We set $m_i = 5 \forall i \in N$. All the elements of q_{s,b^i} are also uniformly sampled from $[0, 1]$. For the Boltzmann policy function we have

$$\nabla_{\theta^i} \log \pi_{\theta^i}^i(s, a^i) = q_{s,a^i} - \sum_{b^i \in \mathcal{A}^i} \pi_{\theta^i}^i(s, b^i) q_{s,b^i}$$

The features for state value function $\varphi(s) \in \mathcal{R}^L$ are uniformly sampled from $[0, 1]$ of dimension $L = 5 \ll |\mathcal{S}|$, whereas the features for the reward function $f(s, a) \in \mathbb{R}^M$ are uniformly sampled from $[0, 1]$ of dimension $M = 10 \ll |\mathcal{S}||\mathcal{A}|$. The communication network \mathcal{G}_t is generated randomly at each time t , such that the links in the network are formed with the connectivity ratio⁴ $4/n$. The step sizes are taken as $\beta_{v,t} = \frac{1}{t^{0.65}}$, and $\beta_{\theta,t} = \frac{1}{t^{0.85}}$ respectively. Initial values of parameters $\mu_0^i, \tilde{\mu}_0^i, v_0^i, \tilde{v}_0^i, \lambda_0^i, \tilde{\lambda}_0^i, \theta_0^i, w_0^i$ are taken as zero vectors of appropriate dimension, $\forall i \in N$. The Fisher information matrix inverse is initialized to $G_0^{i-1} = 1.5 \times I$, $\forall i \in N$. We compared the MAAC with the multi-agent natural actor-critic algorithms FI-MAN, AP-MAN, and FIAP-MAN. The globally averaged reward, standard deviation and 95% confidence intervals (averaged over 25 iterations) for all multi-agent natural actor-critic algorithms are given in Table 6.

Algorithm	Avg Rewards	Std Dvn	Confidence interval
MAAC	1.993280	0.066421	(1.967243, 2.019316)
FI-MAN	2.008412	0.055538	(1.986642, 2.030183)
AP-MAN	1.982451	0.079404	(1.951325, 2.013576)
FIAP-MAN	1.981089	0.093754	(1.944338, 2.017839)

Table 6: Globally averaged rewards, standard deviation and 95% confidence for all the algorithms for the abstract multi-agent RL problem. We observe that globally averaged rewards and standard deviation are almost same for all the algorithms with high confidence. All the values are averaged over 25 runs.

⁴Ratio of total degree of the graph and the degree of complete graph, i.e., $\frac{2E}{n(n-1)}$, where E is the number of edges in the graph.

We see that the globally averaged returns from all the algorithms are almost close with high confidence. Since the performance of all the algorithms are same, we have compared the relative V values, defined as $V(s; v^i) = v^{i\top} \varphi(s)$ for all agents $i \in N$ averaged over 25 runs with each run involving 12000 iterations. These values are available in Table 7 (maximum values in each row are bold).

Agents	Algorithms			
	FI-MAN	AP-MAN	FIAP-MAN	MAAC
1	0.099790	-0.081895	0.096078	-0.011488
2	0.082189	-0.006449	0.030639	0.012191
3	0.055486	-0.078218	0.082690	-0.082770
4	0.076051	-0.079353	0.012621	0.015753
5	0.083763	-0.063922	0.061808	0.002050
6	0.020304	-0.052126	0.108242	-0.008364
7	0.056736	-0.105311	0.087904	0.042844
8	0.036493	-0.039098	-0.004051	0.052373
9	0.101874	-0.026014	0.153574	0.030972
10	0.040236	-0.041242	0.045329	0.016195
11	0.024138	-0.035986	0.101919	-0.006431
12	0.106377	-0.054188	-0.018450	0.012857
13	0.058369	-0.049010	0.078504	0.003431
14	0.049588	-0.090194	0.056069	-0.003832
15	0.090342	-0.057247	0.066245	0.013376

Table 7: Relative V values for each agent for all algorithms averaged over 25 runs. The values in bold represent the maximum in each row, i.e., for each agent. The V values are maximum either for FI-MAN or FIAP-MAN algorithm for all the agents except agent 8, suggesting that natural actor-critic algorithms have better relative V value than standard gradient-based algorithm MAAC. However, the globally averaged returns are almost the same for all the algorithms as shown in Table 6.

Though the globally averaged returns are almost the same for all the algorithms, the relative V values are maximum for all but agent 8 in the FI-MAN or FIAP-MAN algorithms showing the usefulness of multi-agent natural actor-critic algorithms.

B.2 Experiments for traffic network control

Here we provide some more details about the traffic network congestion model for both arrival patterns.

B.2.1 More performance details for arrival pattern 1

Though we aim to minimize the network congestion only, in Table 8, we also provide the congestion to each traffic light for the last 200 decision epochs (all the values are round off to 3 decimal places). Because of the $p_{s,m}$'s for arrival pattern 1, as expected the traffic light T_2 is heavily congested; T_1, T_4 are almost equally congested and T_3 is the least congested. We also present the correction factor (CF) that is calculated as $1.96 \times \frac{std \, dvn}{\sqrt{10}}$. It captures the 95% confidence about the average congestion of each traffic light and the overall network congestion.

For completeness, we now provide the plots of norm of the differences for agents T_2, T_3, T_4 in Figure 8.

B.2.2 More performance details of arrival pattern 2

Table 9 provides the average network congestion and the congestion to each traffic light for last 200 decision epochs. As expected from the arrival pattern 1, all the traffic lights are almost equally congested. Again CF is the correction factor defined earlier.

We again plot the norm of the difference of the actor parameter for remaining agent T_2, T_3 and T_4 in Figure 9.

Algos	Decision Epochs	Congestion (Avg \pm CF)				
		T_1	T_2	T_3	T_4	Network
MAAC	1300	3.742 \pm 0.071	4.344 \pm 0.049	2.241 \pm 0.012	3.716 \pm 0.045	14.042 \pm 0.053
	1350	3.737 \pm 0.072	4.345 \pm 0.050	2.239 \pm 0.011	3.717 \pm 0.041	14.037 \pm 0.054
	1400	3.742 \pm 0.065	4.344 \pm 0.049	2.242 \pm 0.011	3.708 \pm 0.042	14.035 \pm 0.043
	1450	3.741 \pm 0.061	4.347 \pm 0.053	2.246 \pm 0.011	3.705 \pm 0.042	14.039 \pm 0.046
	1500	3.733 \pm 0.067	4.336 \pm 0.050	2.249 \pm 0.013	3.699 \pm 0.040	14.017 \pm 0.052
FI	1300	2.652 \pm 0.114	4.515 \pm 0.838	2.359 \pm 0.159	2.598 \pm 0.041	12.124 \pm 0.896
	1350	2.638 \pm 0.112	4.516 \pm 0.851	2.358 \pm 0.159	2.589 \pm 0.042	12.100 \pm 0.903
	1400	2.633 \pm 0.110	4.514 \pm 0.856	2.358 \pm 0.160	2.579 \pm 0.039	12.084 \pm 0.910
	1450	2.623 \pm 0.111	4.515 \pm 0.871	2.361 \pm 0.161	2.569 \pm 0.039	12.068 \pm 0.921
	1500	2.613 \pm 0.110	4.492 \pm 0.868	2.359 \pm 0.161	2.564 \pm 0.038	12.028 \pm 0.918
AP	1300	3.754 \pm 0.077	4.349 \pm 0.045	2.236 \pm 0.013	3.758 \pm 0.041	14.097 \pm 0.048
	1350	3.747 \pm 0.078	4.346 \pm 0.046	2.235 \pm 0.011	3.761 \pm 0.036	14.089 \pm 0.047
	1400	3.755 \pm 0.072	4.345 \pm 0.045	2.238 \pm 0.011	3.751 \pm 0.037	14.091 \pm 0.039
	1450	3.756 \pm 0.068	4.348 \pm 0.048	2.243 \pm 0.011	3.752 \pm 0.041	14.099 \pm 0.041
	1500	3.748 \pm 0.073	4.338 \pm 0.046	2.247 \pm 0.013	3.746 \pm 0.039	14.079 \pm 0.051
FIAP	1300	2.757 \pm 0.245	3.855 \pm 0.376	1.929 \pm 0.148	2.939 \pm 0.165	11.479 \pm 0.691
	1350	2.743 \pm 0.236	3.833 \pm 0.372	1.923 \pm 0.149	2.926 \pm 0.161	11.424 \pm 0.680
	1400	2.735 \pm 0.229	3.827 \pm 0.383	1.916 \pm 0.147	2.910 \pm 0.156	11.388 \pm 0.675
	1450	2.723 \pm 0.222	3.809 \pm 0.380	1.913 \pm 0.149	2.897 \pm 0.152	11.342 \pm 0.662
	1500	2.711 \pm 0.214	3.785 \pm 0.371	1.907 \pm 0.148	2.883 \pm 0.147	11.287 \pm 0.645

Table 8: Table shows the average congestion \pm correction factor (averaged over 10 runs) to each traffic light and to the entire network in last 200 decision epochs for arrival pattern 1. As expected, the average congestion is the highest for traffic light T_2 in all the algorithms, almost same for traffic lights T_1, T_4 and least for traffic light T_3 . The overall network congestion is simply the sum of congestion at all the traffic lights. Moreover, for the last 200 decision epochs all the values are close to each other with high confidence implying that the algorithms indeed are attaining the local minima.

Algos	Decision Epochs	Congestion (Avg \pm CF)				
		T_1	T_2	T_3	T_4	Network
MAAC	1300	3.486 \pm 0.074	3.378 \pm 0.031	3.348 \pm 0.042	3.445 \pm 0.037	13.658 \pm 0.130
	1350	3.485 \pm 0.073	3.375 \pm 0.031	3.361 \pm 0.041	3.448 \pm 0.035	13.670 \pm 0.130
	1400	3.482 \pm 0.071	3.373 \pm 0.034	3.355 \pm 0.040	3.448 \pm 0.033	13.656 \pm 0.129
	1450	3.489 \pm 0.073	3.381 \pm 0.035	3.350 \pm 0.034	3.442 \pm 0.036	13.662 \pm 0.130
	1500	3.481 \pm 0.070	3.379 \pm 0.034	3.348 \pm 0.032	3.438 \pm 0.033	13.646 \pm 0.122
FI	1300	2.560 \pm 0.048	2.554 \pm 0.041	2.541 \pm 0.046	2.609 \pm 0.052	10.264 \pm 0.087
	1350	2.554 \pm 0.047	2.547 \pm 0.044	2.539 \pm 0.045	2.605 \pm 0.048	10.244 \pm 0.083
	1400	2.545 \pm 0.047	2.540 \pm 0.043	2.534 \pm 0.044	2.599 \pm 0.047	10.217 \pm 0.079
	1450	2.541 \pm 0.046	2.535 \pm 0.040	2.524 \pm 0.044	2.593 \pm 0.045	10.194 \pm 0.073
	1500	2.532 \pm 0.047	2.530 \pm 0.040	2.519 \pm 0.045	2.589 \pm 0.045	10.170 \pm 0.074
AP	1300	3.515 \pm 0.070	3.400 \pm 0.026	3.377 \pm 0.046	3.488 \pm 0.037	13.780 \pm 0.129
	1350	3.514 \pm 0.067	3.398 \pm 0.028	3.388 \pm 0.045	3.490 \pm 0.031	13.792 \pm 0.126
	1400	3.513 \pm 0.064	3.397 \pm 0.032	3.383 \pm 0.043	3.490 \pm 0.029	13.783 \pm 0.123
	1450	3.518 \pm 0.066	3.407 \pm 0.033	3.377 \pm 0.037	3.488 \pm 0.035	13.790 \pm 0.126
	1500	3.511 \pm 0.064	3.404 \pm 0.032	3.376 \pm 0.034	3.485 \pm 0.033	13.776 \pm 0.117
FIAP	1300	2.591 \pm 0.043	2.558 \pm 0.037	2.570 \pm 0.043	2.579 \pm 0.038	10.298 \pm 0.140
	1350	2.586 \pm 0.042	2.549 \pm 0.036	2.564 \pm 0.043	2.576 \pm 0.034	10.275 \pm 0.134
	1400	2.577 \pm 0.042	2.544 \pm 0.035	2.557 \pm 0.041	2.569 \pm 0.035	10.247 \pm 0.135
	1450	2.574 \pm 0.039	2.540 \pm 0.034	2.549 \pm 0.041	2.562 \pm 0.034	10.226 \pm 0.128
	1500	2.566 \pm 0.041	2.534 \pm 0.034	2.543 \pm 0.041	2.556 \pm 0.036	10.199 \pm 0.132

Table 9: Table shows the average congestion \pm correction factor (averaged over 10 runs) to each traffic light and to the entire network in last 200 decision epochs for arrival pattern 2. As expected, the average congestion is almost the same for all traffic lights in all the algorithms.

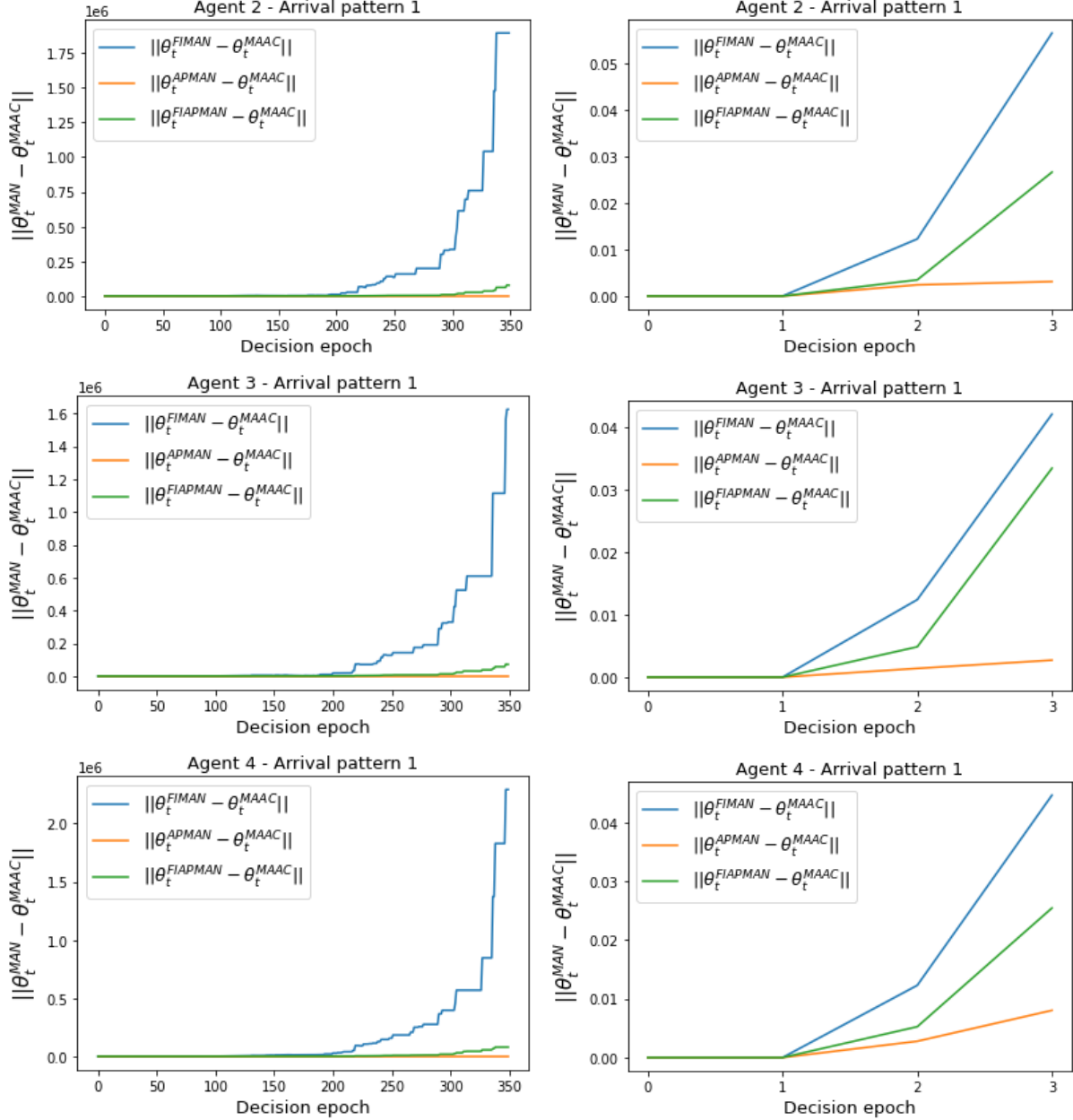


Figure 8: Norm of difference of agent T_2, T_3, T_4 for all the algorithms. The left panel is shown upto 350 epochs, however to show that actor parameters are actually differing from iterate 2 itself, we zoom them in the left figure. These observations illustrate Theorem 3 in Section 3.4.

B.2.3 Justification of Equation (48)

We first use the law of total probability to show that for a given arrival pattern m the number of arrivals to the source node s at time t follows the binomial distribution as given in Equation (48).

$$\begin{aligned}
 \mathbb{P}(N_t^s = k | M_t = m) &= \sum_{j=0}^{N_v} \mathbb{P}(N_t^s = k | N_t = j, M_t = m) \mathbb{P}(N_t = j | M_t = m) \\
 &= \sum_{j=k}^{N_v} \binom{j}{k} p_{s,m}^k (1 - p_{s,m})^{j-k} \mathbb{P}(N_t = j)
 \end{aligned}$$

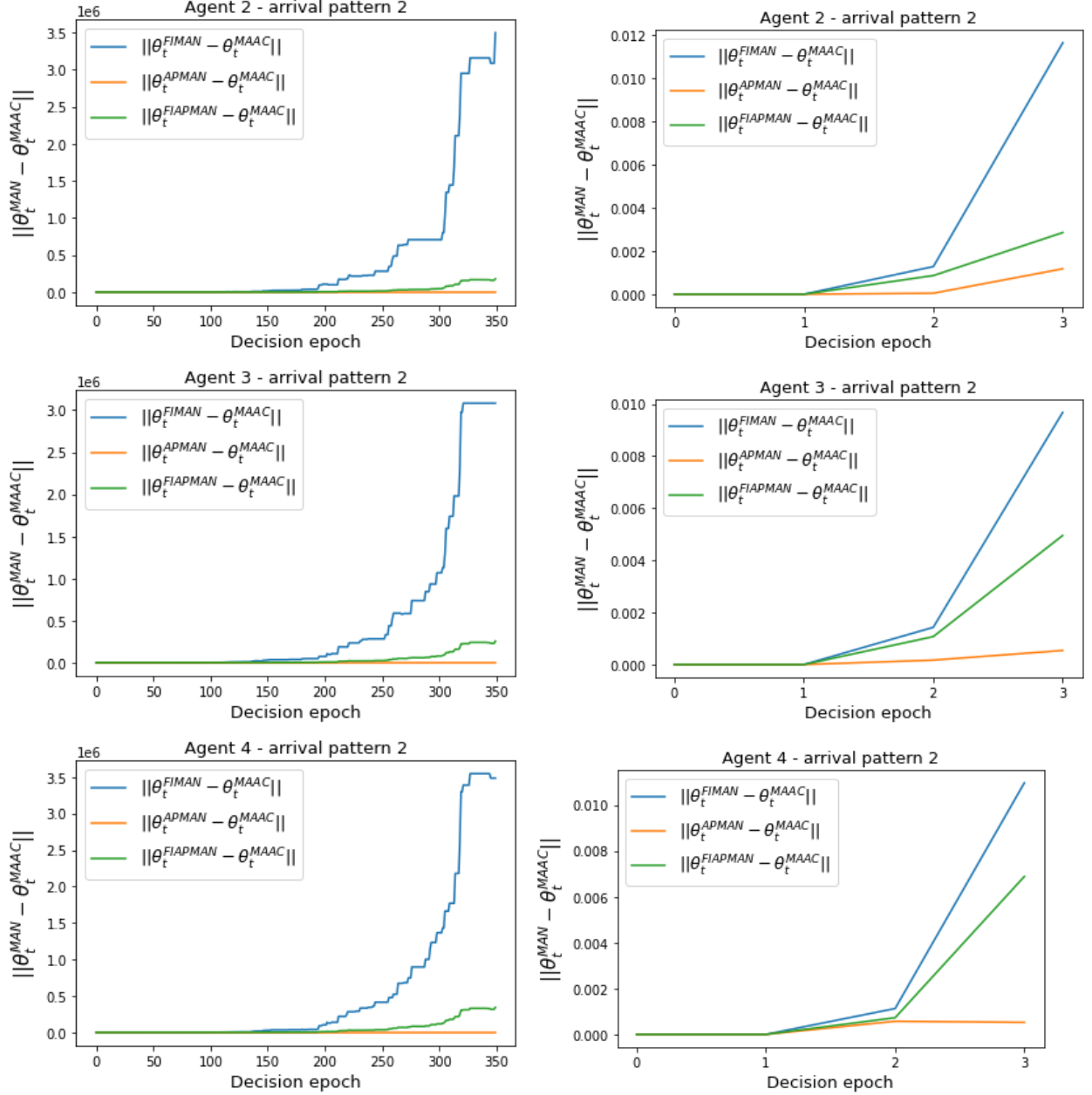


Figure 9: For arrival pattern 2, norm of difference of agent T_2, T_3, T_4 for all the algorithms. The left panel is shown upto 350 epochs, however to show that actor parameters are actually differing from iterate 2 itself, we zoom them in the left figure. These observations illustrate Theorem 3 in Section 3.4.

$$\begin{aligned}
 &= p_{s,m}^k \sum_{j=0}^{N_v} \binom{j}{k} \binom{N_v}{j} (1-p_{s,m})^{j-k} \left(\frac{1}{T}\right)^j \left(1-\frac{1}{T}\right)^{N_v-j} \\
 &= \binom{N_v}{k} p_{s,m}^k \sum_{l=0}^{N_v-k} \binom{N_v-k}{l} (1-p_{s,m})^{N_v-k-l} \left(\frac{1}{T}\right)^{N_v-l} \left(1-\frac{1}{T}\right)^l \\
 &= \binom{N_v}{k} \left(\frac{p_{s,m}}{T}\right)^k \left(1-\frac{p_{s,m}}{T}\right)^{N_v-k}.
 \end{aligned}$$

C Some relevant background

In this Section, we will provide details of single agent MDP, actor-critic algorithm, the MAAC algorithm [Zhang et al., 2018], and the Kushner-Clark Lemma.

C.1 Markov decision processes and actor-critic algorithms with linear function approximation

Markov decision process (MDP) is a stochastic control process that provides a mathematical framework for sequential decision making. Formally it is defined as below.

Definition 1 (MDP [Puterman, 2014]). *A MDP is characterised by a quadruple $\mathcal{M} = \langle \mathcal{S}, \mathcal{A}, P, r \rangle$, where \mathcal{S} and \mathcal{A} are finite state and action space respectively. $P(s'|s, a) : \mathcal{S} \times \mathcal{A} \times \mathcal{S} \rightarrow [0, 1]$ is the transition probability of taking action a from state s and going to state s' . $R(s, a) : \mathcal{S} \times \mathcal{A} \rightarrow \mathbb{R}$ is the reward function defined as $R(s, a) = \mathbb{E}[r_{t+1} | s_t = s, a_t = a]$ where r_{t+1} is the instantaneous reward at time t .*

The policy of an agent is a decision rule using which agent takes action in each state; formally, it is a mapping $\pi : \mathcal{S} \times \mathcal{A} \rightarrow [0, 1]$. It represents the probability of taking action a in the state s . The goal of the agent is to maximize the expected average reward, i.e.,

$$J(\pi) = \lim_T \frac{1}{T} \sum_{t=0}^{T-1} \mathbb{E}(r_{t+1}) = \sum_{s \in \mathcal{S}} d_\pi(s) \sum_{a \in \mathcal{A}} \pi(s, a) R(s, a),$$

where $d_\pi(s) = \lim_t \mathbb{P}(s_t = s | \pi)$ is the stationary state distribution of the Markov chain under policy π . The action value function for a policy, $Q_\pi(\cdot, \cdot)$ is defined as

$$Q_\pi(s, a) = \sum_t \mathbb{E}[r_{t+1} - J(\pi) | s_0 = s, a_0 = a, \pi].$$

The state value function $V(s)$ for any state s is defined as

$$V_\pi(s) = \sum_{a \in \mathcal{A}} \pi(s, a) Q_\pi(s, a).$$

In most real-life scenarios, the state space, the action space, or both are large and infinite, and hence finding the optimal policy is computationally heavy. It is useful to consider the parameterized policies. Let the parameterized policy is denoted by π_θ . We need following regularity assumption on the parameterized policy function [Bhatnagar et al., 2009, Sutton and Barto, 2018]. For any $s \in \mathcal{S}$, and $a \in \mathcal{A}$, the policy function $\pi_\theta(s, a) > 0$ for any $\theta \in \Theta$. Also, $\pi_\theta(s, a)$ is continuously differentiable with respect to the parameter θ over Θ . Moreover, for any $\theta \in \Theta$, let P^θ be the transition matrix for the Markov chain $\{s_t\}_{t \geq 0}$ induced by policy π_θ , that is, for any $s, s' \in \mathcal{S}$,

$$P^\theta(s' | s) = \sum_{a \in \mathcal{A}} \pi_\theta(s, a) P(s' | s, a).$$

Futhermore, the Markov chain $\{s_t\}_{t \geq 0}$ is assumed to be ergodic under π_θ with stationary distribution denoted by $d_\theta(s)$ over \mathcal{S} .

Under this parameterization, the policy gradient theorem [Sutton and Barto, 2018] is given by: $\nabla_\theta J(\theta) = \mathbb{E}_{s \sim d_\theta, a \sim \pi_\theta} [\nabla_\theta \log \pi_\theta(s, a) \cdot \{Q_\theta(s, a) - b(s)\}]$. The term $b(s)$ is usually referred to as the baseline. This baseline helps in reducing the variance in the gradient of the objective function. It turns out that $V_\theta(s)$ serves as the minimum variance baseline. We define the advantage function as follows: $A_\theta(s, a) = Q_\theta(s, a) - V_\theta(s)$.

The actor-critic algorithm is obtained by parameterizing the state value function. Let the state value function is parameterized as $V_t(v) := V_t(s; v)$. Moreover, let μ_t be the estimate of the objective function at time t . The actor-critic algorithms use the following to update the critic and actor parameters

$$\begin{aligned} \mu_{t+1} &= (1 - \beta_{v,t}) \cdot \mu_t + \beta_{v,t} \cdot r_{t+1} \\ v_{t+1} &= v_t + \beta_{v,t} \cdot \delta_t \cdot \nabla_v V_t(v_t) \\ \theta_{t+1} &= \theta_t + \beta_{\theta,t} \cdot \delta_t \cdot \psi_t, \end{aligned}$$

where δ_t is the TD error involving the state value function and defined as $\delta_t = r_{t+1} - \mu_t + V_{t+1}(v_t) - V_t(v_t)$, and it is known to be an unbiased estimator of the advantage function [Bhatnagar et al., 2009], i.e., $\mathbb{E}[\delta_t | s_t = s, a_t = s, \pi_\theta] = A_\theta(s, a)$. Here $\beta_{\theta,t}$ and $\beta_{v,t}$ are step-sizes and satisfy the following assumptions

$$a) \sum_t \beta_{v,t} = \sum_t \beta_{\theta,t} = \infty; \quad b) \sum_t \beta_{v,t}^2 + \beta_{\theta,t}^2 < \infty,$$

moreover, $\beta_{\theta,t} = o(\beta_{v,t})$, and $\lim_t \frac{\beta_{v,t+1}}{\beta_{v,t}} = 1$. Next, we provide the Kushner-Clark lemma that we use often in the proof of convergence.

C.2 Kushner-Clark Lemma [Kushner and Yin, 2003, Metivier and Priouret, 1984]

Let $\mathcal{X} \subseteq \mathbb{R}^p$ be a compact set and let $h : \mathcal{X} \rightarrow \mathbb{R}^p$ be a continuous function. Consider the following recursion in p -dimensions

$$x_{t+1} = \Gamma\{x_t + \gamma_t[h(x_t) + \zeta_t + \beta_t]\}. \quad (58)$$

Let $\hat{\Gamma}(\cdot)$ is transformed projection operator defined for any $x \in \mathcal{X} \subseteq \mathbb{R}^p$ as

$$\hat{\Gamma}(h(x)) = \lim_{0 < \eta \rightarrow 0} \left\{ \frac{\Gamma(x + \eta h(x)) - x}{\eta} \right\},$$

then the ODE associated with Equation (58) is $\dot{x} = \hat{\Gamma}(h(x))$.

A. 6. *Kushner-Clark lemma requires following assumptions*

1. Stepsize $\{\gamma_t\}_{t \geq 0}$ satisfy $\sum_t \gamma_t = \infty$, and $\gamma_t \rightarrow 0$ as $t \rightarrow \infty$.
2. The sequence $\{\beta_t\}_{t \geq 0}$ is a bounded random sequence with $\beta_t \rightarrow 0$ almost surely as $t \rightarrow \infty$.
3. For any $\epsilon > 0$, the sequence $\{\zeta_t\}_{t \geq 0}$ satisfy

$$\lim_t \mathbb{P} \left(\sup_{p \geq t} \left\| \sum_{\tau=t}^p \gamma_\tau \zeta_\tau \right\| \geq \epsilon \right) = 0.$$

Kushner-Clark lemma is as follows: suppose that ODE $\dot{x} = \hat{\Gamma}(h(x))$ has a compact set \mathcal{K}^* as its asymptotically stable equilibria, then under assumption A. 6, x_t in Equation (58) converges almost surely to \mathcal{K}^* as $t \rightarrow \infty$.

C.3 Multi-agent actor-critic algorithm based on state value function

For completeness, we reproduce the multi-agent actor-critic (MAAC) algorithm based on the state value function [Zhang et al., 2018].

MAAC: Multi-agent actor-critic based on state value function

Input: Initial values of $\mu_0^i, \tilde{\mu}_0^i, v_0^i, \tilde{v}_0^i, \lambda_0^i, \tilde{\lambda}_0^i, \theta_0^i, G_0^i, G_0^{i-1} \forall i \in N$, initial state s_0 , and stepsizes $\{\beta_{v,t}\}_{t \geq 0}, \{\beta_{\theta,t}\}_{t \geq 0}$.

Each agent i implements $a_0^i \sim \pi_{\theta_0^i}(s_0, \cdot)$.

Initialize the step counter $t \leftarrow 0$.

repeat

for all $i \in N$ **do**

 Observe state s_{t+1} , and reward r_{t+1}^i .

 Update: $\tilde{\mu}_t^i \leftarrow (1 - \beta_{v,t}) \cdot \mu_t^i + \beta_{v,t} \cdot r_{t+1}^i$.

$\tilde{\lambda}_t^i \leftarrow \lambda_t^i + \beta_{v,t} \cdot [r_{t+1}^i - \bar{R}_t(\lambda_t^i)] \cdot \nabla_{\lambda} \bar{R}_t(\lambda_t^i)$, where $\bar{R}_t(\lambda_t^i) = \lambda_t^{i\top} f(s_t, a_t)$.

 Update: $\delta_t^i \leftarrow r_{t+1}^i - \mu_t^i + V_{t+1}(v_t^i) - V_t(v_t^i)$, where $V_{t+1}(v_t^i) = v_t^{i\top} \varphi(s_{t+1})$.

Critic Step: $\tilde{v}_t^i \leftarrow v_t^i + \beta_{v,t} \cdot \delta_t^i \cdot \nabla_v V_t(v_t^i)$

 Update $\tilde{\delta}_t^i \leftarrow \bar{R}_t(\lambda_t^i) - \mu_t^i + V_{t+1}(v_t^i) - V_t(v_t^i)$; $\psi_t^i \leftarrow \nabla_{\theta^i} \log \pi_{\theta_t^i}(s_t, a_t^i)$.

Actor Step: $\theta_{t+1}^i \leftarrow \theta_t^i + \beta_{\theta,t} \cdot \tilde{\delta}_t^i \cdot \psi_t^i$.

 Send $\tilde{\mu}_t^i, \tilde{\lambda}_t^i, \tilde{v}_t^i$ to the neighbors over \mathcal{G}_t .

for all $i \in N$ **do**

Consensus update: $\mu_{t+1}^i \leftarrow \sum_{j \in N} c_t(i, j) \tilde{\mu}_t^j$;

$\lambda_{t+1}^i \leftarrow \sum_{j \in N} c_t(i, j) \tilde{\lambda}_t^j$; $v_{t+1}^i \leftarrow \sum_{j \in N} c_t(i, j) \tilde{v}_t^j$.

 Update: $t \leftarrow t + 1$.

until Convergence;
